A posteriori estimates distinguishing the error components and adaptive stopping criteria for numerical approximations of parabolic variational inequalities

Jad Dabaghi, Vincent Martin, Martin Vohralík

A posteriori estimates distinguishing the error components and adaptive stopping criteria for numerical approximations of parabolic variational inequalities *

Jad Dabaghi[†‡] Vincent Martin[§] Martin Vohralík[†‡]

August 29, 2019

Abstract

We consider in this paper a model parabolic variational inequality. This problem is discretized with conforming Lagrange finite elements of order $p \geq 1$ in space and with the backward Euler scheme in time. The nonlinearity coming from the complementarity constraints is treated with any semismooth Newton algorithm and we take into account in our analysis an arbitrary iterative algebraic solver. In the case $p = 1$, when the system of nonlinear algebraic equations is solved exactly, we derive an a posteriori error estimate on both the energy error norm and a norm approximating the time derivative error. When $p \geq 1$, we provide a fully computable and guaranteed a posteriori estimate in the energy error norm which is valid at each step of the linearization and algebraic solvers. Our estimate, based on equilibrated flux reconstructions, also distinguishes the discretization, linearization, and algebraic error components. We build an adaptive inexact semismooth Newton algorithm based on stopping the iterations of both solvers when the estimators of the corresponding error components do not affect significantly the overall estimate. Numerical experiments are performed with the semismooth Newton-min algorithm and the semismooth Newton–Fischer–Burmeister algorithm in combination with the GMRES iterative algebraic solver to illustrate the strengths of our approach.

Keywords: parabolic variational inequality, complementarity condition, semismooth Newton method, algebraic solver, a posteriori error estimate, adaptivity, stopping criterion

1 Introduction

Let $\Omega \subset \mathbb{R}^2$ be a polygonal domain and let $T > 0$ denote the final time. Let $H^1(\Omega)$ be the space of L^2 functions on the domain Ω which admit a weak gradient in $[L^2(\Omega)]^2$ and $H^1_0(\Omega)$ its zero-trace subspace. Consider the affine space $H^1_g(\Omega) := \{v \in H^1(\Omega),\ v = g \text{ on } \partial\Omega\}$, where g is a positive constant and denote the dual space of $H^1_0(\Omega)$ by $H^{-1}(\Omega)$, with the duality pairing $\langle \cdot, \cdot \rangle$. Consider a bilinear continuous form $a(\cdot,\cdot) : \left[H^1(\Omega)\right]^2 \times \left[H^1(\Omega)\right]^2 \to \mathbb{R}$, coercive on $\left[H^1_0(\Omega)\right]^2$. Let $\boldsymbol{\mathcal{K}}_g$ be a nonempty closed convex subset of $H^1_g(\Omega) \times H^1_0(\Omega)$ and let $\boldsymbol{\mathcal{K}}^{\mathrm{t}}_g$ be its evolutive-in-time version

$$\boldsymbol{\mathcal{K}}^{\mathrm{t}}_g := \left\{\boldsymbol{v} \in L^2(0,T;H^1_g(\Omega)) \times L^2(0,T;H^1_0(\Omega)),\ \boldsymbol{v}(t) \in \boldsymbol{\mathcal{K}}_g \text{ a.e. in }]0,T[\right\}. \tag{1.1}$$

We consider the following parabolic variational inequality: for the data $\boldsymbol{f} := (f_1, f_2) \in \left[L^2(0,T;L^2(\Omega))\right]^2$ and the initial condition $\boldsymbol{u}^0 = (u^0_1, u^0_2) \in \boldsymbol{\mathcal{K}}_g$, find $\boldsymbol{u} = (u_1, u_2) \in \boldsymbol{\mathcal{K}}^{\mathrm{t}}_g$ such that $\partial_t \boldsymbol{u} \in \left[L^2(0,T;H^{-1}(\Omega))\right]^2$

*This project has received funding from the European Research Council (ERC) under the European Union's Horizon 2020 research and innovation program (grant agreement No 647134 GATIPOR).

[†]Inria, 2 rue Simone Iff, 75589 Paris, France

[‡]Université Paris-Est, CERMICS (ENPC), 77455 Marne-la-Vallée 2, France

[§]Sorbonne universités, Université de technologie de Compiègne (UTC), LMAC, CS 60319, 60203 Compiègne Cedex

and such that for all $\boldsymbol{v} \in \boldsymbol{\mathcal{K}}_g^{\mathrm{t}}$

$$\begin{aligned} &\int_0^T \langle \partial_t \boldsymbol{u}, \boldsymbol{v} - \boldsymbol{u} \rangle(t) \,\mathrm{dt} + \int_0^T a(\boldsymbol{u}, \boldsymbol{v} - \boldsymbol{u})(t) \,\mathrm{dt} \geq \int_0^T (\boldsymbol{f}, \boldsymbol{v} - \boldsymbol{u})_\Omega(t) \,\mathrm{dt}, \\ &\boldsymbol{u}(0) = \boldsymbol{u}^0. \end{aligned} \tag{1.2}$$

Problem (1.2) belongs to the wide class of parabolic variational inequalities of the first kind, see Glowinski [1] and Lions [2] for a general introduction. Evolutionnary variational inequalities have attracted recent interest in a wide variety of applications. We mention the problems in modeling pricing of American options [3, 4], the applications in stochastic control [5], and obstacle problems in mechanics [2, 6, 7, 8]. Existence and uniqueness of a weak solution $\boldsymbol{u} \in \boldsymbol{\mathcal{K}}_g^{\mathrm{t}}$ for (1.2) is classical, see [2, 9, 10] and the references therein.

For spatial discretization of variational inequalities, the finite element method is commonly employed, see Chen and Nochetto [11], Veeser [12], Braess [13], or Ben Belgacem *et al.* [14] for a $\mathbb{P}_1$ conforming solution, and Bürg and Schröder [15], Dabaghi *et al.* [16] for a $\mathbb{P}_p$ nonconforming solution. Discontinuous Galerkin methods have been studied in Wang *et al.* [17] and Gudi and Porwal [18, 19, 20], finite volumes in Herbin and Marchand [21], Berton and Eymard [22], and Steinbach [23], and discontinuous skeletal methods in the recent work of Cicuttin, Ern, and Gudi [24]. The discretization in time often uses the backward Euler scheme.

Among the spectrum of methods for the solution of the systems of algebraic inequalities arising from discretizations of (1.2), let us mention the interior point method of Wright [25], the active set strategy by Kanzow [26], the primal-dual active set strategy by Hintermüller *et al.* [27], and the the family of the semismooth Newton methods (see [28, 29, 30, 31]). In this work, we use a saddle-point Lagrangian formulation giving rise at each time step n to a nonlinear system of algebraic equations of the form

$$\mathcal{S}^n(\boldsymbol{X}_h^n) = 0, \tag{1.3}$$

where $\mathcal{S}$ is a nonlinear operator and $\boldsymbol{X}_h^n \in \mathbb{R}^m$, $m \geq 1$, is the unknown vector of degrees of freedom. We employ any semismooth linearization procedure starting from an initial guess $\boldsymbol{X}_h^{n,0} \in \mathbb{R}^m$ and giving at each step $k \geq 1$ the system of linear algebraic equations

$$\mathbb{A}^{n,k-1} \boldsymbol{X}_h^{n,k} = \boldsymbol{F}^{n,k-1}, \tag{1.4}$$

where the matrix $\mathbb{A}^{n,k-1} \in \mathbb{R}^{m,m}$ and the vector $\boldsymbol{F}^{n,k-1} \in \mathbb{R}^m$ are constructed from $\boldsymbol{X}_h^{n,k-1} \in \mathbb{R}^m$. Solving (1.4) with a direct method may be very expensive. A popular approach is to employ an inexact algebraic solver giving at each iterative linear algebraic step $i \geq 0$ and each linearization step $k \geq 1$ a residual vector $\boldsymbol{R}_h^{n,k,i} \in \mathbb{R}^m$ defined by

$$\boldsymbol{R}_h^{n,k,i} := \boldsymbol{F}^{n,k-1} - \mathbb{A}^{n,k-1} \boldsymbol{X}_h^{n,k,i}. \tag{1.5}$$

In the present work, we focus on answering the following questions: To which precision should (1.4) be solved? To which precision should (1.3) be resolved? Can we estimate the total error, as well as each error component (discretization, linearization, algebraic) of the overall numerical approximation? Can we reduce the typical number of iterations of both linearization and algebraic solvers?

Our key tool to propose answers to the above questions is the a posteriori error analysis. A huge amount of work has been performed in the recent past on a posteriori error estimates for partial differential equations. We can mention the pioneering work of Prager and Synge [32], Babuška and Rheinboldt [33], Ainsworth and Oden [34], and Verfürth [35] for a general introduction. For elliptic variational inequalities, we can mention the contributions [36, 37, 38, 15, 11, 12, 13, 18, 20, 39]. In contrast to the last references, in Bürg and Schröder [15] and Dabaghi *et al.* [16], a $\mathbb{P}_p$ conforming finite element discretization, yielding a nonconforming approximation of variational inequalities for $p \geq 2$ are employed. In [16], three components of the error are distinguished: the discretization error, the semismooth linearization error, and the iterative algebraic error.

In the context of parabolic problems, a posteriori analysis has received significant attention over the past decade. For parabolic equations, we mention Verfürth [40], Bernardi, Bergham, and Mghazli [41], and Ern, Smears, and Vohralík [42, 43], where in particular in [42], local efficiency in space and in time for the estimators is proven. For parabolic variational inequalities, the edifice seems still under construction. We

can mention Moon, Nochetto, Petersdorff, and Zhang [44] for a study of the Black–Scholes model, Achdou, Hecht, and Pommier [7] for a study of the parabolic obstacle problem, and Gimperlein and Stocek [45] for a large variety of parabolic variational inequalities. In the present work, we follow the methodology of [42] and [16] to derive a posteriori error estimates for a parabolic variational inequality with distinction of each component of the error. In particular, this enables us to define adaptive stopping criteria for nonlinear semismooth and linear algebraic solvers, which is new to the best of our knowledge. Importantly, it enables to save many unnecessary iterations.

To exemplify our approach, we consider the system of unsteady parabolic variational inequalities as an extension of the stationary model problem studied in [16]. Two important difficulties arise for the a posteriori analysis in this setting:

1) Denoting by $\boldsymbol{u}_{h\tau}^{k,i} := \left(u_{1h\tau}^{k,i}, u_{2h\tau}^{k,i}\right)$ the space-time numerical approximation, where the indices k, i indicate the presence of inexact linearization and algebraic solvers and where $\boldsymbol{u}_{h\tau}^{k,i}$ is piecewise affine and continuous in time and piecewise polynomial of degree p and continuous for each variable in space, $\boldsymbol{u}_{h\tau}^{k,i}$ is nonconforming in the sense that $\boldsymbol{u}_{h\tau}^{k,i} \notin \boldsymbol{\mathcal{K}}_g^{\mathrm{t}}$. Denoting by $\lambda_{h\tau}^{k,i}$ the discrete counterpart of the Lagrange multiplier λ, the same phenomenon occurs in the sense that $\lambda_{h\tau}^{k,i}$ is not also conforming. 2) We cannot easily provide, as for the parabolic heat equation, an a posteriori upper bound for the time derivative $\left\|\partial_t\left(\boldsymbol{u} - \boldsymbol{u}_{h\tau}^{k,i}\right)\right\|_{[L^2(0,T;H^{-1}(\Omega))]^2}$. To tackle this difficulty at least for $p = 1$ and exact solvers, where we simply denote $\boldsymbol{u}_{h\tau} = \boldsymbol{u}_{h\tau}^{k,i}$, we construct an element $\boldsymbol{z} \in \boldsymbol{\mathcal{K}}_g^{\mathrm{t}}$ such that $\|\boldsymbol{u} - \boldsymbol{z}\|_{\left[L^2(0,T;H_0^1(\Omega))\right]^2}$ is closely linked to $\|\partial_t\left(\boldsymbol{u} - \boldsymbol{u}_{h\tau}\right)\|_{[L^2(0,T;H^{-1}(\Omega))]^2}$ and such that the a posteriori error estimate holds as

$$\|\boldsymbol{u} - \boldsymbol{u}_{h\tau}\|^2_{\left[L^2(0,T;H_0^1(\Omega))\right]^2} + \|\boldsymbol{u} - \boldsymbol{z}\|^2_{\left[L^2(0,T;H_0^1(\Omega))\right]^2} + \|\left(\boldsymbol{u} - \boldsymbol{u}_{h\tau}\right)(\cdot,T)\|^2_{L^2(\Omega)} \leq \left(\eta(\boldsymbol{u}_{h\tau})\right)^2, \tag{1.6}$$

with $\eta(\boldsymbol{u}_{h\tau})$ depending only on the approximate solution $\boldsymbol{u}_{h\tau}$.

This contribution is structured as follows. We first present the model problem, its weak formulation, and its discretization with the backward Euler scheme in time and the conforming $\mathbb{P}_p$ ($p \geq 1$) finite element method in space. In particular, we show that our nonlinear system may be seen as a system of parabolic partial differential equations with complementarity constraints. Then, we present the concept of inexact semismooth Newton methods to solve our system of algebraic inequalities at each time step. Next, we provide the a posteriori analysis following the approach of the equilibrated flux reconstructions. In particular, we derive an a posteriori error estimate for affine finite elements ($p = 1$) at each time step n when the semismooth Newton solver as well as the algebraic iterative solver have converged. Then we can estimate the error as shown in (1.6). We next provide a second a posteriori error estimate, valid for any $p \geq 1$ at each semismooth linearization iteration $k \geq 1$ and at each iterative algebraic solver iteration $i \geq 0$. This estimate only bounds the first component on the left-hand side of (1.6), but distinguishes the different error components, namely the discretization error, the semismooth linearization error, the algebraic error, and the initial error, taking the form

$$\left\|\boldsymbol{u} - \boldsymbol{u}_{h\tau}^{k,i}\right\|_{\left[L^2(0,T;H_0^1(\Omega))\right]^2} \leq \eta(\boldsymbol{u}_{h\tau}^{k,i}) \leq \eta_{\mathrm{disc}}^{k,i} + \eta_{\mathrm{lin}}^{k,i} + \eta_{\mathrm{alg}}^{k,i} + \eta_{\mathrm{init}}.$$

This lead us to a proposition of an adaptive inexact semismooth Newton algorithm for parabolic problems. Finally, we present numerical experiments when $p = 1$ with the Newton-min algorithm as well as with the Newton–Fischer–Burmeister algorithm in combination with the GMRES algebraic solver, assessing the strengths of our approach.

2 Model problem and setting

Let $\Omega \subset \mathbb{R}^2$ be a polygonal domain and $T > 0$ be the final simulation time. The model problem we consider here is to find u_1, u_2, and λ such that

$$\begin{cases} \partial_t u_1 - \mu_1 \Delta u_1 - \lambda = f_1 & \text{in} \quad \Omega \times]0,T[\\ \partial_t u_2 - \mu_2 \Delta u_2 + \lambda = f_2 & \text{in} \quad \Omega \times]0,T[\\ (u_1 - u_2)\lambda = 0, \quad u_1 - u_2 \geq 0, \quad \lambda \geq 0 & \text{in} \quad \Omega \times]0,T[\\ u_1 = g & \text{on} \quad \partial\Omega \times]0,T[\\ u_2 = 0 & \text{on} \quad \partial\Omega \times]0,T[\\ u_1(0) = u_1^0, \ u_2(0) = u_2^0, \ u_1^0 - u_2^0 \geq 0 & \text{in} \quad \Omega \end{cases} \tag{2.1}$$

Here, the real coefficients μ_1 and μ_2 are supposed constant and strictly positive, and, for the sake of simplicity, we assume that the Dirichlet boundary condition $g > 0$ is also a constant. The source term $\boldsymbol{f} := (f_1, f_2)$ is supposed to belong to $\left[L^2(0,T;L^2(\Omega))\right]^2$. Finally, the initial conditions are supposed to satisfy $\boldsymbol{u}^0 := \left(u_1^0, u_2^0\right) \in H_g^1(\Omega) \times H_0^1(\Omega)$ and $u_1^0 - u_2^0 \geq 0$ a.e. in Ω. The two first equations of (2.1) are of parabolic type. The third line of (2.1) states linear complementarity conditions expressing that either $u_1 - u_2 = 0$ and $\lambda > 0$, or $u_1 - u_2 > 0$ and $\lambda = 0$. Observe that when $u_1 - u_2 > 0$ and $\lambda = 0$ everywhere in $\Omega \times]0,T[$, problem (2.1) is equivalent to solving two separated heat equations. On the other hand, when f_1 and f_2 are independent of time and $\partial_t u_1 = \partial_t u_2 = 0$, (2.1) becomes the stationary contact problem between two membranes studied in [14, 46, 47, 16].

We define the sets

$$\Lambda := \left\{\chi \in L^2(\Omega), \ \chi \geq 0 \text{ a.e. in } \Omega\right\} \quad \text{and} \quad \Psi := L^2(0,T;\Lambda).$$

We also introduce the nonempty closed convex set

$$\boldsymbol{\mathcal{K}}_g := \left\{(v_1, v_2) \in H_g^1(\Omega) \times H_0^1(\Omega), \ v_1 - v_2 \geq 0 \text{ a.e. in } \Omega\right\}, \tag{2.2}$$

as well as its evolutive-in-time version $\boldsymbol{\mathcal{K}}_g^{\mathrm{t}}$ defined by (1.1). Note that since $(g,0) \in L^2(0,T;H_g^1(\Omega)) \times L^2(0,T;H_0^1(\Omega))$, $\boldsymbol{\mathcal{K}}_g^{\mathrm{t}}$ is nonempty. The compact notations

$$a(\boldsymbol{u},\boldsymbol{v}) := \sum_{\alpha=1}^{2} \mu_\alpha \left(\boldsymbol{\nabla} u_\alpha, \boldsymbol{\nabla} v_\alpha\right)_\Omega, \quad b(\boldsymbol{v},\chi) := (\chi, v_1 - v_2)_\Omega \tag{2.3}$$

will be useful henceforth, where $\boldsymbol{u} = (u_1, u_2)$, $\boldsymbol{v} = (v_1, v_2)$, a is continuous and coercive as described in the introduction, and b is a continuous bilinear form on $\left[H^1(\Omega)\right]^2 \times L^2(\Omega)$.

The weak formulation of problem (2.1) is given by the parabolic variational inequality (1.2) and it is well-posed. To illustrate the construction of the numerical discretization in Section 3 below, let us also mention that alternatively, one could look for $(u_1, u_2, \lambda) \in L^2(0,T;H_g^1(\Omega)) \times L^2(0,T;H_0^1(\Omega)) \times \Psi$ such that $\partial_t u_\alpha \in L^2(0,T;H^{-1}(\Omega))$, $\alpha = 1,2$, and satisfying for almost all $t \in]0,T[$ and for all $(v_1, v_2, \chi) \in H_0^1(\Omega) \times H_0^1(\Omega) \times \Lambda$

$$\begin{aligned} &\sum_{\alpha=1}^{2} \langle \partial_t u_\alpha(t), v_\alpha \rangle + \sum_{\alpha=1}^{2} \mu_\alpha \left(\boldsymbol{\nabla} u_\alpha(t), \boldsymbol{\nabla} v_\alpha\right)_\Omega - \left(\lambda(t), v_1 - v_2\right)_\Omega = \sum_{\alpha=1}^{2} \left(f_\alpha(t), v_\alpha\right)_\Omega, \\ &\left(\chi - \lambda(t), u_1(t) - u_2(t)\right)_\Omega \geq 0, \\ &\boldsymbol{u}(0) = \boldsymbol{u}^0. \end{aligned} \tag{2.4}$$

The second line in (2.4) can also be interpreted as a linear complementarity constraint, cf. a derivation in the case of a stationary problem in [47, 16], reading as

$$\left(u_1 - u_2\right)(t) \geq 0, \quad \lambda(t) \geq 0, \quad \lambda(t)\left(u_1 - u_2\right)(t) = 0. \tag{2.5}$$

Finally, standard notations $\boldsymbol{\nabla}$ and $\boldsymbol{\nabla}\cdot$ are used respectively for the weak gradient and divergence operators. For a nonempty set $\mathcal{O}$ of $\mathbb{R}^2$, we denote its Lebesgue measure by $|\mathcal{O}|$ and the $L^2(\mathcal{O})$ scalar product for

$u, v \in L^2(\mathcal{O})$ by $(u,v)_{\mathcal{O}} := \int_{\mathcal{O}} uv \,\mathrm{dx}$. We also use the notations $\|v\|_{\mathcal{O}}^2 := (v,v)_{\mathcal{O}}$, $\|\boldsymbol{w}\|_{\mathcal{O}}^2 := \sum_{\alpha=1,2} \|w_\alpha\|_{\mathcal{O}}^2$ for $\boldsymbol{w} = (w_1, w_2) \in [L^2(\mathcal{O})]^2$, and $\|\boldsymbol{\nabla} v\|_{\mathcal{O}}^2 := (\boldsymbol{\nabla} v, \boldsymbol{\nabla} v)_{\mathcal{O}}$. Then, we define the space energy norm:

$$\forall \boldsymbol{v} = (v_1, v_2) \in [H_0^1(\mathcal{O})]^2, \quad |||\boldsymbol{v}|||_{\mathcal{O}} := \left\{ \sum_{\alpha=1}^{2} \mu_\alpha \, \|\boldsymbol{\nabla} v_\alpha\|_{\mathcal{O}}^2 \right\}^{\frac{1}{2}}. \tag{2.6}$$

For a function $\boldsymbol{v} = (v_1, v_2) \in [L^2(0,T; H_0^1(\Omega))]^2$, we then define the space-time energy norm by

$$|||\boldsymbol{v}|||_{\Omega,T} := \left\{ \int_0^T |||\boldsymbol{v}|||_{\Omega}^2 (t) \,\mathrm{dt} \right\}^{\frac{1}{2}}. \tag{2.7}$$

3 Discretization and semismooth Newton linearization

The discretization relies on the backward Euler scheme in time and on the conforming finite element method of degree $p \geq 1$ in space.

3.1 Setting

For the time discretization, we introduce a division of the interval $[0,T]$ into subintervals $I_n := [t_{n-1}, t_n]$, $1 \leq n \leq N_{\mathrm{t}}$, such that $0 = t_0 < t_1 < \cdots < t_{N_{\mathrm{t}}} = T$. The time steps are denoted by $\Delta t_n = t_n - t_{n-1}$, $n = 1, \cdots, N_{\mathrm{t}}$. For the space discretization, we consider a conforming simplicial mesh $\mathcal{T}_h$ of the domain Ω, *i.e.*, $\mathcal{T}_h$ is a set of triangles K verifying

$$\bigcup_{K \in \mathcal{T}_h} \overline{K} = \overline{\Omega},$$

where the intersection of the closure of two elements of $\mathcal{T}_h$ is either an empty set, a vertex, or an edge. The set of vertices of $\mathcal{T}_h$ is denoted by $\mathcal{V}_h$ and is partitioned into interior vertices $\mathcal{V}_h^{\mathrm{int}}$ and boundary vertices $\mathcal{V}_h^{\mathrm{ext}}$. We denote by $\mathcal{N}_h^{\mathrm{int}}$ the number of interior vertices. The vertices of an element $K \in \mathcal{T}_h$ are collected in the set $\mathcal{V}_K$. Denote by h_K the diameter of a triangle K and $h := \max_{K \in \mathcal{T}_h} h_K$. Furthermore, for the vertex $\boldsymbol{a} \in \mathcal{V}_h$, let the patch $\omega_h^{\boldsymbol{a}} \subset \Omega$ be the domain made up of the elements of $\mathcal{T}_h$ that share $\boldsymbol{a}$. The vector $\mathbf{n}_{\omega_h^{\boldsymbol{a}}}$ stands for its outward unit normal. In the sequel, we use the discrete conforming space of piecewise polynomial and continuous functions

$$X_h^p := \left\{ v_h \in \mathcal{C}^0(\overline{\Omega});\ v_h|_K \in \mathbb{P}_p(K) \ \ \forall K \in \mathcal{T}_h \right\} \subset H^1(\Omega),$$

where $\mathbb{P}_p(K)$ stands for the set of polynomials of total degree less than or equal to p on the element K. We also denote by $\mathcal{V}_{\mathrm{d}}^p$ the set of the Lagrange nodes of the space X_h^p and by $\mathcal{N}_{\mathrm{d}}^p$ its cardinality. The internal degrees of freedom are collected in the set $\mathcal{V}_{\mathrm{d}}^{p,\mathrm{int}}$ whose cardinality is $\mathcal{N}_{\mathrm{d}}^{p,\mathrm{int}}$, and the boundary ones are collected in the set $\mathcal{V}_{\mathrm{d}}^{p,\mathrm{ext}}$. The Lagrange basis functions of X_h^p are denoted by $(\psi_{h,\boldsymbol{x}_l})_{1 \leq l \leq \mathcal{N}_{\mathrm{d}}^p}$ for $\boldsymbol{x}_l \in \mathcal{V}_{\mathrm{d}}^p$. We recall that $\psi_{h,\boldsymbol{x}_l}(\boldsymbol{x}_l) = 1$ for all $\boldsymbol{x}_l \in \mathcal{V}_{\mathrm{d}}^p$ and $\psi_{h,\boldsymbol{x}_l}(\boldsymbol{x}_{l'}) = 0$ for all $(\boldsymbol{x}_{l'})_{1 \leq l' \neq l \leq \mathcal{N}_{\mathrm{d}}^p} \in \mathcal{V}_{\mathrm{d}}^p$. In the particular case $p = 1$, the set $\mathcal{V}_{\mathrm{d}}^1$ coincides with $\mathcal{V}_h$ and the Lagrange basis functions are the "hat" basis functions that are denoted by $\psi_{h,\boldsymbol{a}}$, $\boldsymbol{a} \in \mathcal{V}_h$. Still in this case, we denote $M_{\boldsymbol{a}} := (\psi_{h,\boldsymbol{a}}, 1)_{\omega_h^{\boldsymbol{a}}} = \frac{|\omega_h^{\boldsymbol{a}}|}{3}$. We also introduce the boundary-aware set and space

$$X_{gh}^p := \{ v_h \in X_h^p,\ v_h = g \text{ on } \partial\Omega \} \subset H_g^1(\Omega), \quad X_{0h}^p := X_h^p \cap H_0^1(\Omega),$$

and the convex set

$$\boldsymbol{\mathcal{K}}_{gh}^p := \left\{ (v_{1h}, v_{2h}) \in X_{gh}^p \times X_{0h}^p,\ v_{1h}(\boldsymbol{x}_l) - v_{2h}(\boldsymbol{x}_l) \geq 0 \ \ \forall (\boldsymbol{x}_l)_{1 \leq l \leq \mathcal{N}_{\mathrm{d}}^p} \in \mathcal{V}_{\mathrm{d}}^p \right\}. \tag{3.1}$$

Recall the defintion (2.2) and observe that $\boldsymbol{\mathcal{K}}_{gh}^1 \subset \boldsymbol{\mathcal{K}}_g$ holds in the case $p = 1$ but $\boldsymbol{\mathcal{K}}_{gh}^p \not\subset \boldsymbol{\mathcal{K}}_g$ for $p \geq 2$, see [11, 12, 14, 16]. For $\alpha = 1, 2$, let us introduce the piecewise constant in time functions $\tilde{f}_\alpha \in L^2(0,T; L^2(\Omega))$ such that

$$(\tilde{f}_\alpha)|_{I_n} := \frac{1}{\Delta t_n} \int_{I_n} f_\alpha(t) \,\mathrm{dt}, \quad \text{and denote } \tilde{f}_\alpha^n := (\tilde{f}_\alpha)|_{I_n} \in L^2(\Omega),\ \tilde{\boldsymbol{f}} := \left(\tilde{f}_1, \tilde{f}_2\right),\ \tilde{\boldsymbol{f}}^n := \left(\tilde{f}_1^n, \tilde{f}_2^n\right). \tag{3.2}$$

3.2 Discrete reduced problem and discrete saddle-point problem

Let

$$c_n(\boldsymbol{u}_h^n, \boldsymbol{v}_h) := \frac{1}{\Delta t_n} \sum_{\alpha=1}^{2} (u_{\alpha h}^n, v_{\alpha h})_\Omega, \quad 1 \le n \le N_\mathrm{t}.$$

Given $\boldsymbol{u}_h^0 \in \boldsymbol{\mathcal{K}}_{gh}^p$, the discrete reduced problem corresponding to (1.2) consists in searching for all $1 \le n \le N_\mathrm{t}$ $\boldsymbol{u}_h^n \in \boldsymbol{\mathcal{K}}_{gh}^p$ such that for all $\boldsymbol{v}_h \in \boldsymbol{\mathcal{K}}_{gh}^p$

$$c_n\left(\boldsymbol{u}_h^n - \boldsymbol{u}_h^{n-1}, \boldsymbol{v}_h - \boldsymbol{u}_h^n\right) + a(\boldsymbol{u}_h^n, \boldsymbol{v}_h - \boldsymbol{u}_h^n) \ge \left(\tilde{\boldsymbol{f}}^n, \boldsymbol{v}_h - \boldsymbol{u}_h^n\right)_\Omega. \tag{3.3}$$

Following the Lions–Stampacchia theorem [48], we have:

Proposition 1. *The discrete problem (3.3) admits a unique solution.*

Recall that when $p \ge 2$, $\boldsymbol{u}_h^n$ is typically nonconforming in the sense that $\boldsymbol{u}_h^n \notin \boldsymbol{\mathcal{K}}_g$. Moreover, following the methodology of [16, 14, 18, 15], knowing $\boldsymbol{u}_h^n$, the solution to (3.3), we define for $1 \le n \le N_\mathrm{t}$ and for all $\alpha = 1, 2$ the functions $\lambda_{\alpha h}^n \in X_h^p$ by

$$\begin{aligned} &\langle \lambda_{\alpha h}^n, z_{\alpha h} \rangle_h := (-1)^\alpha \left[-\frac{1}{\Delta t_n} \left(u_{\alpha h}^n - u_{\alpha h}^{n-1}, z_{\alpha h}\right)_\Omega - \mu_\alpha \left(\boldsymbol{\nabla} u_{\alpha h}^n, \boldsymbol{\nabla} z_{\alpha h}\right)_\Omega + \left(\tilde{f}_\alpha^n, z_{\alpha h}\right)_\Omega \right] \quad \forall z_{\alpha h} \in X_{0h}^p, \\ &\langle \lambda_{\alpha h}^n, \psi_{h,\boldsymbol{x}_l} \rangle_h := 0 \quad \forall \boldsymbol{x}_l \in \mathcal{V}_\mathrm{d}^{p,\mathrm{ext}}, \end{aligned} \tag{3.4}$$

where for all $(w_h, v_h) \in X_h^p \times X_h^p$,

$$\langle w_h, v_h \rangle_h := \sum_{\boldsymbol{a} \in \mathcal{V}_h} w_h(\boldsymbol{a}) v_h(\boldsymbol{a}) M_{\boldsymbol{a}} \quad \text{if} \quad p = 1, \quad \text{and} \quad \langle w_h, v_h \rangle_h := (w_h, v_h)_\Omega \quad \text{if} \quad p \ge 2.$$

Lemma 3.1. *Let $1 \le n \le N_\mathrm{t}$ be a time step and $(u_{1h}^n, u_{2h}^n) \in \boldsymbol{\mathcal{K}}_{gh}^p$ be the solution of the reduced discrete problem (3.3). Then, the functions λ_{1h}^n and λ_{2h}^n defined by (3.4) coincide.*

Proof. From (3.4) and taking $z_{1h} = z_{2h} = \psi_{h,\boldsymbol{x}_l}$ with $\boldsymbol{x}_l$ any internal Lagrange node, we get

$$\langle \lambda_{1h}^n - \lambda_{2h}^n, \psi_{h,\boldsymbol{x}_l} \rangle_h = \frac{1}{\Delta t_n} \sum_{\alpha=1}^{2} \left[\left(u_{\alpha h}^n - u_{\alpha h}^{n-1}, \psi_{h,\boldsymbol{x}_l}\right)_\Omega + \left(\mu_\alpha \boldsymbol{\nabla} u_{\alpha h}^n, \boldsymbol{\nabla} \psi_{h,\boldsymbol{x}_l}\right)_\Omega \right] - \left(\tilde{f}_1^n + \tilde{f}_2^n, \psi_{h,\boldsymbol{x}_l}\right)_\Omega.$$

Taking $v_{1h} := u_{1h}^n + \psi_{h,\boldsymbol{x}_l}$ and $v_{2h} := u_{2h}^n + \psi_{h,\boldsymbol{x}_l}$ so that $(v_{1h}, v_{2h}) \in \boldsymbol{\mathcal{K}}_{gh}^p$, we see

$$\langle \lambda_{1h}^n - \lambda_{2h}^n, \psi_{h,\boldsymbol{x}_l} \rangle_h \ge 0 \quad \forall l = 1 \ldots \mathcal{N}_\mathrm{d}^{p,\mathrm{int}}. \tag{3.5}$$

In the same way, taking $v_{1h} := u_{1h}^n - \psi_{h,\boldsymbol{x}_l}$ and $v_{2h} := u_{2h}^n - \psi_{h,\boldsymbol{x}_l}$, we have $(v_{1h}, v_{2h}) \in \boldsymbol{\mathcal{K}}_{gh}^p$ and we get

$$\langle \lambda_{1h}^n - \lambda_{2h}^n, \psi_{h,\boldsymbol{x}_l} \rangle_h \le 0 \quad \forall l = 1 \ldots \mathcal{N}_\mathrm{d}^{p,\mathrm{int}}. \tag{3.6}$$

The conclusion follows the last lines of [16, Lemma 2.1]. □

Following Lemma 3.1, we can set $\lambda_h^n := \lambda_{1h}^n = \lambda_{2h}^n \in X_h^p$. Moreover, λ_h^n satisfies the following property:

Lemma 3.2. *Let $1 \le n \le N_\mathrm{t}$, let $(u_{1h}^n, u_{2h}^n) \in \boldsymbol{\mathcal{K}}_{gh}^p$ be the solution of the reduced discrete problem (3.3), and let λ_h^n be defined by (3.4). Then, there holds*

$$\langle \lambda_h^n, \psi_{h,\boldsymbol{x}_l} \rangle_h \ge 0 \quad \forall \boldsymbol{x}_l \in \mathcal{V}_\mathrm{d}^{p,\mathrm{int}}.$$

Proof. For $\boldsymbol{x}_l \in \mathcal{V}_\mathrm{d}^{p,\mathrm{int}}$, observe that $(v_{1h}, v_{2h}) := (u_{1h}^n + \psi_{h,\boldsymbol{x}_l}, u_{2h}^n) \in \boldsymbol{\mathcal{K}}_{gh}^p$. Using the reduced problem (3.3), the characterization (3.4) with $z_{1h} = \psi_{h,\boldsymbol{x}_l} \in X_{0h}^p$, and Lemma 3.1, we get for all $l = 1 \ldots \mathcal{N}_\mathrm{d}^{p,\mathrm{int}}$

$$\frac{1}{\Delta t_n} \left(u_{1h}^n - u_{1h}^{n-1}, \psi_{h,\boldsymbol{x}_l}\right)_\Omega + \mu_1 \left(\boldsymbol{\nabla} u_{1h}^n, \boldsymbol{\nabla} \psi_{h,\boldsymbol{x}_l}\right)_\Omega - \left(\tilde{f}_1^n, \psi_{h,\boldsymbol{x}_l}\right)_\Omega = \langle \lambda_h, \psi_{h,\boldsymbol{x}_l} \rangle_h \ge 0.$$

□

Following Lemma 3.2 we suggest the following definition for the discrete convex set associated to λ_h^n

Definition 3.3. *Let, for all $p \geq 1$,*

$$\Lambda_h^p := \left\{ v_h \in X_h^p;\ \langle v_h, \psi_{h,\boldsymbol{x}_l} \rangle_h \geq 0\ \forall \boldsymbol{x}_l \in \mathcal{V}_{\mathrm{d}}^{p,\mathrm{int}},\ \langle v_h, \psi_{h,\boldsymbol{x}_l} \rangle_h = 0\ \forall \boldsymbol{x}_l \in \mathcal{V}_{\mathrm{d}}^{p,\mathrm{ext}} \right\}. \tag{3.7}$$

Remark 3.4. *Observe that $\Lambda_h^p \not\subset \Lambda$ for $p \geq 2$. In the case $p = 1$, Λ_h^p reduces to*

$$\Lambda_h^1 = \left\{ v_h \in X_{0h}^1;\ v_h(\boldsymbol{a}) \geq 0 \quad \forall \boldsymbol{a} \in \mathcal{V}_h^{\mathrm{int}} \right\} \subset \Lambda. \tag{3.8}$$

For $p = 1$, the construction above provides the positivity of the discrete Lagrange multiplier λ_h^n in internal vertices of the mesh. In the case $p \geq 2$, the positivity of $\lambda_h^n \in \Lambda_h^p$ only holds in a weak sense, which will in particular allow for the equivalence stated in Lemma 3.5 below. We also note that for any $\chi_h^n \in \Lambda_h^p$ and any $\boldsymbol{v}_h \in \boldsymbol{\mathcal{K}}_{gh}^p$,

$$\langle \chi_h^n, v_{1h}^n - v_{2h}^n \rangle_h = \sum_{\boldsymbol{x}_l \in \mathcal{V}_{\mathrm{d}}^{p,\mathrm{int}}} (v_{1h}^n - v_{2h}^n)(\boldsymbol{x}_l) \langle \chi_h^n, \psi_{h,\boldsymbol{x}_l} \rangle_h \geq 0. \tag{3.9}$$

It will be useful to also consider the discrete formulation corresponding to problem (2.4). Given $\left(u_{1h}^0, u_{2h}^0\right) \in \boldsymbol{\mathcal{K}}_{gh}^p$, it consists, for each $n = 1 \cdots N_{\mathrm{t}}$, in searching $(u_{1h}^n, u_{2h}^n, \lambda_h^n) \in X_{gh}^p \times X_{0h}^p \times \Lambda_h^p$ such that for all $(z_{1h}, z_{2h}, \chi_h) \in X_{0h}^p \times X_{0h}^p \times \Lambda_h^p$,

$$\begin{aligned} &\frac{1}{\Delta t_n} \sum_{\alpha=1}^{2} \left(u_{\alpha h}^n - u_{\alpha h}^{n-1}, z_{\alpha h} \right)_\Omega + \sum_{\alpha=1}^{2} \mu_\alpha \left(\boldsymbol{\nabla} u_{\alpha h}^n, \boldsymbol{\nabla} z_{\alpha h} \right)_\Omega - \langle \lambda_h^n, z_{1h} - z_{2h} \rangle_h = \sum_{\alpha=1}^{2} \left(\tilde{f}_\alpha^n, z_{\alpha h} \right)_\Omega, \\ &\langle \chi_h - \lambda_h^n, u_{1h}^n - u_{2h}^n \rangle_h \geq 0. \end{aligned} \tag{3.10}$$

Let us also construct the basis $(\Theta_{h,\boldsymbol{x}_l})_{1 \leq l \leq \mathcal{N}_{\mathrm{d}}^p}$ of X_h^p, dual to $(\psi_{h,\boldsymbol{x}_l})_{1 \leq l \leq \mathcal{N}_{\mathrm{d}}^p}$, satisfying

$$\begin{aligned} &\langle \Theta_{h,\boldsymbol{x}_l}, \psi_{h,\boldsymbol{x}_l} \rangle_h = 1 \quad \forall \boldsymbol{x}_l \in \mathcal{V}_{\mathrm{d}}^p, \\ &\left\langle \Theta_{h,\boldsymbol{x}_l}, \psi_{h,\boldsymbol{x}_l^*} \right\rangle_h = 0 \quad \forall \boldsymbol{x}_{l^*} \in \mathcal{V}_{\mathrm{d}}^p,\ \boldsymbol{x}_{l^*} \neq \boldsymbol{x}_l, \end{aligned} \tag{3.11}$$

as in [16]. Note that each vector $\Theta_{h,\boldsymbol{x}_l}$ of the dual basis can be determined by inverting a diagonal (lumped mass) matrix for $p = 1$ and the finite element mass matrix for $p \geq 2$; importantly, all $\Theta_{h,\boldsymbol{x}_l}$, $1 \leq l \leq \mathcal{N}_{\mathrm{d}}^{p,\mathrm{int}}$, belong to Λ_h^p. Note also that the support of $\Theta_{h,\boldsymbol{x}_l}$ is typically not local. We can now link formulations (3.3) and (3.10):

Lemma 3.5. *Let $1 \leq n \leq N_{\mathrm{t}}$ be a time step. For any solution $(u_{1h}^n, u_{2h}^n, \lambda_h^n)$ of problem (3.10), the pair (u_{1h}^n, u_{2h}^n) is a solution of problem (3.3). Conversely, for any solution (u_{1h}^n, u_{2h}^n) of problem (3.3), defining the function $\lambda_h^n = \lambda_{\alpha h}^n$, $\alpha = 1, 2$, by (3.4), the triple $(u_{1h}^n, u_{2h}^n, \lambda_h^n)$ is a solution to problem (3.10).*

Proof. For the case $p = 1$, the proof is a direct extension of [46, Lemma 13] and for $p \geq 2$ it employs the arguments of [16, Lemma 2.3]. Let $p \geq 1$ and let $(u_{1h}^n, u_{2h}^n, \lambda_h^n)$ be the solution of problem (3.10). The first lines of [16, Lemma 2.3] prove that the discrete vector $\boldsymbol{u}_h^n$ is an element of $\boldsymbol{\mathcal{K}}_{gh}^p$. Now, we prove (3.3). Let $(v_{1h}, v_{2h}) \in \boldsymbol{\mathcal{K}}_{gh}^p$. Taking $z_{1h} := v_{1h} - u_{1h}^n \in X_{0h}^p$ and $z_{2h} := v_{2h} - u_{2h}^n \in X_{0h}^p$ as test functions in (3.10) provides

$$\langle \lambda_h^n, v_{1h} - v_{2h} \rangle_h - \langle \lambda_h^n, u_{1h}^n - u_{2h}^n \rangle_h = a(\boldsymbol{u}_h^n, \boldsymbol{v}_h - \boldsymbol{u}_h^n) - \left(\tilde{\boldsymbol{f}}^n, \boldsymbol{v}_h - \boldsymbol{u}_h^n \right)_\Omega + c_n \left(\boldsymbol{u}_h^n - \boldsymbol{u}_h^{n-1}, \boldsymbol{v}_h - \boldsymbol{u}_h^n \right). \tag{3.12}$$

Using (3.9) with $\lambda_h^n \in \Lambda_h^p$ and $\boldsymbol{v}_h \in \boldsymbol{\mathcal{K}}_{gh}^p$ and taking $\chi_h = 0 \in \Lambda_h^p$ in (3.10) gives

$$\langle \lambda_h^n, v_{1h} - v_{2h} \rangle_h \geq 0, \quad \langle -\lambda_h^n, u_{1h}^n - u_{2h}^n \rangle_h \geq 0. \tag{3.13}$$

Combining (3.12) and (3.13) provides (3.3).

Conversely, let $(u_{1h}^n, u_{2h}^n) \in \boldsymbol{\mathcal{K}}_{gh}^p$ be the solution of the reduced problem (3.3) and let $(z_{1h}, z_{2h}) \in X_{0h}^p \times X_{0h}^p$ be arbitrary. The Lagrange multiplier λ_h^n defined by (3.4) combined with Lemma 3.1 and Lemma 3.2 yields $\lambda_h^n \in \Lambda_h^p$. Next, considering the first line of (3.4) with $\alpha = 1, 2$ and subtracting these

equations gives the first line of (3.10). It remains to prove the second line of (3.10). Let now $(v_{1h}, v_{2h}) \in \boldsymbol{\mathcal{K}}_{gh}^p$. The first line in (3.10) now implies (3.12) and the reduced problem (3.3) yields

$$-\langle \lambda_h^n, u_{1h}^n - u_{2h}^n \rangle_h + \langle \lambda_h^n, v_{1h} - v_{2h} \rangle_h \geq 0 \quad \forall\, (v_{1h}, v_{2h}) \in \boldsymbol{\mathcal{K}}_{gh}^p. \tag{3.14}$$

For $v_{1h} := u_{1h}^n - \sum_{\boldsymbol{x}_l \in \mathcal{V}_{\rm d}^{p,\rm int}} u_{1h}(\boldsymbol{x}_l)\psi_{h,\boldsymbol{x}_l} \in X_{gh}^p$ and $v_{2h} := 0 \in X_{0h}^p$, $(v_{1h}, v_{2h}) \in \boldsymbol{\mathcal{K}}_{gh}^p$, and using the definition of Λ_h^p, we have $\langle \lambda_h^n, v_{1h} - v_{2h} \rangle_h = 0$ and the inequality (3.14) yields $-\langle \lambda_h^n, u_{1h}^n - u_{2h}^n \rangle_h \geq 0$. To conclude the proof, we use (3.9) with $\boldsymbol{u}_h^n \in \boldsymbol{\mathcal{K}}_{gh}^p$ and for any $\chi_h \in \Lambda_h^p$. □

As a consequence of Lemma 3.5 and Proposition 1, problem (3.10) is well-posed and admits a unique weak solution for each $n = 1, \cdots, N_{\rm t}$. We finish this section by the following remark:

Remark 3.6. *Taking in* (3.10) $\chi_h = 0$ *and next* $\chi_h = 2\lambda_h^n \in \Lambda_h^p$ *gives* $\langle \lambda_h^n, u_{1h}^n - u_{2h}^n \rangle_h = 0$. *As* $\boldsymbol{u}_h^n \in \boldsymbol{\mathcal{K}}_{gh}^p$ *and* $\lambda_h^n \in \Lambda_h^p$, *we obtain a discrete equivalent of the complementarity condition* (2.5) *valid for all polynomial degrees* $p \geq 1$:

$$\begin{array}{l} (u_{1h}^n - u_{2h}^n)(\boldsymbol{x}_l) \geq 0 \ \forall \boldsymbol{x}_l \in \mathcal{V}_{\rm d}^{p,\rm int}, \langle \lambda_h^n, \psi_{h,\boldsymbol{x}_l} \rangle_h \geq 0, \ \forall \boldsymbol{x}_l \in \mathcal{V}_{\rm d}^{p,\rm int}, \langle \lambda_h^n, \psi_{h,\boldsymbol{x}_l} \rangle_h = 0 \ \forall \boldsymbol{x}_l \in \mathcal{V}_{\rm d}^{p,\rm ext}, \\ \langle \lambda_h^n, u_{1h}^n - u_{2h}^n \rangle_h = 0. \end{array} \tag{3.15}$$

3.3 Numerical resolution and discrete complementarity constraints

Let n be fixed in $\{1, \ldots, N_{\rm t}\}$. We write in an algebraic form the discrete problem (3.10), using the expression (3.15) for the constraints. We employ the subset $(\Theta_{h,\boldsymbol{x}_l})_{1 \leq l \leq \mathcal{N}_{\rm d}^{p,\rm int}}$ of the basis $(\Theta_{h,\boldsymbol{x}_l})_{1 \leq l \leq \mathcal{N}_{\rm d}^{p}}$ of Λ_h^p, dual to $(\psi_{h,\boldsymbol{x}_l})_{1 \leq l \leq \mathcal{N}_{\rm d}^{p,\rm int}}$ in the sense of (3.11). For the first component of the discrete solution $u_{1h}^n \in X_{gh}^p$, we use the lifting $u_{1h}^n = u_{1h}^{*,n} + g$ where $u_{1h}^{*,n} \in X_{0h}^p$ and $g > 0$ is the constant boundary value. The algebraic representation of the lifting is denoted by $\boldsymbol{X}_{1h}^n \in \mathbb{R}^{\mathcal{N}_{\rm d}^{p,\rm int}}$, so that

$$u_{1h}^n = \sum_{l=1}^{\mathcal{N}_{\rm d}^{p,\rm int}} (\boldsymbol{X}_{1h}^n)_l \, \psi_{h,\boldsymbol{x}_l} + g \quad \text{where} \quad (\boldsymbol{X}_{1h}^n)_l = u_{1h}^{*,n}(\boldsymbol{x}_l). \tag{3.16}$$

The second component of the discrete solution u_{2h}^n is expressed in the Lagrange basis $(\psi_{h,\boldsymbol{x}_l})_{1 \leq l \leq \mathcal{N}_{\rm d}^{p,\rm int}}$ as

$$u_{2h}^n = \sum_{l=1}^{\mathcal{N}_{\rm d}^{p,\rm int}} (\boldsymbol{X}_{2h}^n)_l \, \psi_{h,\boldsymbol{x}_l} \quad \text{where} \quad (\boldsymbol{X}_{2h}^n)_l = u_{2h}^n(\boldsymbol{x}_l). \tag{3.17}$$

The initial value $\boldsymbol{u}_h^0 \in \boldsymbol{\mathcal{K}}_{gh}^p$ is decomposed in the same way into $(u_{1h}^{*,0} + g, u_{2h}^0)$, and $(u_{1h}^{*,0}, u_{2h}^0) \in [X_{0h}^p]^2$ is represented by $\boldsymbol{X}_h^0 = \left[\boldsymbol{X}_{1h}^0, \boldsymbol{X}_{2h}^0\right]^T \in \mathbb{R}^{2\mathcal{N}_{\rm d}^{p,\rm int}}$. The discrete Lagrange multiplier λ_h^n is decomposed in the basis $(\Theta_{h,\boldsymbol{x}_l})_{1 \leq l \leq \mathcal{N}_{\rm d}^{p}}$ as

$$\lambda_h^n = \sum_{l=1}^{\mathcal{N}_{\rm d}^{p,\rm int}} (\boldsymbol{X}_{3h}^n)_l \, \Theta_{h,\boldsymbol{x}_l} \quad \text{with} \quad \boldsymbol{X}_{3h}^n \in \mathbb{R}^{\mathcal{N}_{\rm d}^{p,\rm int}}, \tag{3.18}$$

because $\lambda_h^n \in \Lambda_h^p$ and thus the components for $\boldsymbol{x}_l \in \mathcal{V}_{\rm d}^{p,\rm ext}$ are 0.

In algebraic form, the first line of (3.10) reads

$$\mathbb{E}_p^n \boldsymbol{X}_h^n = \boldsymbol{F}^n,$$

where $\boldsymbol{X}_h^n := [\boldsymbol{X}_{1h}^n, \boldsymbol{X}_{2h}^n, \boldsymbol{X}_{3h}^n]^T \in \mathbb{R}^{3\mathcal{N}_{\rm d}^{p,\rm int}}$ is the unknown algebraic vector and $\mathbb{E}_p^n \in \mathbb{R}^{2\mathcal{N}_{\rm d}^{p,\rm int}, 3\mathcal{N}_{\rm d}^{p,\rm int}}$ is the rectangular matrix defined by

$$\mathbb{E}_p^n := \begin{bmatrix} \mu_1 \mathbb{S} + \frac{1}{\Delta t_n}\mathbb{M} & \mathbf{0} & -\mathbb{I}_{\rm d} \\ \mathbf{0} & \mu_2 \mathbb{S} + \frac{1}{\Delta t_n}\mathbb{M} & +\mathbb{I}_{\rm d} \end{bmatrix},$$

$\mathbb{I}_{\rm d} \in \mathbb{R}^{\mathcal{N}_{\rm d}^{p,\rm int},\mathcal{N}_{\rm d}^{p,\rm int}}$ is the identity matrix, and the finite element mass matrix $\mathbb{M}$ and the stiffness matrix $\mathbb{S}$ belonging to $\mathbb{R}^{\mathcal{N}_{\rm d}^{p,\rm int},\mathcal{N}_{\rm d}^{p,\rm int}}$ are defined by

$$\mathbb{M}_{l,m} := (\psi_{h,\boldsymbol{x}_l}, \psi_{h,\boldsymbol{x}_m})_\Omega\,, \qquad \mathbb{S}_{l,m} := (\boldsymbol{\nabla}\psi_{h,\boldsymbol{x}_l}, \boldsymbol{\nabla}\psi_{h,\boldsymbol{x}_m})_\Omega\,, \qquad 1 \le l,m \le \mathcal{N}_{\rm d}^{p,\rm int}. \tag{3.19}$$

The right-hand side vector $\boldsymbol{F}^n$ is defined by blocks ($[\boldsymbol{F}^n]^T := [\boldsymbol{F}_1^n, \boldsymbol{F}_2^n]^T$) as

$$(\boldsymbol{F}_\alpha^n)_l := \left(\tilde{f}_\alpha^n + \frac{1}{\Delta t_n} u_{\alpha h}^{n-1}, \psi_{h,\boldsymbol{x}_l}\right)_\Omega \quad 1 \le l \le \mathcal{N}_{\rm d}^{p,\rm int}, \quad \alpha = 1,2. \tag{3.20}$$

With $\mathbf{1} = (1,1,\cdots,1)^T \in \mathbb{R}^{\mathcal{N}_{\rm d}^{p,\rm int}}$, the first complementarity constraint of (3.15) is expressed as

$$\boldsymbol{X}_{1h}^n + g\mathbf{1} - \boldsymbol{X}_{2h}^n \ge 0.$$

Next, using (3.11), the second complementarity constraint of (3.15) is given for any $\boldsymbol{x}_l \in \mathcal{V}_{\rm d}^{p,\rm int}$ by

$$\langle \lambda_h^n, \psi_{h,\boldsymbol{x}_l}\rangle_h = \sum_{l'=1}^{\mathcal{N}_{\rm d}^{p,\rm int}} (\boldsymbol{X}_{3h}^n)_{l'} \left\langle \Theta_{h,\boldsymbol{x}_{l'}}, \psi_{h,\boldsymbol{x}_l}\right\rangle_h = (\boldsymbol{X}_{3h}^n)_l \ge 0.$$

For the last constraint in (3.15), using again (3.11), we get

$$\langle \lambda_h^n, u_{1h}^n - u_{2h}^n\rangle_h = (\boldsymbol{X}_{1h}^n - \boldsymbol{X}_{2h}^n)\cdot \boldsymbol{X}_{3h}^n + g\mathbf{1}\cdot\boldsymbol{X}_{3h}^n. \tag{3.21}$$

Thus, for any $p \ge 1$, problem (3.10) can be written as: given $\boldsymbol{X}_h^0 \in \mathbb{R}^{2\mathcal{N}_{\rm d}^{p,\rm int}}$, for $n = 1,\cdots,N_{\rm t}$, search $\boldsymbol{X}_h^n \in \mathbb{R}^{3\mathcal{N}_{\rm d}^{p,\rm int}}$ such that

$$\begin{aligned} &\mathbb{E}_p^n \boldsymbol{X}_h^n = \boldsymbol{F}^n, \\ &\boldsymbol{X}_{1h}^n + g\mathbf{1} - \boldsymbol{X}_{2h}^n \ge 0, \quad \boldsymbol{X}_{3h}^n \ge 0, \quad (\boldsymbol{X}_{1h}^n + g\mathbf{1} - \boldsymbol{X}_{2h}^n)\cdot \boldsymbol{X}_{3h}^n = 0. \end{aligned} \tag{3.22}$$

Remark 3.7. *Note that $u_{1h}^{*,n}$ and u_{2h}^n are expressed in the Lagrange basis $(\psi_{h,\boldsymbol{x}_l})_{1\le l\le \mathcal{N}_{\rm d}^{p,\rm int}}$, while the discrete lagrange multiplier λ_h^n is expressed in a subset $(\Theta_{h,\boldsymbol{x}_l})_{1\le l\le \mathcal{N}_{\rm d}^{p,\rm int}}$ of the dual basis to $(\psi_{h,\boldsymbol{x}_l})_{1\le l\le \mathcal{N}_{\rm d}^{p}}$. It is also possible to express λ_h^n in the Lagrange basis $(\psi_{h,\boldsymbol{x}_l})_{1\le l\le \mathcal{N}_{\rm d}^{p}}$ of X_h^p, see [49, Sect. 1.2.3]. In such a case, the complementary constraints are expressed with submatrices of the finite element mass matrix and the identity matrix blocks in the matrix $\mathbb{E}_p^n$ are replaced by the mass matrix.*

3.4 Equivalent rewriting using C-functions

We now express the complementarity constraints given by the second line of (3.22) via non-differentiable equations. Let us recall that a function $f : (\mathbb{R}^m)^2 \to \mathbb{R}^m$, $m \ge 1$, is a C-function or a complementarity function, see [29, 30], if

$$\forall (\boldsymbol{x},\boldsymbol{y}) \in (\mathbb{R}^m)^2 \qquad f(\boldsymbol{x},\boldsymbol{y}) = \mathbf{0} \quad \Longleftrightarrow \quad \boldsymbol{x} \ge \mathbf{0}, \quad \boldsymbol{y} \ge \mathbf{0}, \quad \boldsymbol{x}\cdot\boldsymbol{y} = 0.$$

Examples of C-functions are the min and max functions

$$(\min\{\boldsymbol{x},\boldsymbol{y}\})_l := \min\{\boldsymbol{x}_l, \boldsymbol{y}_l\}\,, \quad (\max\{\boldsymbol{x},\boldsymbol{y}\})_l := \max\{\boldsymbol{x}_l,\boldsymbol{y}_l\} \qquad l = 1,\ldots,m, \tag{3.23}$$

the Fischer–Burmeister function

$$(f_{\rm FB}(\boldsymbol{x},\boldsymbol{y}))_l := \sqrt{\boldsymbol{x}_l^2 + \boldsymbol{y}_l^2} - (\boldsymbol{x}_l + \boldsymbol{y}_l) \quad l = 1,\ldots,m, \tag{3.24}$$

or the Mangasarian function

$$(f_{\rm M}(\boldsymbol{x},\boldsymbol{y}))_l := \xi(|\boldsymbol{x}_l - \boldsymbol{y}_l|) - \xi(\boldsymbol{y}_l) - \xi(\boldsymbol{x}_l) \quad l = 1,\ldots,m,$$

where $\xi : \mathbb{R} \mapsto \mathbb{R}$ is an increasing function satisfying $\xi(\mathbf{0}) = \mathbf{0}$. The min function, the max function, the Fischer–Burmeister function, and the Mangasarian function are not Fréchet differentiable everywhere. Let $\tilde{\mathbf{C}}$ be any C-function satisfying for $m = \mathcal{N}_{\rm d}^{p,\rm int}$ $\tilde{\mathbf{C}}(\boldsymbol{X}_{1h}^n + g\mathbf{1} - \boldsymbol{X}_{2h}^n, \boldsymbol{X}_{3h}^n) = 0 \iff \{\boldsymbol{X}_{1h}^n + g\mathbf{1} - \boldsymbol{X}_{2h}^n \geq 0,\ \boldsymbol{X}_{3h}^n \geq 0, \text{ and } (\boldsymbol{X}_{1h}^n + g\mathbf{1} - \boldsymbol{X}_{2h}^n)\cdot\boldsymbol{X}_{3h}^n = 0\}$. Then, introducing the function $\mathbf{C} : \mathbb{R}^{3\mathcal{N}_{\rm d}^{p,\rm int}} \to \mathbb{R}^{\mathcal{N}_{\rm d}^{p,\rm int}}$ defined as $\mathbf{C}(\boldsymbol{X}_h^n) = \tilde{\mathbf{C}}(\boldsymbol{X}_{1h}^n + g\mathbf{1} - \boldsymbol{X}_{2h}^n, \boldsymbol{X}_{3h}^n)$, problem (3.22) can be equivalently rewritten as: given $\boldsymbol{X}_h^0 \in \mathbb{R}^{2\mathcal{N}_{\rm d}^{p,\rm int}}$, for each $n \geq 1$, search $\boldsymbol{X}_h^n \in \mathbb{R}^{3\mathcal{N}_{\rm d}^{p,\rm int}}$ such that

$$\left\{ \begin{array}{ll} \mathbb{E}_p^n \boldsymbol{X}_h^n & = \boldsymbol{F}^n, \\ \mathbf{C}(\boldsymbol{X}_h^n) & = \mathbf{0}. \end{array} \right. \tag{3.25}$$

3.5 Linearization by semismooth Newton methods

Let a time step $n \geq 1$ be fixed and let $\boldsymbol{X}_h^0 \in \mathbb{R}^{2\mathcal{N}_{\rm d}^{p,\rm int}}$ be given. We provide in this section the linearization of system (3.25). Observe that the $2\mathcal{N}_{\rm d}^{p,\rm int}$ first lines of (3.25) are linear and the nonlinearity occurs in the last $\mathcal{N}_{\rm d}^{p,\rm int}$ lines of (3.25). Even if the function $\mathbf{C}$ is not Fréchet differentiable, it is locally Lipschitz and continuous. As a result of the Rademacher theorem (see [50, 29, 30]), the function $\mathbf{C}$ is differentiable almost everywhere, or more precisely, it belongs to the class of strong semismooth functions. The semismooth Newton linearization is defined as follows: let an initial guess $\boldsymbol{X}_h^{n,0} \in \mathbb{R}^{3\mathcal{N}_{\rm d}^{p,\rm int}}$ be given; typically, $\boldsymbol{X}_h^{n,0} := \boldsymbol{X}_h^{n-1}$, where $\boldsymbol{X}_h^{n-1}$ is the last iterate from the previous time step (including possibly inexact solvers). At step $k \geq 1$, one looks for $\boldsymbol{X}_h^{n,k} \in \mathbb{R}^{3\mathcal{N}_{\rm d}^{p,\rm int}}$ such that

$$\mathbb{A}^{n,k-1} \boldsymbol{X}_h^{n,k} = \boldsymbol{B}^{n,k-1}, \tag{3.26}$$

where $\mathbb{A}^{n,k-1} \in \mathbb{R}^{3\mathcal{N}_{\rm d}^{p,\rm int}, 3\mathcal{N}_{\rm d}^{p,\rm int}}$ is a matrix and $\boldsymbol{B}^{n,k-1} \in \mathbb{R}^{3\mathcal{N}_{\rm d}^{p,\rm int}}$ is the right-hand side vector given by

$$\mathbb{A}^{n,k-1} := \left[\begin{array}{c} \mathbb{E}_p^n \\ \mathbf{J}_{\mathbf{C}}(\boldsymbol{X}_h^{n,k-1}) \end{array} \right] \quad \boldsymbol{B}^{n,k-1} := \left[\begin{array}{c} \boldsymbol{F}^n \\ \mathbf{J}_{\mathbf{C}}(\boldsymbol{X}_h^{n,k-1}) \boldsymbol{X}_h^{n,k-1} - \mathbf{C}(\boldsymbol{X}_h^{n,k-1}) \end{array} \right]. \tag{3.27}$$

Here, the notation $\mathbf{J}_{\mathbf{C}}(\boldsymbol{X}_h^{n,k-1})$ stands for the Jacobian matrix in the sense of Clarke. For example, considering the semismooth min function (3.23), we have, for $p \geq 1$,

$$\min\{\boldsymbol{X}_{1h}^n + g\mathbf{1} - \boldsymbol{X}_{2h}^n, \boldsymbol{X}_{3h}^n\} = \min\left\{ \left(\begin{array}{c} u_{1h}^n(\boldsymbol{x}_1) - u_{2h}^n(\boldsymbol{x}_1) \\ \vdots \\ u_{1h}^n(\boldsymbol{x}_{\mathcal{N}_{\rm d}^{p,\rm int}}) - u_{2h}^n(\boldsymbol{x}_{\mathcal{N}_{\rm d}^{p,\rm int}}) \end{array} \right), \left(\begin{array}{c} (\boldsymbol{X}_{3h}^n)_1 \\ \vdots \\ (\boldsymbol{X}_{3h}^n)_{\mathcal{N}_{\rm d}^{p,\rm int}} \end{array} \right) \right\},$$

and if the block matrices $\mathbb{K}$ and $\mathbb{G}$ in $\mathbb{R}^{\mathcal{N}_{\rm d}^{p,\rm int}, 3\mathcal{N}_{\rm d}^{p,\rm int}}$ are defined respectively by

$$\mathbb{K} := \left[\mathbb{I}_{\mathrm{d}_{\mathcal{N}_{\rm d}^{p,\rm int} \times \mathcal{N}_{\rm d}^{p,\rm int}}}, -\mathbb{I}_{\mathrm{d}_{\mathcal{N}_{\rm d}^{p,\rm int} \times \mathcal{N}_{\rm d}^{p,\rm int}}}, \mathbf{0}_{\mathcal{N}_{\rm d}^{p,\rm int} \times \mathcal{N}_{\rm d}^{p,\rm int}} \right], \tag{3.28}$$

$$\mathbb{G} := \left[\mathbf{0}_{\mathcal{N}_{\rm d}^{p,\rm int} \times \mathcal{N}_{\rm d}^{p,\rm int}}, \mathbf{0}_{\mathcal{N}_{\rm d}^{p,\rm int} \times \mathcal{N}_{\rm d}^{p,\rm int}}, \mathbb{I}_{\mathrm{d}_{\mathcal{N}_{\rm d}^{p,\rm int} \times \mathcal{N}_{\rm d}^{p,\rm int}}} \right], \tag{3.29}$$

the $l^{\rm th}$ row of the Jacobian matrix in the sense of Clarke $\mathbf{J}_{\mathbf{C}}(\boldsymbol{X}_h^{n,k-1})$ is either given by the $l^{\rm th}$ row of $\mathbb{K}$ if $u_{1h}^{n,k-1}(\boldsymbol{x}_l) - u_{2h}^{n,k-1}(\boldsymbol{x}_l) \leq \left(\boldsymbol{X}_{3h}^{n,k-1}\right)_l$, or by the $l^{\rm th}$ row of $\mathbb{G}$ if $u_{1h}^{n,k-1}(\boldsymbol{x}_l) - u_{2h}^{n,k-1}(\boldsymbol{x}_l) > \left(\boldsymbol{X}_{3h}^{n,k-1}\right)_l$.

For an "exact semismooth Newton" resolution of (3.25), choose a tolerance $\varepsilon_{\rm lin}$ close to the machine precision and stop the linearization procedure when the relative linearization residual satisfies

$$\left\| \begin{pmatrix} \boldsymbol{F}^n - \mathbb{E}_p^n \boldsymbol{X}_h^{n,k} \\ \mathbf{C}(\boldsymbol{X}_h^{n,k}) \end{pmatrix} \right\| \Big/ \left\| \begin{pmatrix} \boldsymbol{F}^n - \mathbb{E}_p^n \boldsymbol{X}_h^{n,0} \\ \mathbf{C}(\boldsymbol{X}_h^{n,0}) \end{pmatrix} \right\| \leq \varepsilon_{\rm lin}. \tag{3.30}$$

3.6 Iterative algebraic solvers and inexact linearization

Let a linearization step $k \geq 1$ be fixed and choose an iterative algebraic solver with iteration index $i \geq 0$. Given an initial guess $\boldsymbol{X}_h^{n,k,0} \in \mathbb{R}^{3\mathcal{N}_{\rm d}^{p,\rm int}}$, often taken as $\boldsymbol{X}_h^{n,k,0} := \boldsymbol{X}_h^{n,k-1}$, where $\boldsymbol{X}_h^{n,k-1}$ is the last available

iterate from the previous semismooth Newton step (including possibly inexact algebraic solver), the residual in (3.26) is defined by

$$\boldsymbol{R}_h^{n,k,i} := \boldsymbol{B}^{n,k-1} - \mathbb{A}^{n,k-1}\boldsymbol{X}_h^{n,k,i}. \tag{3.31}$$

In fact, the residual $\boldsymbol{R}_h^{n,k,i} \in \mathbb{R}^{3\mathcal{N}_{\mathrm{d}}^{p,\mathrm{int}}}$ is a block vector

$$\boldsymbol{R}_h^{n,k,i} := \left[\boldsymbol{R}_{1h}^{n,k,i}, \boldsymbol{R}_{2h}^{n,k,i}, \boldsymbol{R}_{3h}^{n,k,i}\right]^T,$$

where $\boldsymbol{R}_{\alpha h}^{n,k,i} \in \mathcal{N}_{\mathrm{d}}^{p,\mathrm{int}}$, $\alpha = 1, 2$, are the components associated to the block equation in (3.22), whereas $\boldsymbol{R}_{3h}^{n,k,i} \in \mathcal{N}_{\mathrm{d}}^{p,\mathrm{int}}$ is associated with the block inequality (constraints) in (3.22).

"Inexact semismooth Newton" resolution of (3.25) consists in, on each step $k \geq 1$, stopping the algebraic iterations when the relative algebraic residual satisfies

$$\left\|\boldsymbol{R}_h^{n,k,i}\right\| \Big/ \left\|\boldsymbol{B}^{n,k-1} - \mathbb{A}^{n,k-1}\boldsymbol{X}_h^{n,k,0}\right\| \leq \varepsilon_{\mathrm{alg}}^k, \tag{3.32}$$

where the term $\varepsilon_{\mathrm{alg}}^k$ is commonly called the "forcing term", see [51, 52, 53, 54]. When the algebraic stopping criterion (3.32) is satisfied, one updates the solution as

$$\boldsymbol{X}_h^{n,k} := \boldsymbol{X}_h^{n,k,i},$$

and once the linearization stopping criterion (3.32) is satisfied, one updates the solution as

$$\boldsymbol{X}_h^{n} := \boldsymbol{X}_h^{n,k}.$$

In this way, u_{1h}^{n-1}, u_{2h}^{n-1} are the functional representations of the vectors $\boldsymbol{X}_{1h}^{n-1}$ and $\boldsymbol{X}_{2h}^{n-1}$, *i.e.* $\boldsymbol{X}_{\alpha h}^{n-1,k,i}$ when the stopping criteria are met.

We provide in Section 5 below the alternative to the classical stopping criteria (3.30) and (3.32).

4 A posteriori error analysis

In this section, we derive two a posteriori error estimates. First, we establish an a posteriori error estimate when $p = 1$ and when both the algebraic and linearization solvers have converged. Next, we derive an a posteriori error estimate when $p \geq 1$ at any semismooth linearization step $k \geq 1$ and any step of the iterative algebraic solver $i \geq 0$.

4.1 Approximate solution

At each time step $1 \leq n \leq N_{\mathrm{t}}$, we try to solve the nonlinear system (3.25) giving in particular the degrees of freedom of the numerical solution $\boldsymbol{X}_h^{n,k,i} \in \mathbb{R}^{3\mathcal{N}_{\mathrm{d}}^{p,\mathrm{int}}}$ where $k \geq 1$ is the semismooth Newton step and $i \geq 0$ is the algebraic solver step. The functional representations of the vectors $\boldsymbol{X}_{1h}^{n,k,i}$ and $\boldsymbol{X}_{2h}^{n,k,i}$, denoted by $u_{1h}^{n,k,i}$ and $u_{2h}^{n,k,i}$ are given as in (3.16) and (3.17), and the function of $\boldsymbol{X}_{3h}^{n,k,i}$ denoted by $\lambda_h^{n,k,i}$ is given as in (3.18). Obviously, $\left(u_{1h}^{n,k,i}, u_{2h}^{n,k,i}, \lambda_h^{n,k,i}\right) \in X_{gh}^p \times X_{0h}^p \times X_h^p \quad \forall 1 \leq n \leq N_{\mathrm{t}}$. Next, we associate to the functions in space $u_{1h}^{n,k,i} \in X_{gh}^p$ and $u_{2h}^{n,k,i} \in X_{0h}^p$, $1 \leq n \leq N_{\mathrm{t}}$, their space-time representations $u_{1h\tau}^{k,i}$, $u_{2h\tau}^{k,i}$

$$u_{1h\tau}^{k,i}|_{I_n} := \frac{u_{1h}^{n,k,i} - u_{1h}^{n-1}}{\Delta t_n}(t - t^n) + u_{1h}^{n,k,i} \qquad \forall 1 \leq n \leq N_{\mathrm{t}},$$

$$u_{2h\tau}^{k,i}|_{I_n} := \frac{u_{2h}^{n,k,i} - u_{2h}^{n-1}}{\Delta t_n}(t - t^n) + u_{2h}^{n,k,i} \qquad \forall 1 \leq n \leq N_{\mathrm{t}}.$$

Concerning the discrete Lagrange multiplier $\lambda_h^{n,k,i} \in X_h^p$, its space-time representation is defined by a piecewise constant-in-time function $\lambda_{h\tau}^{k,i}$

$$\lambda_{h\tau}^{k,i}|_{I_n} := \lambda_h^{n,k,i}.$$

Note that this construction ensures that $u_{\alpha h\tau}^{k,i}$, $\alpha = 1, 2$, are continuous and piecewise affine in time, so that $\partial_t u_{\alpha h\tau}^{k,i} \in L^2(0,T;H^{-1}(\Omega))$. In the expressions of $u_{1h\tau}^{k,i}$, $u_{2h\tau}^{k,i}$, and $\lambda_{h\tau}^{k,i}$, the indices k, i are kept to indicate the presence of inexact solvers; more precisely, $u_{\alpha h}^{n-1}$ are equal to $u_{\alpha h}^{n-1,k,i}$ for the last iterates k and i when the stopping criteria are met. For each time step n, we also denote

$$u_{1h\tau}^{n,k,i} := u_{1h\tau}^{k,i}|_{I_n}, \quad u_{2h\tau}^{n,k,i} := u_{2h\tau}^{k,i}|_{I_n}, \tag{4.1}$$

so that

$$\partial_t u_{1h\tau}^{n,k,i}|_{I_n} = \frac{1}{\Delta t_n}\left(u_{1h}^{n,k,i} - u_{1h}^{n-1}\right), \quad \partial_t u_{2h\tau}^{n,k,i}|_{I_n} = \frac{1}{\Delta t_n}\left(u_{2h}^{n,k,i} - u_{2h}^{n-1}\right).$$

4.2 Representation of the residual

We first start by giving a functional representation to (3.31), following [55]. We associate respectively with $\boldsymbol{R}_{1h}^{n,k,i}$ and $\boldsymbol{R}_{2h}^{n,k,i}$ elementwise discontinuous polynomials $r_{1h}^{n,k,i}$ and $r_{2h}^{n,k,i}$ of degree $p \geq 1$ that vanish on the boundary of Ω. These can be easily computed solving on each element $K \in \mathcal{T}_h$ a small problem with an element mass matrix given as follows. For $\boldsymbol{x}_l \in \mathcal{V}_{\mathrm{d}}^{p,\mathrm{int}}$, denote by $N_{h,\boldsymbol{x}_l}$ the number of mesh elements forming the support of the basis function $\psi_{h,\boldsymbol{x}_l}$. Then, for all $K \in \mathcal{T}_h$ and for all $\alpha \in \{1,2\}$, define $r_{\alpha h}^{n,k,i}|_K \in \mathbb{P}_p(K)$ such that:

$$(r_{\alpha h}^{n,k,i}, \psi_{h,\boldsymbol{x}_l})_K := \frac{(\boldsymbol{R}_{\alpha h}^{n,k,i})_l}{N_{h,\boldsymbol{x}_l}} \quad \text{and} \quad r_{\alpha h}^{k,i}|_{\partial K \cap \partial\Omega} := 0$$

for all Lagrange basis functions $\psi_{h,\boldsymbol{x}_l} \in X_h^p$, $\boldsymbol{x}_l \in \mathcal{V}_{\mathrm{d}}^{p,\mathrm{int}}$, nonzero on K. It is easily seen that the first $2\mathcal{N}_{\mathrm{d}}^{p,\mathrm{int}}$ lines of (3.31) then read

$$\begin{aligned}
\mu_1 \left(\boldsymbol{\nabla} u_{1h}^{n,k,i}, \boldsymbol{\nabla}\psi_{h,\boldsymbol{x}_l}\right)_\Omega &= \left(\tilde{f}_1^n + \tilde{\lambda}_{h,l}^{n,k,i} - r_{1h}^{n,k,i} - \partial_t u_{1h\tau}^{n,k,i}, \psi_{h,\boldsymbol{x}_l}\right)_\Omega \quad \forall l = 1, \dots, \mathcal{N}_{\mathrm{d}}^{p,\mathrm{int}}, \\
\mu_2 \left(\boldsymbol{\nabla} u_{2h}^{n,k,i}, \boldsymbol{\nabla}\psi_{h,\boldsymbol{x}_l}\right)_\Omega &= \left(\tilde{f}_2^n - \tilde{\lambda}_{h,l}^{n,k,i} - r_{2h}^{n,k,i} - \partial_t u_{2h\tau}^{n,k,i}, \psi_{h,\boldsymbol{x}_l}\right)_\Omega \quad \forall l = 1, \dots, \mathcal{N}_{\mathrm{d}}^{p,\mathrm{int}},
\end{aligned} \tag{4.2}$$

where

$$\tilde{\lambda}_{h,l}^{n,k,i} = \begin{cases} \lambda_h^{n,k,i}(\boldsymbol{x}_l) \text{ if } p = 1, \\ \lambda_h^{n,k,i} \text{ (function } \lambda_h^{n,k,i}\text{, the index } l \text{ is discarded) if } p \geq 2. \end{cases} \tag{4.3}$$

We also use the shorthand notation

$$\tilde{\lambda}_{h,\boldsymbol{a}}^{n,k,i} = \begin{cases} \lambda_h^{n,k,i}(\boldsymbol{a}) & \text{if} \quad p = 1, \\ \lambda_h^{n,k,i} & \text{if} \quad p \geq 2. \end{cases}$$

The functional representation of (3.31) given by (4.2) is essential for our a posteriori analysis as we will see in the sequel.

4.3 Flux reconstructions

Our a posteriori analysis relies on the equilibrated flux reconstructions following the concepts of [56, 57, 58, 16]. We construct a discretization flux reconstruction $\boldsymbol{\sigma}_{\alpha h,\mathrm{disc}}^{n,k,i} \in \mathbf{H}(\mathrm{div},\Omega)$ and an algebraic error flux reconstruction $\boldsymbol{\sigma}_{\alpha h,\mathrm{alg}}^{n,k,i} \in \mathbf{H}(\mathrm{div},\Omega)$. More precisely, the discretization flux reconstruction is obtained by solving mixed finite element systems on the patches $\omega_h^{\boldsymbol{a}}$ around the mesh vertices $\boldsymbol{a} \in \mathcal{V}_h$ on the mesh $\mathcal{T}_h$, while the algebraic flux $\boldsymbol{\sigma}_{\alpha h,\mathrm{alg}}^{n,k,i}$ is obtained via solving local problems on a hierarchy of nested grids. The fluxes $\boldsymbol{\sigma}_{\alpha h,\mathrm{alg}}^{n,k,i}, \boldsymbol{\sigma}_{\alpha h,\mathrm{disc}}^{n,k,i}$ are reconstructed in the Raviart–Thomas subspaces of $\mathbf{H}(\mathrm{div},\Omega)$. The Raviart–Thomas spaces of order $p \geq 1$ [59, 60, 61] are defined by

$$\mathbf{RT}_p(\Omega) := \{\boldsymbol{\tau}_h \in \mathbf{H}(\mathrm{div},\Omega),\ \boldsymbol{\tau}_h|_K \in \mathbf{RT}_p(K)\ \ \forall K \in \mathcal{T}_h\},$$

where $\mathbf{RT}_p(K) := [\mathbb{P}_p(K)]^2 + \vec{\boldsymbol{x}}\mathbb{P}_p(K)$, with $\vec{\boldsymbol{x}} = [x_1, x_2]^T$. For $\boldsymbol{a} \in \mathcal{V}_h$, let

$$\mathbf{RT}_p(\omega_h^{\boldsymbol{a}}) := \{\boldsymbol{\tau}_h \in \mathbf{H}(\mathrm{div},\omega_h^{\boldsymbol{a}}),\ \boldsymbol{\tau}_h|_K \in \mathbf{RT}_p(K),\ \forall K \in \mathcal{T}_h \text{ such that } K \subset \omega_h^{\boldsymbol{a}}\},$$

and let $\mathbb{P}_p^{\rm d}(\mathcal{T}_h|_{\omega_h^{\boldsymbol{a}}})$ stand for piecewise discontinuous polynomials of order p in the patch $\omega_h^{\boldsymbol{a}}$. Define consequently the spaces $\mathbf{V}_h^{\boldsymbol{a}}$ and $Q_h^{\boldsymbol{a}}$ by

$$\mathbf{V}_h^{\boldsymbol{a}} := \left\{\boldsymbol{\tau}_h \in \mathbf{RT}_p(\omega_h^{\boldsymbol{a}}),\, \boldsymbol{\tau}_h{\cdot}\mathbf{n}_{\omega_h^{\boldsymbol{a}}} = 0 \text{ on } \partial\omega_h^{\boldsymbol{a}}\right\}, \quad Q_h^{\boldsymbol{a}} := \left\{q_h \in \mathbb{P}_p^{\rm d}(\mathcal{T}_h|_{\omega_h^{\boldsymbol{a}}}),\, (q_h,1)_{\omega_h^{\boldsymbol{a}}} = 0\right\}, \tag{4.4}$$

when $\boldsymbol{a} \in \mathcal{V}_h^{\rm int}$ and

$$\mathbf{V}_h^{\boldsymbol{a}} := \left\{\boldsymbol{\tau}_h \in \mathbf{RT}_p(\omega_h^{\boldsymbol{a}}),\ \boldsymbol{\tau}_h{\cdot}\mathbf{n}_{\omega_h^{\boldsymbol{a}}} = 0 \ \text{ on } \ \partial\omega_h^{\boldsymbol{a}}\backslash\partial\Omega\right\}, \quad Q_h^{\boldsymbol{a}} := \mathbb{P}_p^{\rm d}(\mathcal{T}_h|_{\omega_h^{\boldsymbol{a}}}) \tag{4.5}$$

when $\boldsymbol{a} \in \mathcal{V}_h^{\rm ext}$.

4.3.1 Discretization flux reconstructions

For all time steps $1 \le n \le N_{\rm t}$, let $\left(u_{1h}^{n,k,i}, u_{2h}^{n,k,i}, \lambda_h^{n,k,i}\right)$ be the approximate solution given by (3.31), verifying in particular (4.2). For each vertex $\boldsymbol{a} \in \mathcal{V}_h$ and each $\alpha \in \{1,2\}$, define $\boldsymbol{\sigma}_{\alpha h,\rm disc}^{n,k,i,\boldsymbol{a}} \in \mathbf{V}_h^{\boldsymbol{a}}$ and $\gamma_{\alpha h}^{n,k,i,\boldsymbol{a}} \in Q_h^{\boldsymbol{a}}$ by solving:

$$\begin{aligned}
\left(\boldsymbol{\sigma}_{\alpha h,\rm disc}^{n,k,i,\boldsymbol{a}}, \boldsymbol{\tau}_h\right)_{\omega_h^{\boldsymbol{a}}} - \left(\gamma_{\alpha h}^{n,k,i,\boldsymbol{a}}, \boldsymbol{\nabla}{\cdot}\boldsymbol{\tau}_h\right)_{\omega_h^{\boldsymbol{a}}} &= -\left(\mu_\alpha \psi_{h,\boldsymbol{a}} \boldsymbol{\nabla} u_{\alpha h}^{n,k,i}, \boldsymbol{\tau}_h\right)_{\omega_h^{\boldsymbol{a}}} && \forall \boldsymbol{\tau}_h \in \mathbf{V}_h^{\boldsymbol{a}},\\
\left(\boldsymbol{\nabla}{\cdot}\boldsymbol{\sigma}_{\alpha h,\rm disc}^{n,k,i,\boldsymbol{a}}, q_h\right)_{\omega_h^{\boldsymbol{a}}} &= \left(\tilde{g}_{\alpha h}^{n,k,i,\boldsymbol{a}}, q_h\right)_{\omega_h^{\boldsymbol{a}}} && \forall q_h \in Q_h^{\boldsymbol{a}},
\end{aligned} \tag{4.6}$$

where the spaces $\mathbf{V}_h^{\boldsymbol{a}}$ and $Q_h^{\boldsymbol{a}}$ are defined by (4.4)–(4.5). The right-hand sides are given as

$$\tilde{g}_{\alpha h}^{n,k,i,\boldsymbol{a}} := \left(\tilde{f}_\alpha^n - (-1)^\alpha \tilde{\lambda}_{h,\boldsymbol{a}}^{n,k,i} - r_{\alpha h}^{n,k,i} - \partial_t u_{\alpha h\tau}^{n,k,i}|_{\omega_h^{\boldsymbol{a}}}\right)\psi_{h,\boldsymbol{a}} - \mu_\alpha \boldsymbol{\nabla} u_{\alpha h}^{n,k,i} \cdot \boldsymbol{\nabla}\psi_{h,\boldsymbol{a}}.$$

Note that it follows from (4.2) with the hat test functions $\psi_{h,\boldsymbol{a}}$ ($\in X_h^p$ for all polynomial degrees $p \ge 1$),

$$\left(\tilde{g}_{\alpha h}^{n,k,i,\boldsymbol{a}}, 1\right)_{\omega_h^{\boldsymbol{a}}} = 0 \qquad \forall \boldsymbol{a} \in \mathcal{V}_h^{\rm int}. \tag{4.7}$$

This implies the Neumann compatibility condition for (4.6). At each time step $1 \le n \le N_{\rm t}$, the discretization flux reconstruction is defined by

$$\boldsymbol{\sigma}_{\alpha h,\rm disc}^{n,k,i} := \sum_{\boldsymbol{a}\in\mathcal{V}_h} \boldsymbol{\sigma}_{\alpha h,\rm disc}^{n,k,i,\boldsymbol{a}}.$$

The following proposition can be shown as in [55, 16]:

Proposition 2. *The flux reconstruction $\boldsymbol{\sigma}_{\alpha h,\rm disc}^{n,k,i} \in \mathbf{H}(\mathrm{div},\Omega)$ and satisfies the equilibration property*

$$\left(\boldsymbol{\nabla}{\cdot}\boldsymbol{\sigma}_{\alpha h,\rm disc}^{n,k,i}, q_h\right)_K = \left(\tilde{f}_\alpha^n - (-1)^\alpha \lambda_h^{n,k,i} - r_{\alpha h}^{n,k,i} - \partial_t u_{\alpha h\tau}^{n,k,i}, q_h\right)_K \quad \forall q_h \in \mathbb{P}_p(K),\, \forall K \in \mathcal{T}_h. \tag{4.8}$$

4.3.2 Algebraic error flux reconstructions

The algebraic error flux reconstructions $\boldsymbol{\sigma}_{\alpha h,\rm alg}^{n,k,i}$, $\alpha = 1,2$, are obtained by the methodology of [55] and yield

$$\boldsymbol{\sigma}_{\alpha h,\rm alg}^{n,k,i} \in \mathbf{H}(\mathrm{div},\Omega) \quad \text{and} \quad \boldsymbol{\nabla}{\cdot}\boldsymbol{\sigma}_{\alpha h,\rm alg}^{n,k,i} = r_{\alpha h}^{n,k,i}.$$

4.3.3 Total flux reconstructions

Finally, the total flux reconstructions are the sums

$$\boldsymbol{\sigma}_{\alpha h}^{n,k,i} := \boldsymbol{\sigma}_{\alpha h,\rm disc}^{n,k,i} + \boldsymbol{\sigma}_{\alpha h,\rm alg}^{n,k,i} \quad \alpha = 1,2, \tag{4.9}$$

so that

$$\left(\boldsymbol{\nabla}{\cdot}\boldsymbol{\sigma}_{\alpha h}^{n,k,i}, q_h\right)_K = \left(\tilde{f}_\alpha^n - (-1)^\alpha \lambda_h^{n,k,i} - \partial_t u_{\alpha h\tau}^{n,k,i}, q_h\right)_K \quad \forall q_h \in \mathbb{P}_p(K),\ \forall K \in \mathcal{T}_h. \tag{4.10}$$

For $\alpha = 1,2$, all these fluxes are extended piecewise constant in time as

$$\begin{aligned}
&\left(\boldsymbol{\sigma}_{\alpha h\tau}^{k,i}, \boldsymbol{\sigma}_{\alpha h\tau,\rm disc}^{k,i}, \boldsymbol{\sigma}_{\alpha h\tau,\rm alg}^{k,i}\right) \in \left[L^2(0,T;\mathbf{H}(\mathrm{div},\Omega))\right]^3,\\
&\boldsymbol{\sigma}_{\alpha h\tau}^{k,i}|_{I_n} = \boldsymbol{\sigma}_{\alpha h}^{n,k,i}, \ \ \boldsymbol{\sigma}_{\alpha h\tau,\rm disc}^{k,i}|_{I_n} = \boldsymbol{\sigma}_{\alpha h,\rm disc}^{n,k,i}, \ \ \boldsymbol{\sigma}_{\alpha h\tau,\rm alg}^{k,i}|_{I_n} = \boldsymbol{\sigma}_{\alpha h,\rm alg}^{n,k,i}, \ \ \forall 1 \le n \le N_{\rm t}.
\end{aligned} \tag{4.11}$$

As a shorthand notation, we will also use $\boldsymbol{\sigma}_{\alpha h\tau}^{n,k,i} := \boldsymbol{\sigma}_{\alpha h\tau}^{k,i}|_{I_n}$.

4.4 An a posteriori error estimate for $p = 1$ and exact solvers

In this section, we establish an a posteriori error estimate between the exact solution $\boldsymbol{u} \in \boldsymbol{\mathcal{K}}_g^{\mathrm{t}}$ given by (1.2) and the approximate numerical solution for $p = 1$ when the semismooth Newton solver and the iterative algebraic solver have converged. In this case, we discard the indices k and i. Note that when $p = 1$, the constraints in (3.15) imply that the approximate solution is conforming in the sense that $\boldsymbol{u}_{h\tau} \in \boldsymbol{\mathcal{K}}_g^{\mathrm{t}}$ and $\lambda_{h\tau} \in \Psi$.

Definition 4.1. *Let $1 \le n \le N_{\mathrm{t}}$, $K \in \mathcal{T}_h$, and $\alpha = 1, 2$. We define the residual estimator $\eta^n_{\mathrm{R},K,\alpha}$, the flux estimator $\eta^n_{\mathrm{F},K,\alpha}$, the constraint estimator $\eta^n_{\mathrm{C},K}$, and the data oscillation estimator $\eta^n_{\mathrm{osc},K,\alpha}$ by the temporal functions, for all $t \in I_n$,*

$$\eta^n_{\mathrm{R},K,\alpha}(t) := \frac{h_K}{\pi}\mu_\alpha^{-\frac{1}{2}} \left\| \tilde{f}^n_\alpha - \partial_t u^n_{\alpha h\tau} - (-1)^\alpha \lambda^n_h - \boldsymbol{\nabla}\cdot\boldsymbol{\sigma}^n_{\alpha h\tau} \right\|_K, \tag{4.12}$$

$$\eta^n_{\mathrm{F},K,\alpha}(t) := \left\| \mu_\alpha^{\frac{1}{2}} \boldsymbol{\nabla} u^n_{\alpha h\tau} + \mu_\alpha^{-\frac{1}{2}} \boldsymbol{\sigma}^n_{\alpha h\tau} \right\|_K, \tag{4.13}$$

$$\eta^n_{\mathrm{C},K}(t) := 2\,(\lambda^n_h, u^n_{1h\tau} - u^n_{2h\tau})_K, \tag{4.14}$$

$$\eta^n_{\mathrm{osc},K,\alpha}(t) := C_{\mathrm{PF}} h_\Omega \mu_\alpha^{-\frac{1}{2}} \left\| f_\alpha - \tilde{f}^n_\alpha \right\|_K. \tag{4.15}$$

Remark 4.2. *The estimators (4.12)–(4.15) are an extension of the estimators of [47] derived in the case of elliptic variational inequations to the parabolic case. They reflect various violations of physical properties of the approximate solution $(u^n_{1h\tau}, u^n_{2h\tau}, \lambda^n_{h\tau})$: $\eta^n_{\mathrm{R},K,\alpha}$ and $\eta^n_{\mathrm{F},K,\alpha}$ represent the nonconformity of the flux,* i.e., *the fact that $-\mu_\alpha \boldsymbol{\nabla} u^n_{\alpha h\tau} \notin L^2(0,T;\mathbf{H}(\mathrm{div},\Omega))$; $\eta^n_{\mathrm{C},K}$ reflects inconsistencies in the complementarity conditions at the discrete level,* i.e., *the fact that $(u^n_{1h\tau} - u^n_{2h\tau})\lambda^n_h \neq 0$. Note that the last constraint in (3.15) for $p = 1$ requires that $(u^n_{1h} - u^n_{2h})\lambda^n_h$ vanishes at each vertex of $\mathcal{T}_h$ but not everywhere in Ω. Finally, $\eta^n_{\mathrm{osc},K,\alpha}$ represents the local distance between the right hand side and its time-averages over I_n. Note that this latter term is an estimator of $\left\| f_\alpha - \tilde{f}^n_\alpha \right\|_{H^{-1}(\Omega)}$ (see (4.21) further) with a rather pessimistic constant, see the discussion in [42, Rem. 5.4] and the references therein).*

4.4.1 A control of the energy error

Recall the Poincaré–Friedrichs and the Poincaré–Wirtinger inequalities, cf. [62, 63]. Denoting by $\overline{v}_{\mathcal{O}}$ the mean value of v over domain $\mathcal{O}$ and $h_{\mathcal{O}}$ the diameter of $\mathcal{O}$,

$$\|v\|_{\mathcal{O}} \le C_{\mathrm{PF}} h_{\mathcal{O}} \|\boldsymbol{\nabla} v\|_{\mathcal{O}} \qquad \forall v \in H^1_0(\mathcal{O}), \tag{4.16a}$$

$$\|v - \overline{v}_{\mathcal{O}}\|_{\mathcal{O}} \le C_{\mathrm{PW}} h_{\mathcal{O}} \|\boldsymbol{\nabla} v\|_{\mathcal{O}} \qquad \forall v \in H^1(\mathcal{O}). \tag{4.16b}$$

We then have:

Theorem 4.3 (case $p = 1$ and exact solvers)**.** *Let $\boldsymbol{u} \in \boldsymbol{\mathcal{K}}_g^{\mathrm{t}}$ be the exact solution given by (1.2). Let $\boldsymbol{u}_{h\tau} \in \boldsymbol{\mathcal{K}}_g^{\mathrm{t}}$ and $\lambda_{h\tau} \in \Psi$ be the approximate solutions for $p = 1$ and exact solvers. Consider the equilibrated flux reconstructions $\boldsymbol{\sigma}_{\alpha h\tau} \in L^2(0,T;\mathbf{H}(\mathrm{div},\Omega))$ given by (4.9), (4.11). Using the error estimators defined by (4.12)–(4.15), there holds*

$$\begin{aligned}
&|||\boldsymbol{u} - \boldsymbol{u}_{h\tau}|||^2_{\Omega,T} + \|(\boldsymbol{u} - \boldsymbol{u}_{h\tau})(\cdot,T)\|^2_\Omega \le \eta^2 := \\
&\left\{ \left(\sum_{n=1}^{N_{\mathrm{t}}} \int_{I_n} \sum_{\alpha=1}^{2} \sum_{K\in\mathcal{T}_h} \left(\eta^n_{\mathrm{R},K,\alpha} + \eta^n_{\mathrm{F},K,\alpha}\right)^2 \right)^{\frac{1}{2}} + \left(\sum_{n=1}^{N_{\mathrm{t}}} \int_{I_n} \sum_{\alpha=1}^{2} \sum_{K\in\mathcal{T}_h} \left(\eta^n_{\mathrm{osc},K,\alpha}\right)^2 (t)\,\mathrm{d}t \right)^{\frac{1}{2}} \right\}^2 \\
&+ \sum_{n=1}^{N_{\mathrm{t}}} \int_{I_n} \sum_{K\in\mathcal{T}_h} \eta^n_{\mathrm{C},K}(t)\,\mathrm{d}t + \|(\boldsymbol{u} - \boldsymbol{u}_{h\tau})(\cdot,0)\|^2_\Omega .
\end{aligned} \tag{4.17}$$

To prove Theorem 4.3, we first introduce the following lemma.

Lemma 4.4. *Let a and b be the forms defined in (2.3). Let $\boldsymbol{u} \in \boldsymbol{\mathcal{K}}_g^{\mathrm{t}}$ be the weak solution from (1.2) and let $\boldsymbol{y} := (y_1, y_2) \in \boldsymbol{\mathcal{K}}_g^{\mathrm{t}}$ be arbitrary. Then, for the vector $\boldsymbol{y}^* := (y_1^*, y_2^*) := (u_1 - y_1, u_2 - y_2) \in \left[L^2(0,T;H_0^1(\Omega))\right]^2$, there holds*

$$
\begin{aligned}
A &:= \int_0^T \left((\boldsymbol{f}, \boldsymbol{y}^*)_\Omega - (\partial_t \boldsymbol{u}_{h\tau}, \boldsymbol{y}^*)_\Omega - a(\boldsymbol{u}_{h\tau}, \boldsymbol{y}^*) + b(\boldsymbol{y}^*, \lambda_{h\tau})\right)(t)\,\mathrm{dt} \\
&\le \left(\left\{ \sum_{n=1}^{N_{\mathrm{t}}} \int_{I_n} \sum_{\alpha=1}^{2} \sum_{K \in \mathcal{T}_h} \left(\eta_{\mathrm{R},K,\alpha}^n + \eta_{\mathrm{F},K,\alpha}^n\right)^2 (t)\,\mathrm{dt} \right\}^{\frac{1}{2}} + \left\{ \sum_{n=1}^{N_{\mathrm{t}}} \int_{I_n} \sum_{\alpha=1}^{2} \sum_{K \in \mathcal{T}_h} \left(\eta_{\mathrm{osc},K,\alpha}^n\right)^2 (t)\,\mathrm{dt} \right\}^{\frac{1}{2}} \right) |||\boldsymbol{y}^*|||_{\Omega,T}\,.
\end{aligned}
\tag{4.18}
$$

Proof. Adding and subtracting $\boldsymbol{\sigma}_{\alpha h\tau}(t) \in \mathbf{H}(\mathrm{div},\Omega)$ and using the Green formula with $y_\alpha^*(t) \in H_0^1(\Omega)$, $\alpha = 1,2$, and employing the decomposition $f_\alpha = \tilde{f}_\alpha^n + \left(f_\alpha - \tilde{f}_\alpha^n\right)$, we have

$$
\begin{aligned}
A = &\int_0^T \sum_{\alpha=1}^{2} \left(\tilde{f}_\alpha^n - \partial_t u_{\alpha h\tau} - \boldsymbol{\nabla}\cdot\boldsymbol{\sigma}_{\alpha h\tau} - (-1)^\alpha \lambda_{h\tau}, y_\alpha^*\right)_\Omega (t)\,\mathrm{dt} \\
&- \int_0^T \sum_{\alpha=1}^{2} \left(\mu_\alpha^{\frac{1}{2}} \boldsymbol{\nabla} u_{\alpha h\tau} + \mu_\alpha^{-\frac{1}{2}} \boldsymbol{\sigma}_{\alpha h\tau}, \mu_\alpha^{\frac{1}{2}} \boldsymbol{\nabla} y_\alpha^*\right)_\Omega (t)\,\mathrm{dt} + \int_0^T \sum_{\alpha=1}^{2} \left(f_\alpha - \tilde{f}_\alpha^n, y_\alpha^*\right)_\Omega (t)\,\mathrm{dt}.
\end{aligned}
$$

Let $\alpha = 1,2$, $1 \le n \le N_{\mathrm{t}}$, $t \in I_n$, and $K \in \mathcal{T}_h$ be fixed. Denoting by $\overline{w}_K$ the mean value over K of $w \in L^2(\Omega)$ and using the property (4.10), one has

$$
\begin{aligned}
&\left(\tilde{f}_\alpha^n - \partial_t u_{\alpha h\tau}^n - (-1)^\alpha \lambda_h^n - \boldsymbol{\nabla}\cdot\boldsymbol{\sigma}_{\alpha h\tau}^n, y_\alpha^*\right)_K (t) \\
&= \left(\mu_\alpha^{-\frac{1}{2}} \left(\tilde{f}_\alpha^n - \partial_t u_{\alpha h\tau}^n - (-1)^\alpha \lambda_h^n - \boldsymbol{\nabla}\cdot\boldsymbol{\sigma}_{\alpha h\tau}^n\right), \mu_\alpha^{\frac{1}{2}} \left(y_\alpha^* - \left(\overline{y_\alpha^*}\right)_K\right)\right)_K (t).
\end{aligned}
$$

Using the Cauchy–Schwarz inequality and next the Poincaré–Wirtinger inequality (4.16b) with $C_{\mathrm{PW}} = \frac{1}{\pi}$ for the convex mesh element K, we get

$$
\left(\tilde{f}_\alpha^n - \partial_t u_{\alpha h\tau}^n - (-1)^\alpha \lambda_h^n - \boldsymbol{\nabla}\cdot\boldsymbol{\sigma}_{\alpha h\tau}^n, y_\alpha^*\right)_K (t) \le \eta_{\mathrm{R},K,\alpha}^n \left\|\mu_\alpha^{\frac{1}{2}} \boldsymbol{\nabla} y_\alpha^*\right\|_K (t). \tag{4.19}
$$

Next, as a result of the Cauchy–Schwarz inequality, we have

$$
\left(\mu_\alpha^{\frac{1}{2}} \boldsymbol{\nabla} u_{\alpha h\tau}^n + \mu_\alpha^{-\frac{1}{2}} \boldsymbol{\sigma}_{\alpha h\tau}^n, \mu_\alpha^{\frac{1}{2}} \boldsymbol{\nabla} y_\alpha^*\right)_K (t) \le \eta_{\mathrm{F},K,\alpha}^n \left\|\mu_\alpha^{\frac{1}{2}} \boldsymbol{\nabla} y_\alpha^*\right\|_K (t). \tag{4.20}
$$

Finally, the Cauchy–Schwarz inequality and the Poincaré–Friedrichs inequality over the entire computational domain Ω give

$$
\begin{aligned}
\left(f_\alpha - \tilde{f}_\alpha^n, y_\alpha^*\right)_\Omega (t) &\le C_{\mathrm{PF}} h_\Omega \mu_\alpha^{-\frac{1}{2}} \left\|f_\alpha - \tilde{f}_\alpha^n\right\|_\Omega \left\|\mu_\alpha^{\frac{1}{2}} \boldsymbol{\nabla} y_\alpha^*\right\|_\Omega (t) \\
&= \left(\sum_{K \in \mathcal{T}_h} (\eta_{\mathrm{osc},K,\alpha}^n)^2 (t)\right)^{\frac{1}{2}} \left\|\mu_\alpha^{\frac{1}{2}} \boldsymbol{\nabla} y_\alpha^*\right\|_\Omega (t).
\end{aligned}
\tag{4.21}
$$

Therefore, combining (4.19)–(4.21) and applying the Cauchy–Schwarz inequality, we get the desired result. □

Proof of Theorem 4.3. Observe that [64, Theorem 5.9.3] gives

$$
\frac{1}{2} \left\|(\boldsymbol{u} - \boldsymbol{u}_{h\tau})(\cdot, T)\right\|_\Omega^2 = \frac{1}{2} \left\|(\boldsymbol{u} - \boldsymbol{u}_{h\tau})(\cdot, 0)\right\|_2^2 + \int_0^T \sum_{\alpha=1}^{2} \langle \partial_t (u_\alpha - u_{\alpha h\tau}), u_\alpha - u_{\alpha h\tau} \rangle (t)\,\mathrm{dt}. \tag{4.22}
$$

Then posing $B := |||\boldsymbol{u} - \boldsymbol{u}_{h\tau}|||_{\Omega,T}^2 + \frac{1}{2} \left\|(\boldsymbol{u} - \boldsymbol{u}_{h\tau})(\cdot, T)\right\|_\Omega^2$, using definition (2.7) and (4.22), we get

$$
B = \int_0^T \left(a(\boldsymbol{u} - \boldsymbol{u}_{h\tau}, \boldsymbol{u} - \boldsymbol{u}_{h\tau}) + \langle \partial_t \boldsymbol{u}, \boldsymbol{u} - \boldsymbol{u}_{h\tau} \rangle - (\partial_t \boldsymbol{u}_{h\tau}, \boldsymbol{u} - \boldsymbol{u}_{h\tau})_\Omega\right)(t)\mathrm{dt} + \frac{1}{2} \left\|(\boldsymbol{u} - \boldsymbol{u}_{h\tau})(\cdot, 0)\right\|_\Omega^2.
$$

Then, using the weak formulation (1.2) with $\boldsymbol{v} = \boldsymbol{u}_{h\tau} \in \boldsymbol{\mathcal{K}}_g^{\mathrm{t}}$, we obtain

$$B \leq \int_0^T \left((\boldsymbol{f} - \partial_t \boldsymbol{u}_{h\tau}, \boldsymbol{u} - \boldsymbol{u}_{h\tau})_\Omega - a(\boldsymbol{u}_{h\tau}, \boldsymbol{u} - \boldsymbol{u}_{h\tau}) \right)(t)\,\mathrm{dt} + \frac{1}{2} \left\| (\boldsymbol{u} - \boldsymbol{u}_{h\tau})(\cdot, 0) \right\|_\Omega^2 .$$

Next, adding and subtracting $\displaystyle\int_0^T b(\boldsymbol{u} - \boldsymbol{u}_{h\tau}, \lambda_{h\tau})(t)\,\mathrm{dt}$ and noting that $(-\lambda_{h\tau}, u_1 - u_2)_\Omega(t) \leq 0$ for a.e $t \in]0, T[$ because $\lambda_{h\tau} \in \Psi$, we obtain

$$\begin{aligned} B \leq \int_0^T & \left((\boldsymbol{f} - \partial_t \boldsymbol{u}_{h\tau}, \boldsymbol{u} - \boldsymbol{u}_{h\tau})_\Omega - a(\boldsymbol{u}_{h\tau}, \boldsymbol{u} - \boldsymbol{u}_{h\tau}) + b(\boldsymbol{u} - \boldsymbol{u}_{h\tau}, \lambda_{h\tau}) \right)(t)\,\mathrm{dt} \\ & + \sum_{n=1}^{N_{\mathrm{t}}} \int_{I_n} \sum_{K \in \mathcal{T}_h} \frac{\eta_{C,K}^n}{2}(t)\,\mathrm{dt} + \frac{1}{2} \left\| (\boldsymbol{u} - \boldsymbol{u}_{h\tau})(\cdot, 0) \right\|_\Omega^2 . \end{aligned}$$

Finally, employing Lemma 4.4 with $\boldsymbol{y} = \boldsymbol{u}_{h\tau} \in \boldsymbol{\mathcal{K}}_g^{\mathrm{t}}$ and using the Young inequality $A_1 A_2 \leq \frac{1}{2}\left(A_1^2 + A_2^2\right)$, $\forall A_1, A_2 \geq 0$, we get the desired result. □

4.4.2 A control of the temporal derivative error

So far, we have established an a posteriori error estimate between the exact solution $\boldsymbol{u} \in \boldsymbol{\mathcal{K}}_g^{\mathrm{t}}$ and its approximate solution $\boldsymbol{u}_{h\tau} \in \boldsymbol{\mathcal{K}}_g^{\mathrm{t}}$ in the energy norm. As we mentioned in the introduction, we cannot easily estimate the norm $\left\| \partial_t (\boldsymbol{u} - \boldsymbol{u}_{h\tau}) \right\|_{[L^2(0,T;H^{-1}(\Omega))]^2}$. We now give our replacement result. Given $\boldsymbol{u} \in \boldsymbol{\mathcal{K}}_g^{\mathrm{t}}$ and for the approximate solution $\boldsymbol{u}_{h\tau} \in \boldsymbol{\mathcal{K}}_g^{\mathrm{t}}$, let $\boldsymbol{z} \in \boldsymbol{\mathcal{K}}_g^{\mathrm{t}}$ be such that, for all $\boldsymbol{v} \in \boldsymbol{\mathcal{K}}_g^{\mathrm{t}}$,

$$\begin{aligned} & \int_0^T a(\boldsymbol{z} - \boldsymbol{u}, \boldsymbol{v} - \boldsymbol{z})(t)\,\mathrm{dt} \geq - \int_0^T \sum_{\alpha=1}^{2} \langle \partial_t \left(u_\alpha - u_{\alpha h\tau} \right) - (-1)^\alpha \lambda_{h\tau}, v_\alpha - z_\alpha \rangle(t)\,\mathrm{dt}, \\ & \boldsymbol{z}(0) = \boldsymbol{u}_{h\tau}(0) \in \boldsymbol{\mathcal{K}}_g. \end{aligned} \tag{4.23}$$

As a result of the Lions–Stampacchia theorem, problem (4.23) is well posed. Now, we give an a posteriori error estimate on the error $|||\boldsymbol{u} - \boldsymbol{z}|||_{\Omega,T}$.

Theorem 4.5 (case $p = 1$ and exact solvers)**.** *Let $\boldsymbol{u} \in \boldsymbol{\mathcal{K}}_g^{\mathrm{t}}$ be the solution of the weak formulation given by (1.2) and let $\boldsymbol{z} \in \boldsymbol{\mathcal{K}}_g^{\mathrm{t}}$ be the solution of (4.23). Assume that the hypotheses of Theorem 4.3 hold and let the total estimator η be defined by (4.17). Then*

$$|||\boldsymbol{u} - \boldsymbol{z}|||_{\Omega,T} \leq 2\eta.$$

Proof. Setting $\boldsymbol{w}^* := \boldsymbol{u} - \boldsymbol{z}$, we have $|||\boldsymbol{w}^*|||_{\Omega,T}^2 = \displaystyle\int_0^T a(\boldsymbol{u} - \boldsymbol{z}, \boldsymbol{u} - \boldsymbol{z})\,\mathrm{dt}$. For $\boldsymbol{v} = \boldsymbol{u} \in \boldsymbol{\mathcal{K}}_g^{\mathrm{t}}$, we in turn get from (4.23)

$$|||\boldsymbol{w}^*|||_{\Omega,T}^2 \leq \int_0^T \left(\langle \partial_t (\boldsymbol{u} - \boldsymbol{u}_{h\tau}), \boldsymbol{w}^* \rangle + b(\boldsymbol{w}^*, \lambda_{h\tau}) \right)(t)\,\mathrm{dt} + \int_0^T \left(a(\boldsymbol{u} - \boldsymbol{u}_{h\tau}, \boldsymbol{w}^*) - a(\boldsymbol{u} - \boldsymbol{u}_{h\tau}, \boldsymbol{w}^*) \right)(t)\,\mathrm{dt}.$$

Employing the weak formulation (1.2) with $\boldsymbol{v} = \boldsymbol{z} \in \boldsymbol{\mathcal{K}}_g^{\mathrm{t}}$ we obtain

$$|||\boldsymbol{w}^*|||_{\Omega,T}^2 \leq \int_0^T \left[(\boldsymbol{f} - \partial_t \boldsymbol{u}_{h\tau}, \boldsymbol{w}^*)_\Omega + b(\boldsymbol{w}^*, \lambda_{h\tau}) - a(\boldsymbol{u}_{h\tau}, \boldsymbol{w}^*) - a(\boldsymbol{u} - \boldsymbol{u}_{h\tau}, \boldsymbol{w}^*) \right](t)\,\mathrm{dt}. \tag{4.24}$$

To bound the three first terms of (4.24), we employ Lemma 4.4 with $\boldsymbol{y} = \boldsymbol{z} \in \boldsymbol{\mathcal{K}}_g^{\mathrm{t}}$ and next the Young inequality ($AB \leq \frac{1}{4}A^2 + B^2$) to see

$$\begin{aligned} |||\boldsymbol{w}^*|||_{\Omega,T}^2 \leq & \left(\left\{ \sum_{n=1}^{N_{\mathrm{t}}} \int_{I_n} \sum_{K \in \mathcal{T}_h} \sum_{\alpha=1}^{2} \left(\eta_{\mathrm{R},K,\alpha}^n + \eta_{\mathrm{F},K,\alpha}^n \right)^2 (t)\,\mathrm{dt} \right\}^{\frac{1}{2}} + \left\{ \int_0^T \sum_{\alpha=1}^{2} \sum_{K \in \mathcal{T}_h} \left(\eta_{\mathrm{osc},K,\alpha}^n \right)^2 (t)\,\mathrm{dt} \right\}^{\frac{1}{2}} \right)^2 \\ & + \frac{1}{4} |||\boldsymbol{w}^*|||_{\Omega,T}^2 - \int_0^T a(\boldsymbol{u} - \boldsymbol{u}_{h\tau}, \boldsymbol{w}^*)(t)\,\mathrm{dt}. \end{aligned} \tag{4.25}$$

The Cauchy–Schwarz inequality and the Young inequality give

$$-\int_0^T a(\boldsymbol{u}-\boldsymbol{u}_{h\tau},\boldsymbol{w}^*)(t)\,\mathrm{d}t \le |||\boldsymbol{u}-\boldsymbol{u}_{h\tau}|||_{\Omega,T}\,|||\boldsymbol{w}^*|||_{\Omega,T} \le |||\boldsymbol{u}-\boldsymbol{u}_{h\tau}|||^2_{\Omega,T}+\frac{1}{4}\,|||\boldsymbol{w}^*|||^2_{\Omega,T}\,. \tag{4.26}$$

Finally, combining (4.25) and (4.26) with (4.17), we get $|||\boldsymbol{w}^*|||^2_{\Omega,T} \le 4\eta^2$ which is the desired result. □

Combining Theorems 4.3 and 4.5, we infer

Corollary 4.6 (case $p=1$ and exact solvers)**.** *Assume the hypotheses of Theorem 4.5. Then*

$$|||\boldsymbol{u}-\boldsymbol{u}_{h\tau}|||^2_{\Omega,T}+|||\boldsymbol{u}-\boldsymbol{z}|||^2_{\Omega,T}+\|(\boldsymbol{u}-\boldsymbol{u}_{h\tau})(\cdot,T)\|^2_{\Omega} \le 5\eta^2. \tag{4.27}$$

In Lemma 4.7, we show that the error measure $|||\boldsymbol{u}-\boldsymbol{z}|||_{\Omega,T}$ is linked to the temporal derivative error, but we could not obtain the (more interesting) converse estimate that would allow to control the temporal derivative error by the estimators.

Lemma 4.7. *Assuming the hypotheses of Theorem 4.5 and denoting by* $\delta := 2/\min\left(\mu_1^{\frac{1}{2}},\mu_2^{\frac{1}{2}}\right)$ *we have*

$$|||\boldsymbol{u}-\boldsymbol{z}|||_{\Omega,T} \le \delta\left(\left(\int_0^T\sum_{\alpha=1}^2\|\partial_t\left(u_\alpha-u_{\alpha h\tau}\right)\|^2_{H^{-1}(\Omega)}(t)\,\mathrm{d}t\right)^{\frac{1}{2}}+\left(\int_0^T\|\lambda_{h\tau}-\lambda\|^2_{H^{-1}(\Omega)}(t)\,\mathrm{d}t\right)^{\frac{1}{2}}\right).$$

Proof. Denoting by $\boldsymbol{w}^* := \boldsymbol{u}-\boldsymbol{z}$, we have

$$|||\boldsymbol{w}^*|||^2_{\Omega,T} \le \int_0^T\sum_{\alpha=1}^2\langle\partial_t\left(u_\alpha-u_{\alpha h\tau}\right),w_\alpha^*\rangle(t)\,\mathrm{d}t+\int_0^T(\lambda_{h\tau},w_1^*-w_2^*)_\Omega(t)\,\mathrm{d}t.$$

Next,

$$\int_0^T(\lambda_{h\tau},w_1^*-w_2^*)_\Omega(t)\,\mathrm{d}t=\int_0^T(\lambda_{h\tau}-\lambda,w_1^*-w_2^*)_\Omega(t)\,\mathrm{d}t+\int_0^T(\lambda,w_1^*-w_2^*)_\Omega(t)\,\mathrm{d}t.$$

Observe that

$$\int_0^T(\lambda,w_1^*-w_2^*)_\Omega(t)\,\mathrm{d}t=\int_0^T(\lambda,u_1-u_2)_\Omega(t)\,\mathrm{d}t-\int_0^T(\lambda,z_1-z_2)_\Omega(t)\,\mathrm{d}t.$$

From (2.1) $\lambda(u_1-u_2)=0$, and as $\lambda\in\Psi$ and $\boldsymbol{z}\in\boldsymbol{\mathcal{K}}_g^{\mathrm{t}}$, we have $\int_0^T(\lambda,w_1^*-w_2^*)_\Omega(t)\,\mathrm{d}t\le 0$ and thus

$$\int_0^T(\lambda_{h\tau},w_1^*-w_2^*)_\Omega(t)\,\mathrm{d}t\le\int_0^T(\lambda_{h\tau}-\lambda,w_1^*-w_2^*)_\Omega(t)\,\mathrm{d}t.$$

Finally,

$$|||\boldsymbol{w}^*|||^2_{\Omega,T} \le \int_0^T\sum_{\alpha=1}^2\langle\partial_t\left(u_\alpha-u_{\alpha h\tau}\right),w_\alpha^*\rangle(t)\,\mathrm{d}t+\int_0^T(\lambda_{h\tau}-\lambda,w_1^*-w_2^*)_\Omega(t)\,\mathrm{d}t. \tag{4.28}$$

Furthermore, denoting by A_1 the first term in the right-hand side of (4.28) we have,

$$\begin{aligned}A_1 &\le \int_0^T\sum_{\alpha=1}^2\sup_{\Phi_\alpha\in H_0^1(\Omega)}\frac{\left\langle\mu_\alpha^{-\frac{1}{2}}\partial_t\left(u_\alpha-u_{\alpha h\tau}\right),\mu_\alpha^{\frac{1}{2}}\Phi_\alpha\right\rangle}{\left\|\mu_\alpha^{\frac{1}{2}}\boldsymbol{\nabla}\Phi_\alpha\right\|_\Omega}\left\|\mu_\alpha^{\frac{1}{2}}\boldsymbol{\nabla}w_\alpha^*\right\|_\Omega(t)\,\mathrm{d}t,\\ &=\int_0^T\sum_{\alpha=1}^2\left\|\mu_\alpha^{-\frac{1}{2}}\partial_t\left(u_\alpha-u_{\alpha h\tau}\right)\right\|_{H^{-1}(\Omega)}\left\|\mu_\alpha^{\frac{1}{2}}\boldsymbol{\nabla}w_\alpha^*\right\|_\Omega(t)\,\mathrm{d}t.\end{aligned}$$

The Cauchy–Schwarz inequality gives

$$A_1\le\left(\int_0^T\sum_{\alpha=1}^2\left\|\mu_\alpha^{-\frac{1}{2}}\partial_t\left(u_\alpha-u_{\alpha h\tau}\right)\right\|^2_{H^{-1}(\Omega)}(t)\,\mathrm{d}t\right)^{\frac{1}{2}}|||\boldsymbol{w}^*|||_{\Omega,T}\,. \tag{4.29}$$

To bound the second term A_2 of (4.28) we employ the Cauchy–Schwarz inequality

$$\begin{aligned} A_2 &= \int_0^T \left(\mu_1^{-\frac12}\left(\lambda_{h\tau}-\lambda\right), \mu_1^{\frac12} w_1^*\right)_\Omega(t)\,\mathrm{dt} - \int_0^T \left(\mu_2^{-\frac12}\left(\lambda_{h\tau}-\lambda\right), \mu_2^{\frac12} w_2^*\right)_\Omega(t)\,\mathrm{dt} \\ &\le \int_0^T \sum_{\alpha=1}^2 \left\|\mu_\alpha^{-\frac12}\left(\lambda_{h\tau}-\lambda\right)\right\|_{H^{-1}(\Omega)} \left\|\mu_\alpha^{\frac12}\boldsymbol{\nabla} w_\alpha^*\right\|_\Omega(t)\,\mathrm{dt} \\ &\le \delta \left(\int_0^T \left\|\lambda_{h\tau}-\lambda\right\|_{H^{-1}(\Omega)}^2(t)\,\mathrm{dt}\right)^{\frac12} |||\boldsymbol{w}^*|||_{\Omega,T}. \end{aligned} \tag{4.30}$$

Combining (4.28), (4.29), and (4.30), we obtain the desired result. □

4.5 An a posteriori error estimate for $p \ge 1$ and each step $k \ge 1$, $i \ge 0$

In this section we devise an a posteriori error estimate which is valid at any time step $1 \le n \le N_\mathrm{t}$, at any semismooth Newton step $k \ge 1$, and at any algebraic step $i \ge 0$. Several difficulties arise. Contrary to the previous case of Section 4.4, the constraints (3.15) are not satisfied because the convergence is not reached. Moreover, even if they were satisfied, the solution remains nonconforming for $p \ge 2$ because $\boldsymbol{\mathcal{K}}_{gh}^p \not\subset \boldsymbol{\mathcal{K}}_g$ and $\Lambda_h^p \not\subset \Lambda$.

Consequently, we have to work with a nonconforming space-time solutions $\boldsymbol{u}_{h\tau}^{k,i} \notin \boldsymbol{\mathcal{K}}_g^\mathrm{t}$ and $\lambda_{h\tau} \notin \Psi$. To cope with these difficulties, we employ the decomposition

$$\lambda_h^{n,k,i} = \lambda_h^{n,k,i,\mathrm{pos}} + \lambda_h^{n,k,i,\mathrm{neg}} \quad \text{where} \quad \lambda_h^{n,k,i,\mathrm{pos}} = \max\left\{\lambda_h^{n,k,i}, 0\right\} \quad \text{and} \quad \lambda_h^{n,k,i,\mathrm{neg}} = \min\left\{\lambda_h^{n,k,i}, 0\right\}.$$

We also introduce the potential $\boldsymbol{s}_{h\tau}^{k,i} := \left(s_{1h\tau}^{k,i}, s_{2h\tau}^{k,i}\right) \in \boldsymbol{\mathcal{K}}_g^\mathrm{t}$ as a piecewise affine and continuous function in time over the whole time interval $]0,T[$, verifying $s_{1h\tau}^{k,i}(t) - s_{2h\tau}^{k,i}(t) \ge 0$ for all $t \in]0,T[$. When $p=1$, a possibility is to construct $\boldsymbol{s}_h^{n,k,i} := \left(s_{1h}^{n,k,i}, s_{2h}^{n,k,i}\right) \in \boldsymbol{\mathcal{K}}_{gh}^1$ by setting, for all $1 \le n \le N_\mathrm{t}$ and for all $\boldsymbol{a} \in \mathcal{V}_h^\mathrm{int}$,

$$\boldsymbol{s}_h^{n,k,i}(\boldsymbol{a}) := \begin{cases} \boldsymbol{u}_h^{k,i}(\boldsymbol{a}) = \left(u_{1h}^{n,k,i}(\boldsymbol{a}), u_{2h}^{n,k,i}(\boldsymbol{a})\right) & \text{if } \left(u_{1h}^{n,k,i} - u_{2h}^{n,k,i}\right)(\boldsymbol{a}) \ge 0, \\ \left(\dfrac{u_{1h}^{n,k,i}(\boldsymbol{a}) + u_{2h}^{n,k,i}(\boldsymbol{a})}{2}, \dfrac{u_{1h}^{n,k,i}(\boldsymbol{a}) + u_{2h}^{n,k,i}(\boldsymbol{a})}{2}\right) & \text{if } \left(u_{1h}^{n,k,i} - u_{2h}^{n,k,i}\right)(\boldsymbol{a}) < 0. \end{cases} \tag{4.31}$$

Definition 4.8. *For all $1 \le n \le N_\mathrm{t}$, we define the error estimators*

$$\begin{aligned} \eta_{\mathrm{R,K},\alpha}^{n,k,i}(t) &:= h_\Omega C_\mathrm{PF} \mu_\alpha^{-\frac12} \left\|\tilde f_\alpha^n - \partial_t s_{\alpha h\tau}^{n,k,i} - \boldsymbol{\nabla}\cdot\boldsymbol{\sigma}_{\alpha h\tau}^{n,k,i} - (-1)^\alpha \lambda_h^{n,k,i}\right\|_K(t), \\ \eta_{\mathrm{F,K},\alpha}^{n,k,i}(t) &:= \left\|\mu_\alpha^{\frac12}\boldsymbol{\nabla} s_{\alpha h\tau}^{n,k,i} + \mu_\alpha^{-\frac12}\boldsymbol{\sigma}_{\alpha h\tau}^{n,k,i}\right\|_K(t), \quad \eta_{\mathrm{C},K}^{n,k,i,\mathrm{pos}}(t) := 2\left(\lambda_h^{n,k,i,\mathrm{pos}}, u_{1h\tau}^{n,k,i} - u_{2h\tau}^{n,k,i}\right)_K(t), \\ \eta_{\mathrm{nonc},1,K}^{n,k,i}(t) &:= h_\Omega C_\mathrm{PF}\left(\frac{1}{\mu_1}+\frac{1}{\mu_2}\right)^{\frac12} \left\|\lambda_h^{n,k,i,\mathrm{neg}}\right\|_K(t), \quad \eta_{\mathrm{nonc},2,K,\alpha}^{n,k,i}(t) := \left\|\mu_\alpha^{\frac12}\boldsymbol{\nabla}\left(s_{\alpha h\tau}^{n,k,i} - u_{\alpha h\tau}^{n,k,i}\right)\right\|_K(t), \\ \eta_{\mathrm{nonc},3,K}^{n,k,i}(t) &:= 2\left(\lambda_h^{n,k,i,\mathrm{pos}}, \left(s_{1h\tau}^{n,k,i} - u_{1h\tau}^{n,k,i}\right) - \left(s_{2h\tau}^{n,k,i} - u_{2h\tau}^{n,k,i}\right)\right)_K(t), \\ \eta_{\mathrm{osc},K,\alpha}^{n}(t) &:= C_\mathrm{PF} h_\Omega \mu_\alpha^{-\frac12} \left\|f_\alpha - \tilde f_\alpha^n\right\|_K. \end{aligned}$$

We observe that the estimators given by Definition 4.8 are slightly different from the ones provided in Definition 4.1. Indeed, in the estimators $\eta_{\mathrm{R,K},\alpha}^{n,k,i}$ and $\eta_{\mathrm{F,K},\alpha}^{n,k,i}$, there appears a $s_{\alpha h\tau}^{n,k,i}$ in place of $u_{\alpha h\tau}^{n,k,i}$, and h_Ω instead of h_K. The constraint estimator $\eta_{\mathrm{C},K}^{n,k,i,\mathrm{pos}}$ is as in Definition 4.1 (remember that $\lambda_h^n \ge 0$ at convergence for $p=1$) and expresses that $\lambda_h^{n,k,i}\left(u_{1h\tau}^{n,k,i} - u_{2h\tau}^{n,k,i}\right) = 0$ is not valid. Next, $\eta_{\mathrm{nonc},1,K}^{n,k,i}$, $\eta_{\mathrm{nonc},2,K,\alpha}^{n,k,i}$, and $\eta_{\mathrm{nonc},3,K}^{n,k,i}$ are nonconformity estimators expressing the possible negativity of the discrete Lagrange multiplier and measuring how far the potential reconstruction $\boldsymbol{s}_{h\tau}^{n,k,i}$ is from the displacements

$\boldsymbol{u}_{h\tau}^{n,k,i}$. Note that for $p = 1$, the estimators $\eta_{\mathrm{nonc},1,K}^{n,k,i}$, $\eta_{\mathrm{nonc},2,K,\alpha}^{n,k,i}$, and $\eta_{\mathrm{nonc},3,K}^{n,k,i}$ turn into semismooth linearization estimators such that we can set $\eta_{\mathrm{lin},1,K}^{n,k,i} := \eta_{\mathrm{nonc},1,K}^{n,k,i}$, $\eta_{\mathrm{lin},2,K,\alpha}^{n,k,i} := \eta_{\mathrm{nonc},2,K,\alpha}^{n,k,i}$, and $\eta_{\mathrm{lin},3,K}^{n,k,i} := \eta_{\mathrm{nonc},3,K}^{n,k,i}$. Indeed, at convergence for $p = 1$, $\lambda_h^{n,k,i,\mathrm{pos}} = \lambda_h^{n,k,i}$, $\lambda_h^{n,k,i,\mathrm{neg}} = 0$, $\boldsymbol{s}_{h\tau}^{n,k,i} = \boldsymbol{u}_{h\tau}^{n,k,i}$, and then $\eta_{\mathrm{lin},1,K}^{n,k,i} = \eta_{\mathrm{lin},2,K,\alpha}^{n,k,i} = \eta_{\mathrm{lin},3,K}^{n,k,i} = 0$.

Theorem 4.9 (case $p \geq 1$ and inexact solvers)**.** *Let $\boldsymbol{u} \in \boldsymbol{\mathcal{K}}_g^{\mathrm{t}}$ be the exact solution given by (1.2) and let $\boldsymbol{u}_{h\tau}^{k,i} \notin \boldsymbol{\mathcal{K}}_g^{\mathrm{t}}$ be the approximate solution issued from inexact linearization and algebraic solvers at each time step $1 \leq n \leq N_{\mathrm{t}}$. Consider the total equilibrated flux reconstruction $\boldsymbol{\sigma}_{\alpha h\tau}^{k,i} \in L^2(0,T,\mathbf{H}(\mathrm{div},\Omega))$ given by (4.9) and (4.11). Let $\boldsymbol{s}_{h\tau}^{k,i} \in \boldsymbol{\mathcal{K}}_g^{\mathrm{t}}$ and consider the estimators of Definition 4.8. Then, for*

$$
\begin{aligned}
\left(\tilde{\eta}^{k,i}\right)^2 := \Bigg(& \left\{ \sum_{n=1}^{N_{\mathrm{t}}} \int_{I_n} \sum_{K\in\mathcal{T}_h} \sum_{\alpha=1}^{2} \left(\eta_{\mathrm{R,K},\alpha}^{n,k,i}\right)^2 (t)\,\mathrm{d}t \right\}^{\frac{1}{2}} + \left\{ \sum_{n=1}^{N_{\mathrm{t}}} \int_{I_n} \sum_{K\in\mathcal{T}_h} \sum_{\alpha=1}^{2} \left(\eta_{\mathrm{F,K},\alpha}^{n,k,i}\right)^2 (t)\,\mathrm{d}t \right\}^{\frac{1}{2}} \\
& + \left\{ \sum_{n=1}^{N_{\mathrm{t}}} \int_{I_n} \sum_{K\in\mathcal{T}_h} \left(\eta_{\mathrm{nonc},1,K}^{n,k,i}\right)^2 (t)\,\mathrm{d}t \right\}^{\frac{1}{2}} + \left\{ \sum_{n=1}^{N_{\mathrm{t}}} \int_{I_n} \sum_{K\in\mathcal{T}_h} \sum_{\alpha=1}^{2} \left(\eta_{\mathrm{osc},K,\alpha}^{n}\right)^2 (t)\,\mathrm{d}t \right\}^{\frac{1}{2}} \Bigg)^2 \\
& + \sum_{n=1}^{N_{\mathrm{t}}} \int_{I_n} \sum_{K\in\mathcal{T}_h} \eta_{\mathrm{C},K}^{n,k,i,\mathrm{pos}}(t)\,\mathrm{d}t + \sum_{n=1}^{N_{\mathrm{t}}} \int_{I_n} \sum_{K\in\mathcal{T}_h} \eta_{\mathrm{nonc},3,K}^{n,k,i}(t)\,\mathrm{d}t + \left\| \left(\boldsymbol{u} - \boldsymbol{s}_{h\tau}^{n,k,i}\right)(\cdot,0) \right\|_{\Omega}^2,
\end{aligned}
$$

we have the a posteriori error estimate

$$
\left|\!\left|\!\left| \boldsymbol{u} - \boldsymbol{u}_{h\tau}^{n,k,i} \right|\!\right|\!\right|_{\Omega,T} \leq \eta^{k,i} := \tilde{\eta}^{k,i} + \left\{ \sum_{n=1}^{N_{\mathrm{t}}} \int_{I_n} \sum_{\alpha=1}^{2} \sum_{K\in\mathcal{T}_h} \left(\eta_{\mathrm{nonc},2,K,\alpha}^{n,k,i}\right)^2 (t)\,\mathrm{d}t \right\}^{\frac{1}{2}}. \tag{4.32}
$$

Proof. We start by the triangle inequality, leading to

$$
\left|\!\left|\!\left| \boldsymbol{u} - \boldsymbol{u}_{h\tau}^{k,i} \right|\!\right|\!\right|_{\Omega,T} \leq \left|\!\left|\!\left| \boldsymbol{u} - \boldsymbol{s}_{h\tau}^{k,i} \right|\!\right|\!\right|_{\Omega,T} + \left|\!\left|\!\left| \boldsymbol{s}_{h\tau}^{k,i} - \boldsymbol{u}_{h\tau}^{k,i} \right|\!\right|\!\right|_{\Omega,T}. \tag{4.33}
$$

The second term of (4.33) immediately equals to

$$
\left|\!\left|\!\left| \boldsymbol{s}_{h\tau}^{k,i} - \boldsymbol{u}_{h\tau}^{k,i} \right|\!\right|\!\right|_{\Omega,T}^2 = \sum_{n=1}^{N_{\mathrm{t}}} \int_{I_n} \sum_{\alpha=1}^{2} \sum_{K\in\mathcal{T}_h} \left(\eta_{\mathrm{nonc},2,K,\alpha}^{n,k,i}\right)^2 (t)\,\mathrm{d}t. \tag{4.34}
$$

Next, observe that

$$
\left|\!\left|\!\left| \boldsymbol{u} - \boldsymbol{s}_{h\tau}^{k,i} \right|\!\right|\!\right|_{\Omega,T}^2 \leq \left|\!\left|\!\left| \boldsymbol{u} - \boldsymbol{s}_{h\tau}^{k,i} \right|\!\right|\!\right|_{\Omega,T}^2 + \frac{1}{2} \left\| \left(\boldsymbol{u} - \boldsymbol{s}_{h\tau}^{k,i}\right)(\cdot,T) \right\|_{\Omega}^2.
$$

Employing the fact that

$$
\frac{1}{2} \left\| \left(\boldsymbol{u} - \boldsymbol{s}_{h\tau}^{k,i}\right)(\cdot,T) \right\|_{\Omega}^2 = \frac{1}{2} \left\| \left(\boldsymbol{u} - \boldsymbol{s}_{h\tau}^{k,i}\right)(\cdot,0) \right\|_{\Omega}^2 + \int_0^T \left\langle \partial_t \left(\boldsymbol{u} - \boldsymbol{s}_{h\tau}^{k,i}\right), \boldsymbol{u} - \boldsymbol{s}_{h\tau}^{k,i} \right\rangle (t)\,\mathrm{d}t,
$$

we have

$$
\begin{aligned}
\left|\!\left|\!\left| \boldsymbol{u} - \boldsymbol{s}_{h\tau}^{k,i} \right|\!\right|\!\right|_{\Omega,T}^2 \leq & \sum_{\alpha=1}^{2} \int_0^T \mu_\alpha \left(\boldsymbol{\nabla} \left(u_\alpha - s_{\alpha h\tau}^{k,i}\right), \boldsymbol{\nabla} \left(u_\alpha - s_{\alpha h\tau}^{k,i}\right) \right)_{\Omega} (t)\,\mathrm{d}t \\
& + \sum_{\alpha=1}^{2} \int_0^T \left\langle \partial_t \left(u_\alpha - s_{\alpha h\tau}^{k,i}\right), u_\alpha - s_{\alpha h\tau}^{k,i} \right\rangle (t)\,\mathrm{d}t + \frac{1}{2} \left\| \left(\boldsymbol{u} - \boldsymbol{s}_{h\tau}^{k,i}\right)(\cdot,0) \right\|_{\Omega}^2.
\end{aligned}
$$

We now use the weak formulation (1.2) with $\boldsymbol{v} = \boldsymbol{s}_{h\tau}^{k,i} \in \boldsymbol{\mathcal{K}}_g^{\mathrm{t}}$ and we add and subtract $\sum_{\alpha=1}^{2} \int_0^T \left(\tilde{f}_\alpha^n, u_\alpha -\right.$

$s_{\alpha h\tau}^{k,i}\big)_\Omega(t)\,\mathrm{dt}$ to get

$$\left|\!\left|\!\left|\boldsymbol{u}-\boldsymbol{s}_{h\tau}^{k,i}\right|\!\right|\!\right|_{\Omega,T}^2 \le \sum_{\alpha=1}^{2}\int_0^T \left(\tilde{f}_\alpha^n-\partial_t s_{\alpha h\tau}^{k,i}, u_\alpha - s_{\alpha h\tau}^{k,i}\right)_\Omega(t) - \sum_{\alpha=1}^{2}\int_0^T \mu_\alpha\left(\boldsymbol{\nabla} s_{\alpha h\tau}^{k,i}, \boldsymbol{\nabla}\left(u_\alpha - s_{\alpha h\tau}^{k,i}\right)\right)_\Omega(t)\,\mathrm{dt}$$
$$+\sum_{\alpha=1}^{2}\int_0^T \left(f_\alpha-\tilde{f}_\alpha^n, u_\alpha - s_{\alpha h\tau}^{k,i}\right)_\Omega(t)\,\mathrm{dt} + \frac{1}{2}\left\|\left(\boldsymbol{u}-\boldsymbol{s}_{h\tau}^{k,i}\right)(\cdot,0)\right\|_\Omega^2.$$

Adding and subtracting $\sum_{\alpha=1}^{2}\int_0^T \left((-1)^\alpha\lambda_{h\tau}^{k,i}, u_\alpha - s_{\alpha h\tau}^{k,i}\right)_\Omega(t)\,\mathrm{dt}$ and $\sum_{\alpha=1}^{2}\int_0^T \left(\boldsymbol{\sigma}_{\alpha h\tau}^{k,i}, \boldsymbol{\nabla}\left(u_\alpha - s_{\alpha h\tau}^{k,i}\right)\right)_\Omega(t)\,\mathrm{dt}$ with $\boldsymbol{\sigma}_{\alpha h\tau}^{k,i}\in L^2(0,T;\mathbf{H}(\mathrm{div},\Omega))$ and using the Green formula with $\left(u_\alpha - s_{\alpha h\tau}^{k,i}\right)(t)\in H_0^1(\Omega)$ a.e. $t\in\,]0,T[$, we obtain

$$\left|\!\left|\!\left|\boldsymbol{u}-\boldsymbol{s}_{h\tau}^{k,i}\right|\!\right|\!\right|_{\Omega,T}^2 \le A_1+A_2+A_3+A_4+\frac{1}{2}\left\|\left(\boldsymbol{u}-\boldsymbol{s}_{h\tau}^{k,i}\right)(\cdot,0)\right\|_\Omega^2 \tag{4.35}$$

with

$$\begin{aligned}
A_1 &:= \sum_{\alpha=1}^{2}\int_0^T \left(\tilde{f}_\alpha^n-\partial_t s_{\alpha h\tau}^{k,i}-\boldsymbol{\nabla}\cdot\boldsymbol{\sigma}_{\alpha h\tau}^{k,i}-(-1)^\alpha\lambda_{h\tau}^{k,i}, u_\alpha - s_{\alpha h\tau}^{k,i}\right)_\Omega(t)\,\mathrm{dt},\\
A_2 &:= -\sum_{\alpha=1}^{2}\int_0^T \left(\mu_\alpha^{\frac12}\boldsymbol{\nabla} s_{\alpha h\tau}^{k,i}+\mu_\alpha^{-\frac12}\boldsymbol{\sigma}_{\alpha h\tau}^{k,i}, \mu_\alpha^{\frac12}\boldsymbol{\nabla}\left(u_\alpha - s_{\alpha h\tau}^{k,i}\right)\right)_\Omega(t)\,\mathrm{dt},\\
A_3 &:= \sum_{\alpha=1}^{2}\int_0^T \left((-1)^\alpha\lambda_{h\tau}^{k,i}, u_\alpha - s_{\alpha h\tau}^{k,i}\right)_\Omega(t)\,\mathrm{dt},\\
A_4 &:= \sum_{\alpha=1}^{2}\int_0^T \left(f_\alpha-\tilde{f}_\alpha^n, u_\alpha - s_{\alpha h\tau}^{k,i}\right)_\Omega(t)\,\mathrm{dt}.
\end{aligned} \tag{4.36}$$

To bound A_1, A_2, and A_4 we proceed as follows. We apply the Cauchy–Schwarz inequality and next the Poincaré–Friedrichs inequality (4.16a) to get

$$A_1 \le \left(\sum_{n=1}^{N_\mathrm{t}}\int_{I_n}\sum_{\alpha=1}^{2}\sum_{K\in\mathcal{T}_h}\left(\eta_{\mathrm{R,K},\alpha}^{n,k,i}\right)^2(t)\,\mathrm{dt}\right)^{\frac12}\left|\!\left|\!\left|\boldsymbol{u}-\boldsymbol{s}_{h\tau}^{n,k,i}\right|\!\right|\!\right|_{\Omega,T}, \tag{4.37}$$

$$A_2 \le \left(\sum_{n=1}^{N_\mathrm{t}}\int_{I_n}\sum_{\alpha=1}^{2}\sum_{K\in\mathcal{T}_h}\left(\eta_{\mathrm{F,K},\alpha}^{n,k,i}\right)^2(t)\,\mathrm{dt}\right)^{\frac12}\left|\!\left|\!\left|\boldsymbol{u}-\boldsymbol{s}_{h\tau}^{n,k,i}\right|\!\right|\!\right|_{\Omega,T}, \tag{4.38}$$

$$A_4 \le \left(\sum_{n=1}^{N_\mathrm{t}}\int_{I_n}\sum_{\alpha=1}^{2}\sum_{K\in\mathcal{T}_h}\left(\eta_{\mathrm{osc},K,\alpha}^{n}\right)^2(t)\,\mathrm{dt}\right)^{\frac12}\left|\!\left|\!\left|\boldsymbol{u}-\boldsymbol{s}_{h\tau}^{n,k,i}\right|\!\right|\!\right|_{\Omega,T}. \tag{4.39}$$

It remains to bound the term A_3. Observe that

$$A_3 = -\int_0^T b(\boldsymbol{u}-\boldsymbol{s}_{h\tau}^{k,i}, \lambda_{h\tau}^{k,i,\mathrm{neg}})(t)\,\mathrm{dt} - \int_0^T b(\boldsymbol{u}-\boldsymbol{s}_{h\tau}^{k,i}, \lambda_{h\tau}^{k,i,\mathrm{pos}})(t)\,\mathrm{dt}.$$

Next, adding and subtracting $b(\boldsymbol{u}_{h\tau}^{k,i}, \lambda_{h\tau}^{k,i,\mathrm{pos}})$ and noting that $-b(\boldsymbol{u}, \lambda_{h\tau}^{k,i,\mathrm{pos}}) \le 0$ since $\boldsymbol{u}\in\boldsymbol{\mathcal{K}}_g^\mathrm{t}$ and $\lambda_{h\tau}^{k,i,\mathrm{pos}}(t)\ge 0$ for all $t\in\,]0,T[$, we have

$$A_3 \le A_{31}+A_{32}+A_{33}$$

with

$$A_{31} := -\int_0^T b(\boldsymbol{u}-\boldsymbol{s}_{h\tau}^{k,i}, \lambda_{h\tau}^{k,i,\mathrm{neg}})(t)\,\mathrm{dt},\ A_{32} := \int_0^T b(\boldsymbol{s}_{h\tau}^{k,i}-\boldsymbol{u}_{h\tau}^{k,i}, \lambda_{h\tau}^{k,i,\mathrm{pos}})(t)\,\mathrm{dt},\ A_{33} := \int_0^T b(\boldsymbol{u}_{h\tau}^{k,i}, \lambda_{h\tau}^{k,i,\mathrm{pos}})(t)\,\mathrm{dt}.$$

The Cauchy–Schwarz inequality and the Poincaré–Friedrichs inequality (4.16a) yield

$$\begin{aligned} A_{31} &\le h_\Omega C_{\mathrm{PF}} \left(\frac{1}{\mu_1}+\frac{1}{\mu_2}\right)^{\frac12} \left(\sum_{n=1}^{N_\mathrm{t}} \int_{I_n} \sum_{K\in\mathcal{T}_h} \left\|\lambda_h^{n,k,i,\mathrm{neg}}\right\|_K^2 (t)\,\mathrm{dt}\right)^{\frac12} \left|\!\left|\!\left|\boldsymbol{u}-\boldsymbol{s}_{h\tau}^{n,k,i}\right|\!\right|\!\right|_{\Omega,T} \\ &= \left(\sum_{n=1}^{N_\mathrm{t}} \int_{I_n} \sum_{K\in\mathcal{T}_h} \left(\eta_{\mathrm{nonc},1,K}^{n,k,i}\right)^2 (t)\,\mathrm{dt}\right)^{\frac12} \left|\!\left|\!\left|\boldsymbol{u}-\boldsymbol{s}_{h\tau}^{n,k,i}\right|\!\right|\!\right|_{\Omega,T}. \end{aligned} \tag{4.40}$$

Next, we have

$$A_{32} = \frac12 \sum_{n=1}^{N_\mathrm{t}} \int_{I_n} \sum_{K\in\mathcal{T}_h} \eta_{\mathrm{nonc},3,K}^{n,k,i}(t)\,\mathrm{dt}. \tag{4.41}$$

Furthermore, we have

$$A_{33} = \frac12 \sum_{n=1}^{N_\mathrm{t}} \int_{I_n} \sum_{K\in\mathcal{T}_h} 2\left(\lambda_h^{n,k,i,\mathrm{pos}}, u_{1h\tau}^{n,k,i}-u_{2h\tau}^{n,k,i}\right)(t)\,\mathrm{dt} = \frac12 \sum_{n=1}^{N_\mathrm{t}} \int_{I_n} \sum_{K\in\mathcal{T}_h} \eta_{\mathrm{C},K}^{n,k,i,\mathrm{pos}}(t). \tag{4.42}$$

Finally, combining (4.35)–(4.42), employing the Young inequality $ab \le \frac12\left(a^2+b^2\right)$, $(a,b)\ge 0$, and using (4.34) provides the desired result.

□

5 Distinguishing the error components and adaptive stopping criteria

In Section 4.5, we have derived an a posteriori error estimate between the exact solution and approximate solution at each semismooth Newton step $k \ge 1$ and each algebraic iterative solver step $i \ge 0$. We now provide an a posteriori error estimate distinguishing the different error components when $p = 1$ and define an adaptive algorithm.

5.1 Distinguishing the error components for $p = 1$

Definition 5.1. *We define the total discretization error estimator $\eta_{\mathrm{disc}}^{k,i}$, the total semismooth linearization error estimator $\eta_{\mathrm{lin}}^{k,i}$, and the total algebraic error estimator $\eta_{\mathrm{alg}}^{k,i}$ respectively by*

$$\begin{aligned} \eta_{\mathrm{disc}}^{k,i} &:= \left\{ 3\left(\left\{\sum_{n=1}^{N_\mathrm{t}} \int_{I_n} \sum_{K\in\mathcal{T}_h} \sum_{\alpha=1}^{2} \left(\eta_{\mathrm{R,K},\alpha}^{n,k,i}\right)^2\right\}^{\frac12} \right.\right. \\ &\quad \left.\left. + \left\{\sum_{n=1}^{N_\mathrm{t}} \int_{I_n} \sum_{K\in\mathcal{T}_h} \sum_{\alpha=1}^{2} \left\|\mu_\alpha^{\frac12}\boldsymbol{\nabla} s_{\alpha h\tau}^{n,k,i} + \mu_\alpha^{-\frac12}\boldsymbol{\sigma}_{\alpha h\tau,\mathrm{disc}}^{n,k,i}\right\|_\Omega^2\right\}^{\frac12}\right)^2 + \left|\sum_{n=1}^{N_\mathrm{t}} \int_{I_n} \sum_{K\in\mathcal{T}_h} \eta_{\mathrm{C},K}^{n,k,i,\mathrm{pos}}\right|\right\}^{\frac12}, \\ \eta_{\mathrm{lin}}^{k,i} &:= \left\{ 3\sum_{n=1}^{N_\mathrm{t}} \int_{I_n} \sum_{K\in\mathcal{T}_h} \left(\eta_{\mathrm{nonc},1,K}^{n,k,i}\right)^2 + \left|\sum_{n=1}^{N_\mathrm{t}} \int_{I_n} \sum_{K\in\mathcal{T}_h} \eta_{\mathrm{nonc},3,K}^{n,k,i}\right|\right\}^{\frac12} + \left\{\sum_{n=1}^{N_\mathrm{t}} \int_{I_n} \sum_{K\in\mathcal{T}_h} \sum_{\alpha=1}^{2} \left(\eta_{\mathrm{nonc},2,K,\alpha}^{n,k,i}\right)^2\right\}^{\frac12}, \\ \eta_{\mathrm{alg}}^{k,i} &:= \left\{ 3\sum_{n=1}^{N_\mathrm{t}} \int_{I_n} \sum_{K\in\mathcal{T}_h} \sum_{\alpha=1}^{2} \left\|\mu_\alpha^{-\frac12}\boldsymbol{\sigma}_{\alpha h\tau,\mathrm{alg}}^{n,k,i}\right\|_K^2 (t)\,\mathrm{dt}\right\}^{\frac12}, \quad \eta_{\mathrm{init}} := \left\{\left\|\left(\boldsymbol{u}-\boldsymbol{s}_{h\tau}^{k,i}\right)(\cdot,0)\right\|_\Omega^2\right\}^{\frac12}. \end{aligned}$$

Using Definition 5.1, we have:

Corollary 5.2. *For $p = 1$, we have the following a posteriori error estimate distinguishing the error components:*

$$\left|\!\left|\!\left|\boldsymbol{u}-\boldsymbol{u}_{h\tau}^{k,i}\right|\!\right|\!\right|_{\Omega,T} \le \eta_{\mathrm{disc}}^{k,i} + \eta_{\mathrm{lin}}^{k,i} + \eta_{\mathrm{alg}}^{k,i} + \eta_{\mathrm{init}}.$$

Proof. The triangle inequality gives $\eta_{\mathrm{F,K},\alpha}^{n,k,i} \le \left\| \mu_\alpha^{\frac{1}{2}} \boldsymbol{\nabla} s_{\alpha h\tau}^{n,k,i} + \mu_\alpha^{-\frac{1}{2}} \boldsymbol{\sigma}_{\alpha h\tau,\mathrm{disc}}^{n,k,i} \right\|_K + \left\| \mu_\alpha^{-\frac{1}{2}} \boldsymbol{\sigma}_{\alpha h\tau,\mathrm{alg}}^{n,k,i} \right\|_K$. Next, using the Minkowski inequality to separate the algebraic contribution from the discretization one and employing after the result $(A_1 + A_2 + A_3)^2 \le 3\left(A_1^2 + A_2^2 + A_3^2\right)$ for $A_1, A_2, A_3 \ge 0$ to gather the discretization terms, we obtain the desired result. □

5.2 Adaptive inexact semismooth Newton algorithm

We finally present our adaptive inexact semismooth Newton algorithm. Following the concept of [16, 58, 55], it is designed to only perform the linearization and algebraic resolutions with minimal necessary precision, and thus to avoid unnecessary iterations. Let γ_{lin} and γ_{alg} be two positive parameters, typically of order 0.1, representing the desired relative sizes of the algebraic and linearization errors. Note that as the estimators of Definition 5.1 are global, we consider their restrictions $\eta_{\mathrm{disc}}^{n,k,i}$, $\eta_{\mathrm{lin}}^{n,k,i}$, and $\eta_{\mathrm{alg}}^{n,k,i}$ to the time interval I_n as follows:

$$\eta_{\mathrm{disc}}^{n,k,i} := \left(\int_{I_n} \sum_{K\in\mathcal{T}_h} \left(\sum_{\alpha=1}^{2} 6 \left(\left(\eta_{\mathrm{R,K},\alpha}^{n,k,i}\right)^2 + \left\| \mu_\alpha^{\frac{1}{2}} \boldsymbol{\nabla} s_{\alpha h\tau}^{n,k,i} + \mu_\alpha^{-\frac{1}{2}} \boldsymbol{\sigma}_{\alpha h\tau,\mathrm{disc}}^{n,k,i} \right\|_K^2 \right) + |\eta_{\mathrm{C},K}^{n,k,i,\mathrm{pos}}| \right)(t)\,\mathrm{dt} \right)^{\frac{1}{2}}, \tag{5.1}$$

$$\eta_{\mathrm{lin}}^{n,k,i} := \left(\int_{I_n} 2 \left(\sum_{K\in\mathcal{T}_h} \left(3 \left(\eta_{\mathrm{nonc},1,K}^{n,k,i}\right)^2 + |\eta_{\mathrm{nonc},3,K}^{n,k,i}| \right) + \left\| \boldsymbol{s}_{h\tau}^{n,k,i} - \boldsymbol{u}_{h\tau}^{n,k,i} \right\|_\Omega^2 \right)(t)\,\mathrm{dt} \right)^{\frac{1}{2}}, \tag{5.2}$$

$$\eta_{\mathrm{alg}}^{n,k,i} := \left(3\Delta t_n \sum_{K\in\mathcal{T}_h} \sum_{\alpha=1}^{2} \left\| \mu_\alpha^{-\frac{1}{2}} \boldsymbol{\sigma}_{\alpha h\tau,\mathrm{alg}}^{n,k,i} \right\|_K^2 \right)^{\frac{1}{2}}. \tag{5.3}$$

Let $n \ge 1$ be fixed. Supposing that η_{init} and $\eta_{\mathrm{osc},\alpha}^{n,k,i}$ are negligible, we propose:

Algorithm 1 Adaptive inexact semismooth Newton algorithm at each time step n

0. Choose an initial vector $\boldsymbol{X}_h^{n,0} \in \mathbb{R}^{3\mathcal{N}_{\mathrm{d}}^{p,\mathrm{int}}}$ and set $k = 1$.

1. From $\boldsymbol{X}_h^{n,k-1}$ define $\mathbb{A}^{n,k-1} \in \mathbb{R}^{3\mathcal{N}_{\mathrm{d}}^{p,\mathrm{int}},3\mathcal{N}_{\mathrm{d}}^{p,\mathrm{int}}}$ and $\boldsymbol{B}^{n,k-1} \in \mathbb{R}^{3\mathcal{N}_{\mathrm{d}}^{p,\mathrm{int}}}$ by (3.27).

2. Consider the linear system

$$\mathbb{A}^{n,k-1} \boldsymbol{X}_h^{n,k} = \boldsymbol{B}^{n,k-1}. \tag{5.4}$$

3. Set $\boldsymbol{X}_h^{n,k,0} = \boldsymbol{X}_h^{n,k-1}$ as initial guess for the iterative linear solver and set $i = 0$.

4*a*. Perform $\nu \ge 1$ steps of a chosen linear solver for (5.4), starting from $\boldsymbol{X}_h^{n,k,i}$. Set $i = i + \nu$. This yields on step i an approximation $\boldsymbol{X}_h^{n,k,i}$ to $\boldsymbol{X}_h^{n,k}$ satisfying

$$\mathbb{A}^{n,k-1} \boldsymbol{X}_h^{n,k,i} = \boldsymbol{B}^{n,k-1} - \boldsymbol{R}^{n,k,i}.$$

4*b*. Compute the estimators of (5.1)–(5.3) and check the stopping criterion for the linear solver in the form:

$$\eta_{\mathrm{alg}}^{n,k,i} \le \gamma_{\mathrm{alg}} \max\left\{ \eta_{\mathrm{disc}}^{n,k,i}, \eta_{\mathrm{lin}}^{n,k,i} \right\}. \tag{5.5}$$

If satisfied, set $\boldsymbol{X}_h^{n,k} = \boldsymbol{X}_h^{n,k,i}$. If not go back to **4*a***.

5. Check the stopping criterion for the nonlinear solver in the form

$$\eta_{\mathrm{lin}}^{n,k,i} \le \gamma_{\mathrm{lin}} \eta_{\mathrm{disc}}^{n,k,i}. \tag{5.6}$$

If satisfied, return $\boldsymbol{X}_h^n = \boldsymbol{X}_h^{n,k}$. If not, set $k = k + 1$ and go back to **1**.

6 Numerical experiments

This section illustrates numerically our theoretical developments in the case of affine finite elements $p = 1$. We first assume that our semismooth Newton solver as well as our iterative algebraic solver have converged, *i.e.*, we apply the "exact semismooth Newton" method as described in Section 3.5. In this scenario, the semismooth Newton index k and the linear iterative algebraic solver index i will be discarded. We extend to the parabolic setting the test case given in [47] in which the domain Ω is given by the unit disk: $\Omega := \{(r, \theta) \in [0, 1] \times [0, 2\pi]\}$. We are interested in the shape of the numerical solution after several time steps and in the behavior of the estimators at convergence of the solvers given by Theorem 4.3.

Second, we will focus on our adaptive inexact semismooth Newton strategy given by Algorithm 1 of Section 5.2. For this purpose, we will consider the geometry given in the first test case with different source terms. We will test our adaptive strategy with two semismooth Newton solvers: the Newton-min solver (see (3.23)) and the Newton–Fischer–Burmeister solver (see (3.24)). The iterative algebraic solver that we employ at each semismooth Newton step $k \geq 1$ is GMRES (see [65, 53, 66]) with an ILU preconditioner with zero level fill-in. For each semismooth method, we compare two different approaches: the exact Newton method and the adaptive inexact Newton method. In the exact Newton case, we simulate an exact resolution in the sense that the nonlinear stopping criterion (3.30) is considered with $\varepsilon_{\mathrm{lin}} = 10^{-9}$ and the linear stopping criterion (3.32) is used with $\varepsilon_{\mathrm{alg}}^k = 10^{-11}$ for all Newton iterations k. For the adaptive inexact semismooth Newton strategy, we consider the stopping criteria (5.5) and (5.6) with $\gamma_{\mathrm{lin}} = \gamma_{\mathrm{alg}} = 10^{-3}$.

For these two studies, the parameters μ_1 and μ_2 are set to 1 and the boundary condition for the first unknown g is equal to 0.05. We consider a mesh containing approximately 21 000 elements. For the sake of simplicity, we consider a constant time step $\Delta t_n = \Delta t = 0.001$ for all $1 \leq n \leq N_{\mathrm{t}} = 300$ and the final time of simulation $t_{\mathrm{F}} = 0.3$. The initial guess $\boldsymbol{X}_h^0 \in \mathbb{R}^{2\mathcal{N}_h^{\mathrm{int}}}$ has its first $\mathcal{N}_h^{\mathrm{int}}$ components equal to g and its next components equal to zero.

6.1 Exact semismooth Newton method

Following [47], we take

$$f_1(r,\theta,t) := \begin{cases} -10g & \text{if } r \leq 1/\sqrt{2}, \\ -8g & \text{if } r \geq 1/\sqrt{2}, \end{cases} \qquad f_2(r,\theta,t) := \begin{cases} -6g & \text{if } r \leq 1/\sqrt{2}, \\ -g\dfrac{1+8r-18r^2}{r}\dfrac{\sqrt{2}}{\sqrt{2}-1} & \text{if } r \geq 1/\sqrt{2}. \end{cases}$$

In this case, $f_\alpha|_{I_n} = \tilde{f}_\alpha^n$, so the data oscillation estimator $\eta_{\mathrm{osc},\alpha}^n$ is zero.

Figure 1 displays for three time values $t = 0.02$, $t = 0.17$, and $t = 0.3$ the behavior of the numerical solution $(u_{1h}^n, u_{2h}^n, \lambda_h^n)$, as well as the behavior of the constraint estimator $\eta_{\mathrm{C},K}^n$. In the first situation, corresponding to the beginning of the simulation $t = 0.02$ (see the top of Figure 1), the complementarity constraint $u_{1h}^n - u_{2h}^n > 0$ is satisfied, and then the discrete Lagrange multiplier λ_h^n as well as the constraint estimator $\eta_{\mathrm{C},K}^n$ vanish. Next, we represent the numerical solution at the time value $t = 0.17$ where u_{1h}^n and u_{2h}^n coincide in a subset of Ω. The constraint estimator detects at each time step the elements where u_{1h}^n and u_{2h}^n become in contact (or detach from one another). Finally, at the end of the simulation $t = 0.3$, see the bottom of Figure 1, the discrete Lagrange multiplier λ_h^n is positive in the whole area $r \leq \frac{1}{\sqrt{2}}$, recovering the numerical result of the stationary case [47]. We note that the constraint estimator $\eta_{\mathrm{C},K}^n$ take very small values.

Figure 2 displays the behavior of the flux estimator $\eta_{\mathrm{F},K,2}^n$ and of the residual estimator $\eta_{\mathrm{R},K,2}^n$ (see Theorem 4.3) associated to the second discrete unknown u_{2h}^n at the final simulation time $t = 0.3$. We observe that the residual estimator $\eta_{\mathrm{R},K,2}^n$ is small with respect to the flux estimator $\eta_{\mathrm{F},K,2}^n$. Furthermore, in several elements $K \in \mathcal{T}_h$, the estimator $\eta_{\mathrm{F},K,2}^n$ is quite large which corresponds to zones where the finite element discretization error is important.

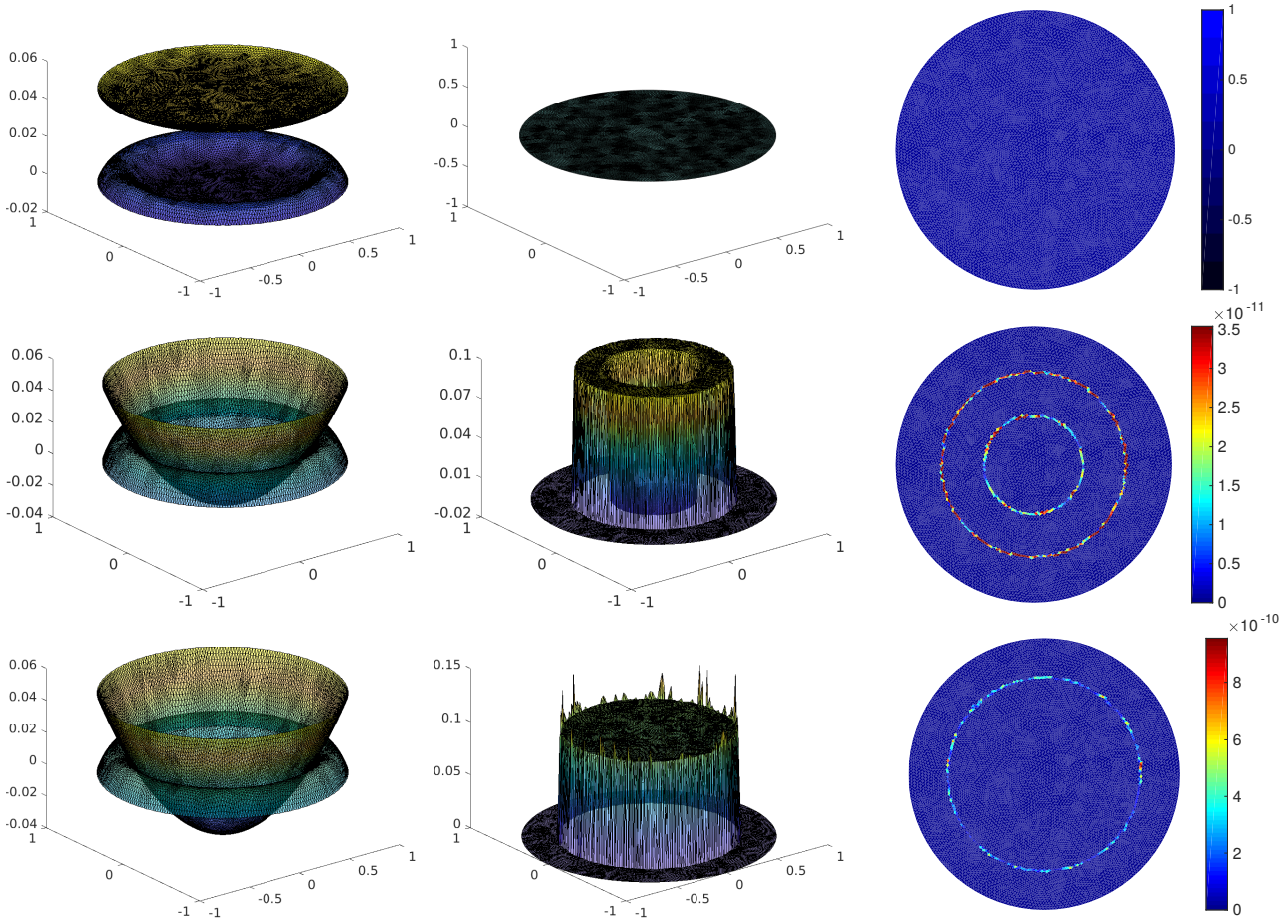

Figure 1: Numerical solution and constraint estimators at convergence for approximately 21 000 elements. First column: approximations u_{1h}^n and u_{2h}^n, second column: Lagrange multipliers λ_h^n, third column: constraint estimators; all respectively at times $t = 0.02$, $t = 0.17$, and $t = 0.3$.

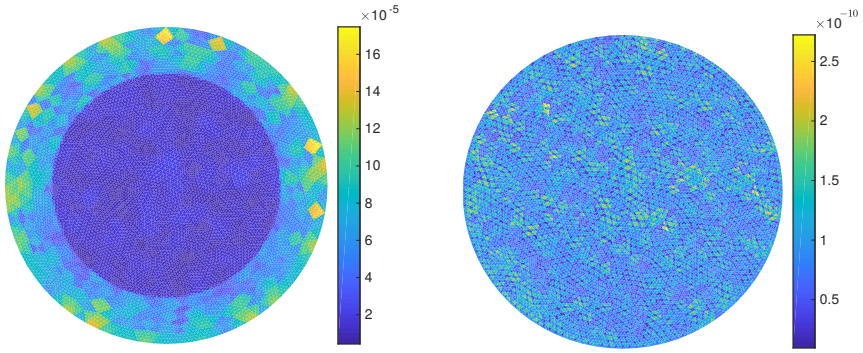

Figure 2: Estimators at convergence for approximately 21 000 elements at $t = 0.3$. Left: flux estimator $\eta_{\mathrm{F},K,2}^n$. Right: residual estimator $\eta_{\mathrm{R},K,2}^n$.

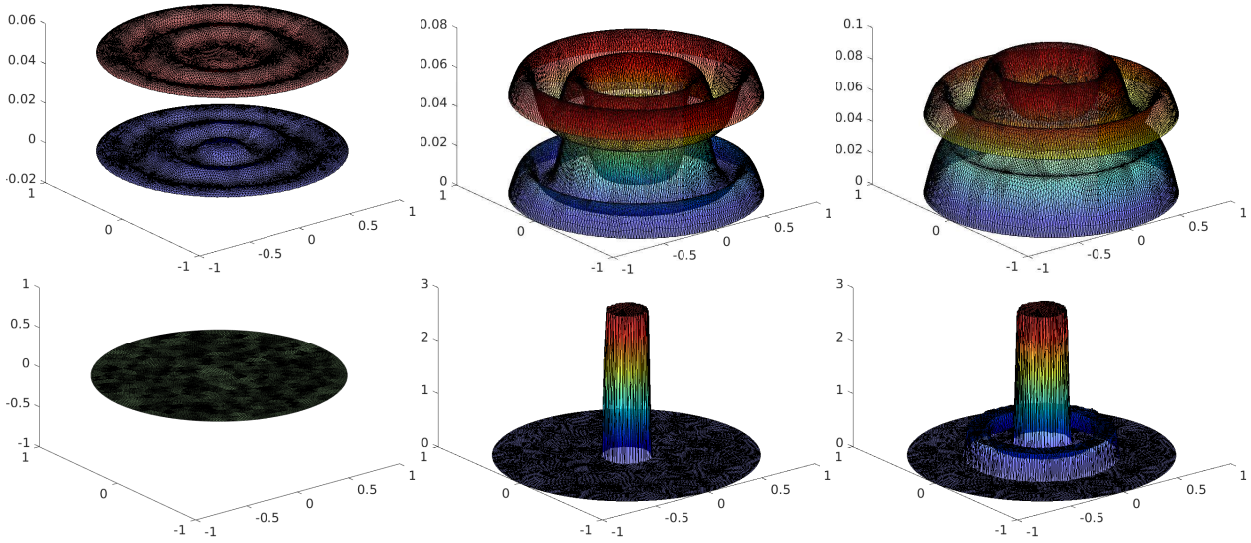

Figure 3: Numerical solution at convergence for approximately 21 000 elements. First row: u_{1h}^n and u_{2h}^n at the time values $t = 0.001$, $t = 0.03$, and $t = 0.3$. Second row: Lagrange multiplier λ_h^n at the time values $t = 0.001$, $t = 0.03$, and $t = 0.3$.

6.2 Adaptive inexact algorithms

The domain Ω is here still the unit disk but we consider the data f_1 and f_2 given by

$$f_1(r,\theta,t) := \begin{cases} -20g & \text{if } r \le 1/5, \\ -50g & \text{if } 1/5 \le r \le 2/5, \\ +50g & \text{if } 2/5 \le r \le 3/5, \\ -50g & \text{if } 3/5 \le r \le 4/5, \\ +50g & \text{if } 4/5 \le r \le 1, \end{cases} \quad f_2(r,\theta,t) := \begin{cases} +90g & \text{if } r \le 1/5, \\ -40g & \text{if } 1/5 \le r \le 2/5, \\ +70g & \text{if } 2/5 \le r \le 3/5, \\ -30g & \text{if } 3/5 \le r \le 4/5, \\ +40g & \text{if } 4/5 \le r \le 1. \end{cases}$$

Here again $\eta_{\mathrm{osc},\alpha}^n$ vanish.

First of all, we display for several time steps the behavior of the numerical solution. Next, for a fixed time value, we represent the estimators as a function of the Newton iterations. Furthermore, for one selected Newton iteration, we also present the evolution of the various estimators as a function of the GMRES iterations. Finally, we test for each adaptive inexact semismooth Newton solver its overall performance and we compare the results with the classical exact resolution.

Figure 3 displays the numerical solution at three time values when the Newton-min solver and GMRES solver have converged. There are three different phases in the simulation: at first, there is no contact, see the left column of Figure 3. In the second period, the contact occurs in a disk around the center of the domain and we observe in the discrete Lagrange multiplier λ_h^n a peak indicating the elements where u_{1h}^n and u_{2h}^n coincide. In the last period (top right and bottom right of Figure 3), there exist two separate contact zones, a disk for $0 \le r \le 1/5$ and a ring for $2/5 \le r \le 3/5$. Furthermore, these contacts occur at $t \approx 0.011$ and $t \approx 0.060$; we will see below in Figures 5 and 8 (left) that more Newton-min iterations will be required at these transition periods.

6.2.1 Newton-min linearization

Figure 4 presents the evolution of the various estimators as a function of the Newton-min iterations (left) and the behavior of the various estimators as a function of the GMRES iterations at the first Newton-min step (right) at the fixed time value $t = 0.084$. From the left part of Figure 4, we observe that the discretization estimator globally dominates and coincides with the total estimator (the two curves are roughly superimposed). The linearization estimator (blue curve) is small from the first Newton-min iteration (around 10^{-6}) and next increases at the second iteration (around 10^{-3}) and afterwards decreases

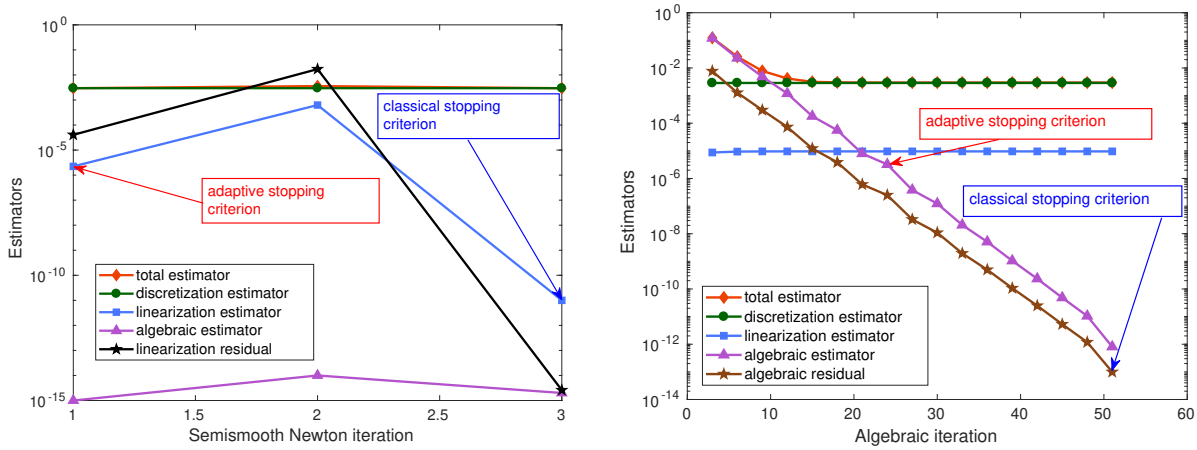

Figure 4: At $t = 0.084$. Left: estimators as a function of the Newton-min iterations. Right: estimators as a function of the GMRES iterations on 1st Newton-min iteration.

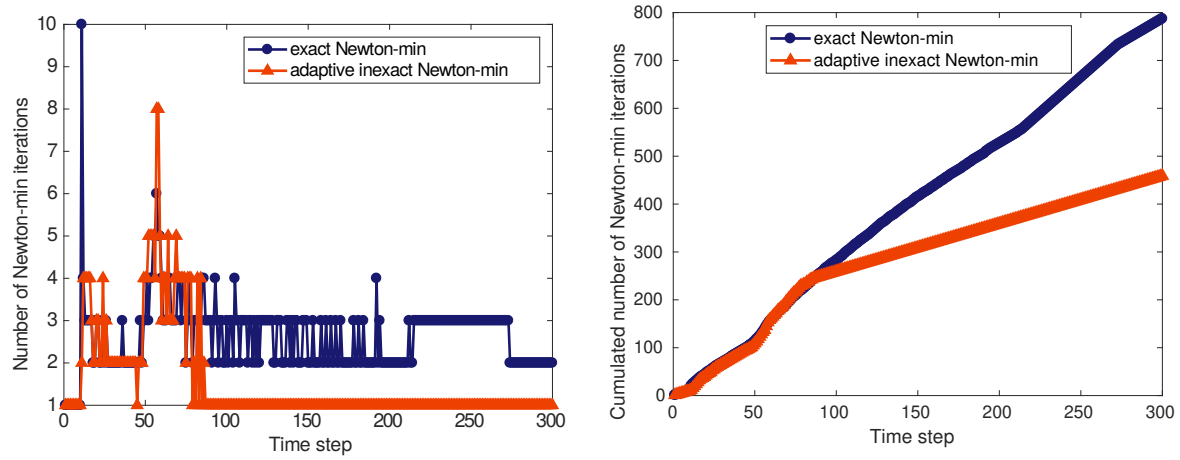

Figure 5: Left: number of Newton-min iterations at each time step. Right: cumulated number of Newton-min iterations as a function of time.

rapidly to reach the value 10^{-11} at the third Newton-min iteration. From the first Newton-min iteration, the discretization estimator (coinciding with the total estimator) stagnates which means that the other components of the error do not influence the behavior of the total error estimator. Then, the Newton-min algorithm performs unnecessary iterations and can be stopped at the first iteration. In right part of Figure 4, we test our adaptive inexact Newton-min strategy in terms of the GMRES iterations for the first Newton-min iteration. We observe that the discretization estimator as well as the linearization estimator roughly stagnate after few iterations. The algebraic estimator is large at the beginning of the iterations and influences the behavior of the total estimator but decreases rapidly to reach at $i = 53$ the value 10^{-12}. The adaptive inexact Newton-min algorithm stops the GMRES after $i = 24$ iterations, when the total estimator almost coincides with the discretization estimator. Note that the curve of the algebraic estimator is here close to the curve of the algebraic residual.

Figure 5 provides the number of Newton-min iterations and the cumulated number of Newton-min iterations required to satisfy the given stopping criteria at each time step of the simulation. In particular, the first graph shows that for almost all time steps, our adaptive strategy is cheaper in terms of Newton-min iterations than the exact resolution. Observe that at some (rare) time steps (13 and 57 for instance), the adaptive approach requires more iterations than the classical resolution: it detects automatically when a few more iterations are necessary to preserve the accuracy. Interestingly, this occurs at times when u^n_{1h} and u^n_{2h} enter in contact. The second graph presents the cumulated number of Newton-min iterations as a

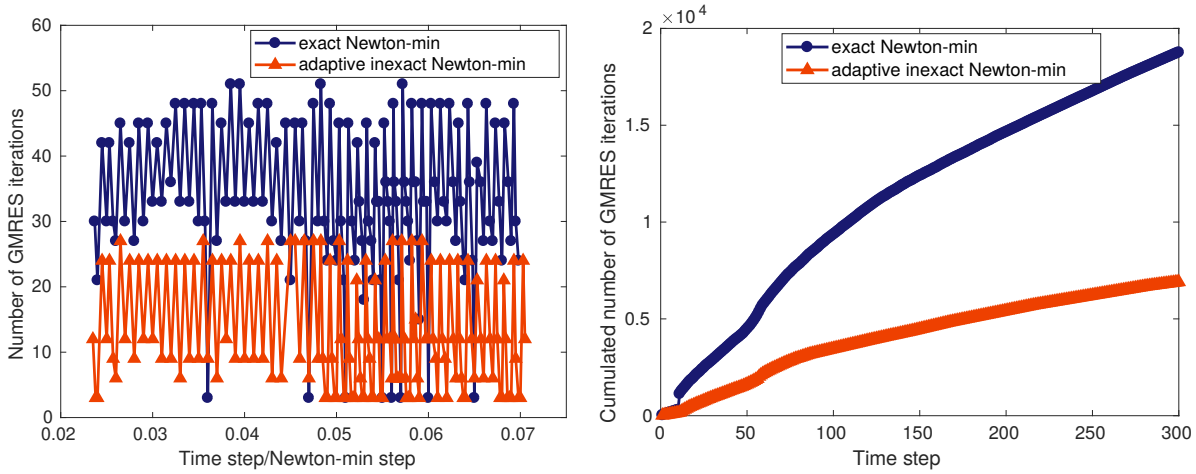

Figure 6: Left: number of GMRES iterations per time and Newton-min steps. Right: cumulated number of GMRES iterations as a function of time.

$\gamma_{\text{alg}} = \gamma_{\text{lin}} = 10^{-3}$	$t_n = 0.001$	$t_n = 0.011$	$t_n = 0.07$	$t_n = 0.15$	$t_n = 0.3$
$\left\|\mu_1^{\frac{1}{2}} \boldsymbol{\nabla}(u_{1h}^{n,\text{exact}} - u_{1h}^{n,\text{adapt}})\right\|_\Omega$	1.41×10^{-7}	1.81×10^{-7}	8.83×10^{-8}	2.03×10^{-7}	3.44×10^{-7}
$\left\|\mu_2^{\frac{1}{2}} \boldsymbol{\nabla}(u_{2h}^{n,\text{exact}} - u_{2h}^{n,\text{adapt}})\right\|_\Omega$	1.32×10^{-7}	1.63×10^{-7}	8.82×10^{-8}	1.71×10^{-7}	3.43×10^{-7}
$\left\|\lambda_h^{n,\text{exact}} - \lambda_h^{n,\text{adapt}}\right\|_\Omega$	0	2.77×10^{-4}	3.19×10^{-4}	4.25×10^{-4}	8.07×10^{-8}

Table 1: Accuracy of the adaptive inexact Newton-min solution for several time values.

function of the time step. We observe a substantial benefit for our adaptive inexact Newton-min approach as it saves at the end of the simulation roughly 50% of the iterations.

In Figure 6, left, we plot the number of GMRES iterations per time and Newton-min steps, between time steps 22 and 72. We can observe that significantly fewer iterations are needed in the adaptive approach. We illustrate the overall performance of the two approaches in Figure 6, right, where we display the cumulated number of GMRES iterations for the two methods as a function of the time steps. The second graph shows that the adaptive inexact Newton-min algorithm requires approximately 7000 cumulated iterations to converge whereas the classical algorithm requires roughly 19 000 iterations. Our adaptive algorithm thus saves many unnecessary iterations.

In Table 1, we give the global energy norm of the difference between the approximate resolution given by the exact solution and the approximate solution provided by the adaptive inexact Newton-min algorithm. We observe that for several time values, the three numerical solutions are close to each other, which confirms that our adaptive strategy does not violate the accuracy of the numerical solution.

6.2.2 Newton–Fischer–Burmeister linearization

In this part, we proceed as in Section 6.2.1 employing this time the C-function of Fischer–Burmeister.

Figure 7 represents the evolution of the various estimators as a function of the Newton–Fischer–Burmeister iterations (left) and the behavior of the various estimators as a function of the GMRES iterations at the first Newton–Fischer–Burmeister step (right), at the fixed time value $t = 0.011$. From the left plot, we observe that the discretization estimator globally dominates and almost coincides with the total estimator (the two curves are roughly superimposed). The linearization estimator (blue curve, squares) is small and decreases rapidly after $k = 5$ steps (adaptive stopping criterion) to reach the value of 10^{-11} at $k = 11$ (classical stopping criterion). Taking $\gamma_{\text{lin}} = 10^{-2}$ instead of $\gamma_{\text{lin}} = 10^{-3}$ in (5.6) will reduce the number of Newton–Fischer–Burmeister iterations at this instant to 4. In the right plot, we take the first Newton–Fischer–Burmeister iteration and we observe that the discretization estimator as well as the linearization estimator stagnate from the beginning of the iterations, while the algebraic estimator is dominant at the

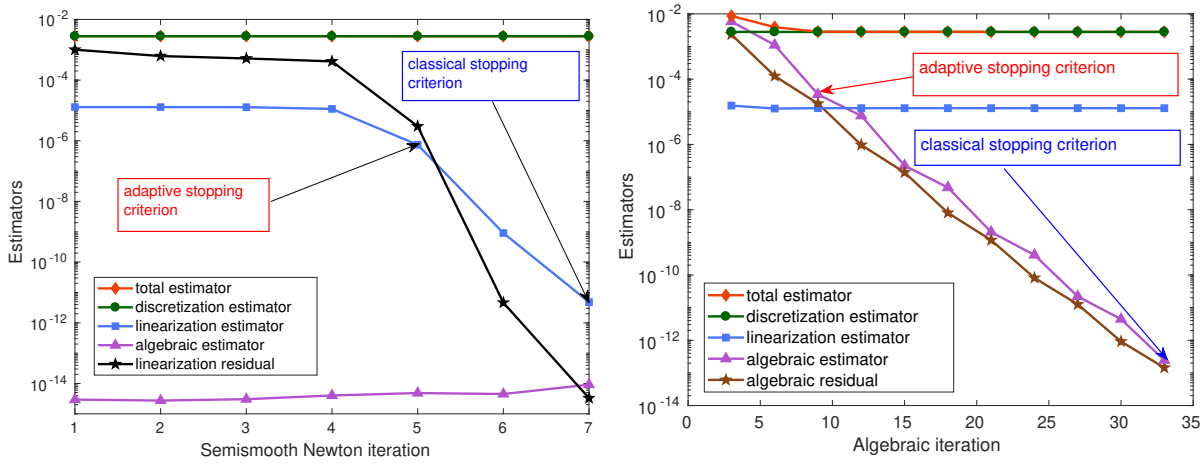

Figure 7: At $t = 0.11$. Left: estimators as a function of the Newton–Fischer–Burmeister iterations. Right: estimators as a function of the GMRES iterations at the first Newton–Fischer–Burmeister step.

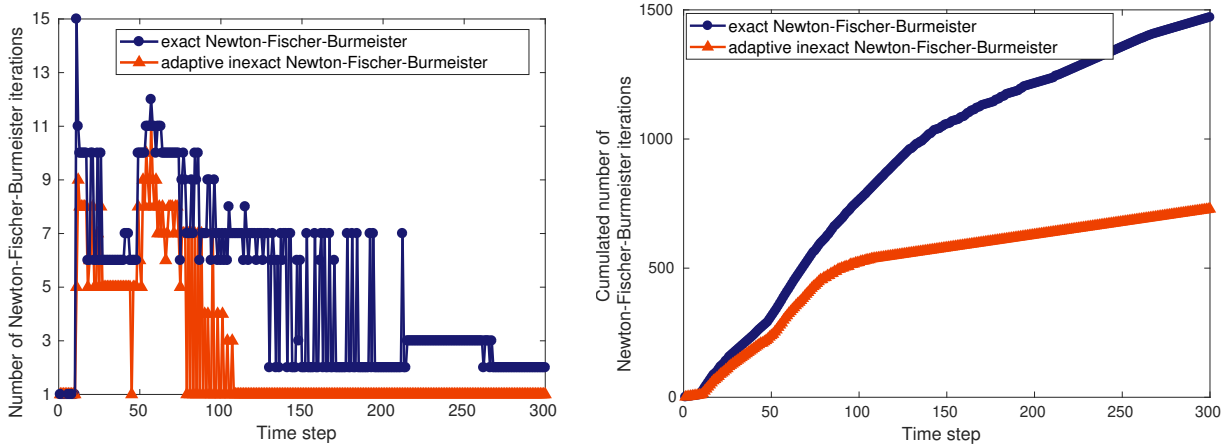

Figure 8: Left: number of Newton–Fischer–Burmeister iterations at each time step. Right: cumulated number of Newton–Fischer–Burmeister iterations as a function of time.

beginning of the iterations. The adaptive inexact Newton–Fischer–Burmeister algorithm stops the GMRES iterations at $i = 9$, whereas the classical criterion stops at $i = 33$. Note that as for the Newton-min case, the behavior of the algebraic estimator follows here closely the one of the algebraic residual.

Figure 8 focuses on the number of Newton–Fischer–Burmeister iterations required to satisfy the various stopping criteria at each time step. We observe from the first figure that the adaptive strategy (red curve) is economic in comparison with the classical resolution (blue curve) especially from $t = 0.1$ onwards, where the adaptive algorithm requires 1 Newton–Fischer–Burmeister iteration at each time step. Furthermore, the right plot depicts the overall performance in terms of Newton–Fischer–Burmeister iterations. With no surprise, the adaptive resolution requires at the end of the simulation much fewer semismooth Newton iterations (approximately 700 for the adaptive algorithm and 1500 for the classical resolution). Thus, our adaptive semismooth approach reduces by 50% the number of Newton–Fischer–Burmeister iterations.

Figure 9 illustrates the overall performance of the two approaches. We display the number of GMRES iterations for each linear system solved as a function of time/Newton–Fischer–Burmeister step between $t = 0.014$ and $t = 0.057$ (left) and the cumulated number of GMRES iterations as a function of time step (right). In particular, we see that our adaptive strategy is very economic in terms of the total algebraic iterations as it requires at the end on the simulation approximately 7000 iterations whereas the classical resolution requires roughly 27 000 iterations. To close this section, we present in Table 2 the energy norm of

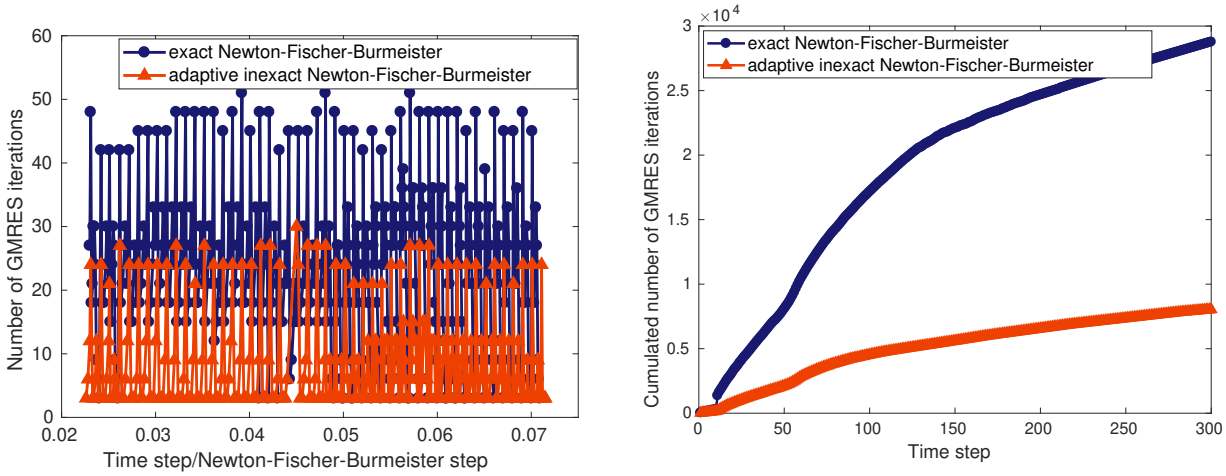

Figure 9: Left: number of GMRES iterations per time and Newton–Fischer–Burmeister step. Right: cumulated number of GMRES iterations per time step.

$\gamma_{\text{alg}} = \gamma_{\text{lin}} = 10^{-3}$	$t_n = 0.001$	$t_n = 0.011$	$t_n = 0.07$	$t_n = 0.15$	$t_n = 0.3$
$\left\|\mu_1^{\frac{1}{2}} \boldsymbol{\nabla}(u_{1h}^{n,\text{exact}} - u_{1h}^{n,\text{adapt}})\right\|_\Omega$	9.9×10^{-6}	1.7×10^{-5}	5.8×10^{-5}	7.7×10^{-5}	2.1×10^{-3}
$\left\|\mu_2^{\frac{1}{2}} \boldsymbol{\nabla}(u_{2h}^{n,\text{exact}} - u_{2h}^{n,\text{adapt}})\right\|_\Omega$	5.5×10^{-6}	2.1×10^{-5}	7.1×10^{-5}	1.8×10^{-4}	2.1×10^{-3}
$\left\|\lambda_h^{n,\text{exact}} - \lambda_h^{n,\text{adapt}}\right\|_\Omega$	0	7.9×10^{-3}	3.3×10^{-4}	2.3×10^{-2}	2.2×10^{-7}

Table 2: Accuracy of the adaptive inexact Newton–Fischer–Burmeister solution for several time values.

the difference between the exact solution given by the classical Newton–Fischer–Burmeister algorithm and the adaptive inexact one for several time values. In particular, it measures the accuracy and precision of our adaptive strategy. We observe that each numerical unknown obtained by the adaptive strategy is close to the unknown given by the classical resolution. Thus, our adaptive algorithm saves many iterations and does not deteriorate the numerical solution.

7 Conclusion

In this work, we focused on deriving a posteriori error estimates for a model parabolic variational inequality. We employed the conforming $\mathbb{P}_p$ finite element method for the discretization in space and the backward Euler scheme for the discretization in time. We designed a posteriori error estimates when $p = 1$ valid at convergence of the semismooth Newton solver and of the iterative algebraic solver. In this case, we estimate both energy and time derivative errors. Next, we extended the study to all polynomial degrees $p \geq 1$ and for each semismooth Newton step $k \geq 1$ and each iterative linear algebraic solver step $i \geq 0$. Here, we only estimate the energy error. We finally proposed an adaptive inexact semismooth Newton algorithm based on the a posteriori error estimators that we derived whose main idea is to stop the two involved iterative solvers at a suitable moment decided adaptively. We have presented numerical experiments for two inexact semismooth Newton solvers for $p = 1$ and we showed that our adaptive inexact semismooth strategy saves many iterations while preserving the accuracy of the numerical solution.

References

[1] R. Glowinski, Numerical methods for nonlinear variational problems, Scientific Computation, Springer-Verlag, Berlin, 2008, reprint of the 1984 original.

[2] J.-L. Lions, Quelques méthodes de résolution des problèmes aux limites non linéaires, Dunod; Gauthier-Villars, Paris, 1969.

[3] P. Jaillet, D. Lamberton, B. Lapeyre, Variational inequalities and the pricing of american options, ACTA APPL. MATH 21 (1990) 263–289.

[4] P. Wilmott, J. Dewynne, S. Howison, Option Pricing: Mathematical Models and Computation, Oxford Financial, 1998.
URL https://books.google.fr/books?id=cGuGcgAACAAJ

[5] A. Bensoussan, J.-L. Lions, Applications of variational inequalities in stochastic control, Vol. 12 of Studies in Mathematics and its Applications, North-Holland Publishing Co., Amsterdam-New York, 1982, translated from the French.

[6] R. Glowinski, J.-L. Lions, R. Trémolières, Numerical analysis of variational inequalities, Vol. 8 of Studies in Mathematics and its Applications, North-Holland Publishing Co., Amsterdam-New York, 1981, translated from the French.

[7] Y. Achdou, F. Hecht, D. Pommier, A posteriori error estimates for parabolic variational inequalities, J. Sci. Comput. 37 (3) (2008) 336–366. doi:10.1007/s10915-008-9215-7.
URL https://doi.org/10.1007/s10915-008-9215-7

[8] T. Gudi, P. Majumder, Convergence analysis of finite element method for a parabolic obstacle problem, J. Comput. Appl. Math. 357 (2019) 85–102. doi:10.1016/j.cam.2019.02.026.
URL https://doi.org/10.1016/j.cam.2019.02.026

[9] R. Glowinski, J.-L. Lions, R. Trémolières, Analyse numérique des inéquations variationnelles. Tome 2, Dunod, Paris, 1976, applications aux phénomènes stationnaires et d'évolution, Méthodes Mathématiques de l'Informatique, 5.

[10] R. Glowinski, J.-L. Lions, R. Trémolières, Analyse numérique des inéquations variationnelles. Tome 1, Dunod, Paris, 1976, théorie générale premiéres applications, Méthodes Mathématiques de l'Informatique, 5.

[11] Z. Chen, R. H. Nochetto, Residual type a posteriori error estimates for elliptic obstacle problems, Numer. Math. 84 (4) (2000) 527–548. doi:10.1007/s002110050009.
URL https://doi.org/10.1007/s002110050009

[12] A. Veeser, Efficient and reliable a posteriori error estimators for elliptic obstacle problems, SIAM J. Numer. Anal. 39 (1) (2001) 146–167. doi:10.1137/S0036142900370812.
URL https://doi.org/10.1137/S0036142900370812

[13] D. Braess, A posteriori error estimators for obstacle problems—another look, Numer. Math. 101 (3) (2005) 415–421. doi:10.1007/s00211-005-0634-1.
URL https://doi.org/10.1007/s00211-005-0634-1

[14] F. Ben Belgacem, C. Bernardi, A. Blouza, M. Vohralík, A finite element discretization of the contact between two membranes, M2AN Math. Model. Numer. Anal. 43 (1) (2008) 33–52. doi:10.1051/m2an/2008041.
URL http://dx.doi.org/10.1051/m2an/2008041

[15] M. Bürg, A. Schröder, A posteriori error control of *hp*-finite elements for variational inequalities of the first and second kind, Comput. Math. Appl. 70 (12) (2015) 2783–2802. doi:10.1016/j.camwa.2015.08.031.
URL https://doi.org/10.1016/j.camwa.2015.08.031

[16] J. Dabaghi, V. Martin, M. Vohralík, Adaptive inexact semismooth Newton methods for the contact problem between two membranes, hAL Preprint 01666845, submitted for publication (2018).
URL https://hal.inria.fr/hal-01666845

[17] F. Wang, W. Han, X.-L. Cheng, Discontinuous Galerkin methods for solving elliptic variational inequalities, SIAM J. Numer. Anal. 48 (2) (2010) 708–733. doi:10.1137/09075891X.
URL https://doi.org/10.1137/09075891X

[18] T. Gudi, K. Porwal, A posteriori error control of discontinuous Galerkin methods for elliptic obstacle problems, Math. Comp. 83 (286) (2014) 579–602. doi:10.1090/S0025-5718-2013-02728-7.
URL https://doi.org/10.1090/S0025-5718-2013-02728-7

[19] T. Gudi, K. Porwal, A remark on the a posteriori error analysis of discontinuous Galerkin methods for the obstacle problem, Comput. Methods Appl. Math. 14 (1) (2014) 71–87. doi:10.1515/cmam-2013-0015.
URL https://doi.org/10.1515/cmam-2013-0015

[20] T. Gudi, K. Porwal, A posteriori error estimates of discontinuous Galerkin methods for the Signorini problem, J. Comput. Appl. Math. 292 (2016) 257–278. doi:10.1016/j.cam.2015.07.008.
URL https://doi.org/10.1016/j.cam.2015.07.008

[21] R. Herbin, E. Marchand, Finite volume approximation of a class of variational inequalities, IMA J. Numer. Anal. 21 (2) (2001) 553–585. doi:10.1093/imanum/21.2.553.
URL https://doi.org/10.1093/imanum/21.2.553

[22] J. Berton, R. Eymard, Finite volume methods for the valuation of American options, M2AN Math. Model. Numer. Anal. 40 (2) (2006) 311–330. doi:10.1051/m2an:2006011.
URL https://doi.org/10.1051/m2an:2006011

[23] J. Steinbach, A variational inequality approach to free boundary problems with applications in mould filling, Vol. 136, Birkhäuser, 2012.

[24] M. Cicuttin, A. Ern, T. Gudi, Hybrid high-order methods for the elliptic obstacle problem, hAL Preprint 01718883, submitted for publication (2019).
URL https://hal.inria.fr/hal-01718883/

[25] S. J. Wright, Primal-dual interior-point methods, Society for Industrial and Applied Mathematics (SIAM), Philadelphia, PA, 1997. doi:10.1137/1.9781611971453.
URL http://dx.doi.org/10.1137/1.9781611971453

[26] C. Kanzow, An active set-type Newton method for constrained nonlinear systems, in: Complementarity: applications, algorithms and extensions (Madison, WI, 1999), Vol. 50 of Appl. Optim., Kluwer Acad. Publ., Dordrecht, 2001, pp. 179–200. doi:10.1007/978-1-4757-3279-5_9.
URL http://dx.doi.org/10.1007/978-1-4757-3279-5_9

[27] M. Hintermüller, K. Ito, K. Kunisch, The primal-dual active set strategy as a semismooth Newton method, SIAM J. Optim. 13 (3) (2002) 865–888 (2003). doi:10.1137/S1052623401383558.
URL http://dx.doi.org/10.1137/S1052623401383558

[28] T. De Luca, F. Facchinei, C. Kanzow, A semismooth equation approach to the solution of nonlinear complementarity problems, Math. Programming 75 (3, Ser. A) (1996) 407–439.
URL https://doi.org/10.1016/S0025-5610(96)00028-7

[29] F. Facchinei, J.-S. Pang, Finite-dimensional variational inequalities and complementarity problems. Vol. I, Springer Series in Operations Research, Springer-Verlag, New York, 2003.

[30] F. Facchinei, J.-S. Pang, Finite-dimensional variational inequalities and complementarity problems. Vol. II, Springer Series in Operations Research, Springer-Verlag, New York, 2003.

[31] F. Facchinei, C. Kanzow, S. Sagratella, Solving quasi-variational inequalities via their KKT conditions, Math. Program. 144 (1-2, Ser. A) (2014) 369–412.
URL https://doi.org/10.1007/s10107-013-0637-0

[32] W. Prager, J. L. Synge, Approximations in elasticity based on the concept of function space, Quart. Appl. Math. 5 (1947) 241–269. doi:10.1090/qam/25902.
URL http://dx.doi.org/10.1090/qam/25902

[33] I. Babuška, W. C. Rheinboldt, Reliable error estimation and mesh adaptation for the finite element method, in: Computational methods in nonlinear mechanics (Proc. Second Internat. Conf., Univ. Texas, Austin, Tex., 1979), North-Holland, Amsterdam-New York, 1980, pp. 67–108.

[34] M. Ainsworth, J. T. Oden, A posteriori error estimation in finite element analysis, Pure and Applied Mathematics (New York), Wiley-Interscience [John Wiley & Sons], New York, 2000. doi:10.1002/9781118032824.
URL http://dx.doi.org/10.1002/9781118032824

[35] R. Verfürth, A posteriori error estimation techniques for finite element methods, Numerical Mathematics and Scientific Computation, Oxford University Press, Oxford, 2013. doi:10.1093/acprof:oso/9780199679423.001.0001.
URL http://dx.doi.org/10.1093/acprof:oso/9780199679423.001.0001

[36] M. Ainsworth, J. T. Oden, C.-Y. Lee, Local a posteriori error estimators for variational inequalities, Numer. Methods Partial Differential Equations 9 (1) (1993) 23–33. doi:10.1002/num.1690090104.
URL https://doi.org/10.1002/num.1690090104

[37] R. Kornhuber, A posteriori error estimates for elliptic variational inequalities, Comput. Math. Appl. 31 (8) (1996) 49–60.
URL https://doi.org/10.1016/0898-1221(96)00030-2

[38] S. I. Repin, Functional a posteriori estimates for elliptic variational inequalities, Zap. Nauchn. Sem. S.-Peterburg. Otdel. Mat. Inst. Steklov. (POMI) 348 (Kraevye Zadachi Matematicheskoĭ Fiziki i Smezhnye Voprosy Teorii Funktsiĭ. 38) (2007) 147–164, 305. doi:10.1007/s10958-008-9093-4.
URL http://dx.doi.org/10.1007/s10958-008-9093-4

[39] F. Chouly, M. Fabre, P. Hild, J. Pousin, Y. Renard, Residual-based *a posteriori* error estimation for contact problems approximated by Nitsche's method, IMA J. Numer. Anal. 38 (2) (2018) 921–954. doi:10.1093/imanum/drx024.
URL https://doi.org/10.1093/imanum/drx024

[40] R. Verfürth, A posteriori error estimates for nonlinear problems: $L^r(0,T;W^{1,\rho}(\Omega))$-error estimates for finite element discretizations of parabolic equations, Numer. Methods Partial Differential Equations 14 (4) (1998) 487–518. doi:10.1002/(SICI)1098-2426(199807)14:4<487::AID-NUM4>3.0.CO;2-G.
URL https://doi.org/10.1002/(SICI)1098-2426(199807)14:4<487::AID-NUM4>3.0.CO;2-G

[41] A. Bergam, C. Bernardi, Z. Mghazli, A posteriori analysis of the finite element discretization of some parabolic equations, Math. Comp. 74 (251) (2005) 1117–1138. doi:10.1090/S0025-5718-04-01697-7.
URL https://doi.org/10.1090/S0025-5718-04-01697-7

[42] A. Ern, I. Smears, M. Vohralík, Guaranteed, locally space-time efficient, and polynomial-degree robust a posteriori error estimates for high-order discretizations of parabolic problems, SIAM J. Numer. Anal. 55 (6) (2017) 2811–2834. doi:10.1137/16M1097626.
URL https://doi.org/10.1137/16M1097626

[43] A. Ern, I. Smears, M. Vohralík, Equilibrated flux a posteriori error estimates in $L^2(H^1)$-norms for high-order discretizations of parabolic problems, IMA Journal of Numerical Analysisdoi:10.1093/imanum.

[44] K.-S. Moon, R. H. Nochetto, T. V. Petersdorff, C.-S. Zhang, A posteriori error analysis for parabolic variational inequalities, ESAIM: Mathematical Modelling and Numerical Analysis - Modélisation Mathématique et Analyse Numérique 41 (3) (2007) 485–511. doi:10.1051/m2an:2007029.
URL http://www.numdam.org/item/M2AN_2007__41_3_485_0

[45] H. Gimperlein, J. Stocek, Space–time adaptive finite elements for nonlocal parabolic variational inequalities, Comput. Methods Appl. Mech. Engrg. 352 (2019) 137–171. doi:10.1016/j.cma.2019.04.019.
URL https://doi.org/10.1016/j.cma.2019.04.019

[46] F. Ben Belgacem, C. Bernardi, A. Blouza, M. Vohralík, On the unilateral contact between membranes. Part 1: Finite element discretization and mixed reformulation, Math. Model. Nat. Phenom. 4 (1) (2009) 21–43. doi:10.1051/mmnp/20094102.
URL http://dx.doi.org/10.1051/mmnp/20094102

[47] F. Ben Belgacem, C. Bernardi, A. Blouza, M. Vohralík, On the unilateral contact between membranes. Part 2: *a posteriori* analysis and numerical experiments, IMA J. Numer. Anal. 32 (3) (2012) 1147–1172. doi:10.1093/imanum/drr003.
URL http://dx.doi.org/10.1093/imanum/drr003

[48] H. Brezis, Functional analysis, Sobolev spaces and partial differential equations, Universitext, Springer, New York, 2011.

[49] J. Dabaghi, Estimations d'erreur a posteriori pour des inégalités variationnelles : application à un écoulement diphasique en milieu poreux, Ph.D. thesis, Sorbonne Université (2019).

[50] F. H. Clarke, Optimization and nonsmooth analysis, 2nd Edition, Vol. 5 of Classics in Applied Mathematics, Society for Industrial and Applied Mathematics (SIAM), Philadelphia, PA, 1990. doi:10.1137/1.9781611971309.
URL https://doi.org/10.1137/1.9781611971309

[51] R. S. Dembo, S. C. Eisenstat, T. Steihaug, Inexact Newton methods, SIAM J. Numer. Anal. 19 (2) (1982) 400–408. doi:10.1137/0719025.
URL https://doi.org/10.1137/0719025

[52] S. C. Eisenstat, H. F. Walker, Globally convergent inexact Newton methods, SIAM J. Optim. 4 (2) (1994) 393–422. doi:10.1137/0804022.
URL http://dx.doi.org/10.1137/0804022

[53] C. T. Kelley, Iterative methods for linear and nonlinear equations, Vol. 16 of Frontiers in Applied Mathematics, Society for Industrial and Applied Mathematics (SIAM), Philadelphia, PA, 1995.
URL https://doi.org/10.1137/1.9781611970944

[54] S. C. Eisenstat, H. F. Walker, Choosing the forcing terms in an inexact Newton method, SIAM J. Sci. Comput. 17 (1) (1996) 16–32, special issue on iterative methods in numerical linear algebra (Breckenridge, CO, 1994). doi:10.1137/0917003.
URL https://doi.org/10.1137/0917003

[55] J. Papež, U. Rüde, M. Vohralík, B. Wohlmuth, Sharp algebraic and total a posteriori error bounds for h and p finite elements via a multilevel approach, hAL Preprint 01662944, submitted for publication (2017).
URL https://hal.inria.fr/hal-01662944/

[56] P. Destuynder, B. Métivet, Explicit error bounds in a conforming finite element method, Math. Comp. 68 (228) (1999) 1379–1396. doi:10.1090/S0025-5718-99-01093-5.
URL http://dx.doi.org/10.1090/S0025-5718-99-01093-5

[57] D. Braess, J. Schöberl, Equilibrated residual error estimator for edge elements, Math. Comp. 77 (262) (2008) 651–672. doi:10.1090/S0025-5718-07-02080-7.
URL http://dx.doi.org/10.1090/S0025-5718-07-02080-7

[58] A. Ern, M. Vohralík, Adaptive inexact Newton methods with a posteriori stopping criteria for nonlinear diffusion PDEs, SIAM J. Sci. Comput. 35 (4) (2013) A1761–A1791. doi:10.1137/120896918.
URL http://dx.doi.org/10.1137/120896918

[59] J. E. Roberts, J.-M. Thomas, Mixed and hybrid methods, in: Handbook of Numerical Analysis, Vol. II, North-Holland, Amsterdam, 1991, pp. 523–639.

[60] F. Brezzi, M. Fortin, Mixed and hybrid finite element methods, Vol. 15 of Springer Series in Computational Mathematics, Springer-Verlag, New York, 1991. doi:10.1007/978-1-4612-3172-1.
URL http://dx.doi.org/10.1007/978-1-4612-3172-1

[61] P.-A. Raviart, J.-M. Thomas, A mixed finite element method for 2nd order elliptic problems, in: Mathematical aspects of finite element methods (Proc. Conf., Consiglio Naz. delle Ricerche (C.N.R.), Rome, 1975, Springer, Berlin, 1977, pp. 292–315. Lecture Notes in Math., Vol. 606.

[62] M. Bebendorf, A note on the Poincaré inequality for convex domains, Z. Anal. Anwendungen 22 (4) (2003) 751–756. doi:10.4171/ZAA/1170.
URL http://dx.doi.org/10.4171/ZAA/1170

[63] L. E. Payne, H. F. Weinberger, An optimal Poincaré inequality for convex domains, Arch. Rational Mech. Anal. 5 (1960) 286–292 (1960). doi:10.1007/BF00252910.
URL http://dx.doi.org/10.1007/BF00252910

[64] L. C. Evans, Partial differential equations, Vol. 19 of Graduate Studies in Mathematics, American Mathematical Society, 1997.

[65] Y. Saad, M. H. Schultz, GMRES: a generalized minimal residual algorithm for solving nonsymmetric linear systems, SIAM J. Sci. Statist. Comput. 7 (3) (1986) 856–869. doi:10.1137/0907058.
URL https://doi.org/10.1137/0907058

[66] Y. Saad, Iterative methods for sparse linear systems, 2nd Edition, Society for Industrial and Applied Mathematics, Philadelphia, PA, 2003. doi:10.1137/1.9780898718003.
URL https://doi.org/10.1137/1.9780898718003